

NBSIR-74-364

**DETECTION OF HUMAN INTRUDERS BY LOW FREQUENCY
SONIC INTERFEROMETRIC TECHNIQUES**

Robert E. Stoltenberg

Electromagnetics Division
Institute for Basic Standards
National Bureau of Standards
Boulder, Colorado 80302

May 1974

Final Report

Prepared for
Sandia Laboratories
U.S. Atomic Energy Commission
Order No. AL-73-356
Albuquerque, New Mexico

NBSIR-74-364

**DETECTION OF HUMAN INTRUDERS BY LOW FREQUENCY
SONIC INTERFEROMETRIC TECHNIQUES**

Robert E. Stoltenberg

Electromagnetics Division
Institute for Basic Standards
National Bureau of Standards
Boulder, Colorado 80302

May 1974

Final Report

Prepared for
Sandia Laboratories
U.S. Atomic Energy Commission
Order No. AL-73-356
Albuquerque, New Mexico



U.S. DEPARTMENT OF COMMERCE, Frederick B. Dent, Secretary

NATIONAL BUREAU OF STANDARDS, Richard W. Roberts, Director

CONTENTS

	<u>Page</u>
1.0 INTRODUCTION-----	1
1.1 Background-----	1
1.2. Concept-----	2
1.2.1 Ambient Acoustical Noise-----	5
1.2.2 Noise Caused by Enviromental Changes---	5
1.2.3 Equipment Noise and Sensitivity-----	6
2.0 OBJECTIVE-----	7
3.0 INSTRUMENTATION REQUIREMENTS-----	8
3.0.1 Ambient Noise Characteristics-----	8
3.0.2 Target Scattering (reflection coef-	8
ficient)-----	8
3.0.3 Sound Pressure Level Field Patterns----	8
3.1 Ambient Sound Pressure Level Measurements-----	9
3.2 Target Scattering Calculations-----	9
3.3 Sound Pressure Level Field Pattern Measurements	12
3.4 Conclusions-----	15
4.0 INSTRUMENTATION-----	17
4.1 Sound Source-----	17
4.1.1 Transducer-----	17
4.1.2 Amplifier and Oscillator-----	18
4.2 Microphones and Preamplifiers-----	18
4.3 Acoustical Hardware Mounting-----	18
4.4 Receivers-----	18
4.4.1 Functional Analysis-----	19
4.5 Recording Capabilities and Signature Analysis-	23
5.0 TEST LOCATION DESCRIPTIONS-----	24
5.1 Room 3082, Radio Building-----	24
5.2 NBS Auditorium-----	24
5.3 NBS Instrument Shop-----	27
5.4 Camco Building #5-----	27

CONTENTS (Continued)

	<u>Page</u>
6.0 PRELIMINARY EVALUATION, ROOM 3082 SPECTRAL DISTRIBUTION OF INTRUDER SIGNATURE AND NOISE-----	27
6.1 Test Description-----	30
6.2 Test Results and Analysis-----	30
6.3 Conclusions-----	36
7.0 INTRUDER TESTS, NBS AUDITORIUM-----	38
7.1 Test Description-----	38
7.2 Test Results and Analysis-----	39
7.2.1 Intruder Signature Analysis-----	39
7.2.2 Sonification Level vs. Noise and In- truder Signature Magnitudes-----	41
7.2.3 Intruder Signature as a Function of Source and Receiver Characteristics----	44
7.2.4 Detection as a Function of Geometry----	48
7.2.5 Spectral Distribution vs. Intruder Velocity-----	48
7.2.6 Intruder Size Comparison-----	48
7.2.7 Additional Exploratory Tests-----	52
7.3 Conclusions-----	55
8.0 INTRUDER TESTS, NBS INSTRUMENT SHOP-----	56
8.1 Test Descriptions-----	56
8.2 Test Results and Analysis-----	57
8.2.1 Intruder Signature Analysis-----	57
8.2.2 Sonification Level vs. Noise and In- truder Signature Magnitude-----	57
8.2.3 Intruder Signature as a Function of Source Characteristics-----	60
8.2.4 Detection as a Function of Geometry----	62
8.2.5 Intruder Signature as a Function of Intruder Velocity and Size-----	62
8.3 Conclusions-----	66

CONTENTS (Continued)

	<u>Page</u>
9.0 WAREHOUSE FEASIBILITY TESTS-----	66
9.1 Test Descriptions-----	66
9.2 Test Results and Analysis-----	67
9.3 Conclusions-----	70
10.0 LONG TERM FALSE ALARMS-----	70
10.1 Test Descriptions-----	72
10.2 Test Results and Analysis-----	72
10.3 Conclusions-----	73
11.0 CONCLUSIONS-----	73
11.1 Conclusion by Parameter-----	73
11.1.1 Intruder Signature-----	74
11.1.2 Background Noise-----	74
11.1.3 Geometry of the Source and Receiver---	75
11.1.4 Area of Coverage-----	75
11.1.5 The Effects of Source and Microphone Characteristics-----	75
11.1.6 General Comments-----	76
11.2 Recommendations-----	76
11.2.1 Minimum Velocity Effects-----	76
11.2.2 Additional Evaluation of Sound Pressure Fields-----	76
11.2.3 Design and Construction of Prototype Engineering Model Detectors-----	76
11.2.4 Detection Capability and False Alarm Tests-----	77
11.2.5 Engineering Model Detector and Test---	77
ACKNOWLEDGMENTS-----	77
REFERENCE-----	77
APPENDIX-----	78

LIST OF ILLUSTRATIONS

		<u>Page</u>
Figure 1.1	Vectorial signal addition-----	3
Figure 3.1	Ambient sound pressure level-----	10
Figure 3.2	Normalized scatter from a rigid sphere-----	11
Figure 3.3	Typical sound pressure level spatial distribution-----	13
Figure 3.4	Circular sound pressure patterns-----	14
Figure 4.1	Receiver block diagram-----	20
Figure 5.1	Room 3082 plan view-----	25
Figure 5.2	Auditorium plan view-----	26
Figure 5.3	Instrument shop plan view-----	28
Figure 5.4	Camco Building plan view-----	29
Figure 6.1	Spectral display carrier frequency dependence	31
Figure 6.2	Corrected spectral display-----	33
Figure 6.3	Receiver output vs. correlation-----	34
Figure 6.4	Target return vs. carrier frequency-----	37
Figure 7.1	Intruder signature, spectral dependence upon carrier frequency-----	40
Figure 7.2	Sonification vs. noise level and intruder signature-----	42
Figure 7.3	Sonification vs. noise and intruder signature	45
Figure 7.4	Intruder signature microphone/preamp vs. sound level meter-----	46
Figure 7.5	Intruder signature speaker vs. horn-----	47
Figure 7.6	Detection vs. geometry-----	49

LIST OF ILLUSTRATIONS (Continued)

	<u>Page</u>
Figure 7.7 Intruder signature vs. intruder velocity-----	50
Figure 7.8 Intruder size comparison-----	51
Figure 7.9 Radio effects upon detection-----	53
Figure 7.10 Random intruder actions-----	54
Figure 8.1 Intruder signature spectral dependence vs. carrier frequencies-----	58
Figure 8.2 Target strength as a function of carrier frequency-----	59
Figure 8.3 Intruder signature as a function of source---	61
Figure 8.4 Detection vs. microphone position-----	63
Figure 8.5 Single speaker-single microphone detection---	64
Figure 8.6 Intruder signature as a function of size and velocity-----	65
Figure 9.1 Intruder signature vs. geometry-----	68
Figure 9.2 Target strength vs. carrier frequency-----	69
Figure 9.3 Sonification vs. noise and intruder signature	71
Figure A.1 Microphone amplifier, speaker amplifier, and DC-DC converter schematics-----	79
Figure A.2 Receiver wiring diagram-----	80
Figure A.3 Amplitude control board 3.4, 5.0 kHz-----	81
Figure A.4 Amplitude control board 1.0, 1.7, 2.2 kHz----	82
Figure A.5 Voltage variable phase shifter-----	83
Figure A.6 Quadrature hybrid-----	84
Figure A.7 Amplitude detector-----	85
Figure A.8 Phase detector-----	86
Figure A.9 Receiver response-----	87

DETECTION OF HUMAN INTRUDERS
BY
LOW FREQUENCY SONIC INTERFEROMETRIC TECHNIQUES

This report examines the theory and evaluates the results of over 200 tests of the use of low frequency sonic interference techniques for the detection of a human intruder in a confined area. The conclusions are that this technique is potentially a significant improvement over conventional methods with regard to area coverage and minimum velocity detection.

This work examined the intruder signature and background noise with respect to sonification frequency, source levels, intruder size, intruder velocity, source types, area coverage (to 692 sq. meters), and geometric position of the source and receiver in four radically different areas.

Interference effects of the intruder signature and noise were analyzed with respect to bandwidth, spectral content, and magnitude by both computer-drawn spectral displays, and specific frequency correlators.

Key words: Human detector; interferometric technique; low frequency acoustics.

1.0 INTRODUCTION

This report describes the results of a test program conducted in FY 1973 to define the various parameters which affect the probability of detecting an intruder by the interferometric measurement of his perturbation of an acoustical sound field. This effort was funded by the Atomic Energy Commission under the direction of Sandia Laboratories.

1.1 Background

The Electromagnetics Division of the National Bureau of Standards has been active in the measurement and evaluation of interferometric techniques utilizing electromagnetic as well as underwater acoustical energy for approximately

3 years. A single test was successfully conducted during this period for determining feasibility of detecting an intruder in a room using this principle. NBS personnel presented the theory and background of this concept in March 1972 for Sandia Laboratory personnel resulting in this contract.

1.2 Concept

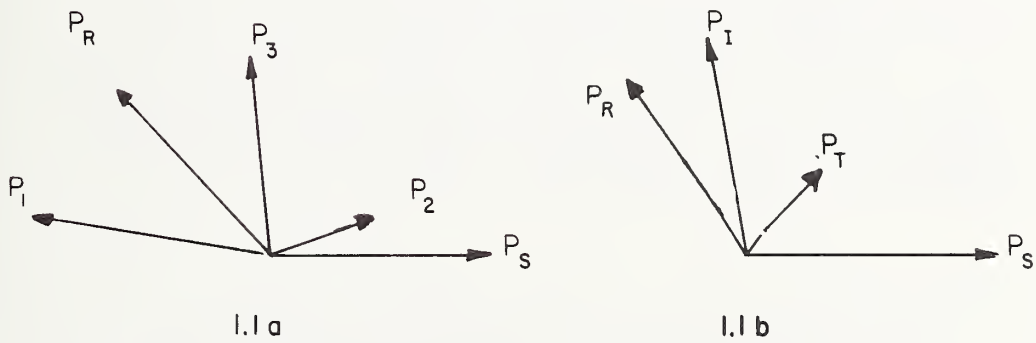
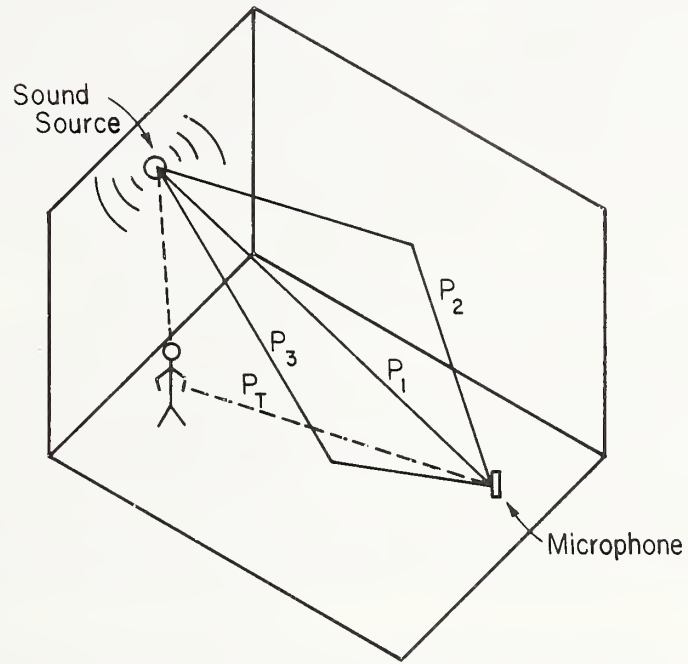
The concept of the technique is as follows. A bounded volume of air (closed room or building) is illuminated with CW acoustical energy from a single speaker. As a result of wall, ceiling, floor, and interior object reflections, multipath transmission produces an acoustical field which, in this report, will be referred to as a standing wave pattern (SWP). This pattern will be uniquely specified by the phase and amplitude of pressure (relative to the source) at all points within the field. The introduction of any new object (scatterer) large enough to disturb the transmission paths will alter this standing wave pattern of the entire volume. Any movement of the object will result in a modulation of the standing wave pattern which is a complex function of the object velocity, acoustical wavelength (λ), and angular direction of the object motion with respect to the geometry of the source, reflectors, and the position of the object.

To illustrate a simple case involving only three reflections the following analysis is presented (see fig. 1.1).

With no intruder present, the resultant pressure wave at the microphone is P_R , which is the vectorial summation of P_1 , P_2 , and P_3 (see fig. 1.1a). P_R will have a phase and magnitude (relative to P_S) which is related to the spreading loss, scattering loss, and acoustical wavelength.

With the introduction of the intruder an additional pressure wave (P_T) (see fig. 1.1b) will be present whose phase and magnitude also will be related to the above parameters and, in addition, to the reflection coefficient (target scattering) at the aspect angle of the intruder. The resultant (P_I) will have some new phase and magnitude different than P_R , which existed prior to the presence of the intruder. Therefore

VECTORIAL SIGNAL ADDITION



- P_S Source Pressure
- P_1 Direct Path
- P_2 Wall Reflection
- P_3 Floor Reflection
- P_R $\Sigma P_1, P_2, P_3$
- P_T Target Reflection
- P_I $\Sigma P_R, P_T$

Figure 1.1

the intruder perturbation does not inherently require intruder movement for detection. The principle is basically different from Doppler techniques. In general, as the intruder traverses any path, the relative phase of P_T will change with respect to P_S through 360° at a rate which is proportional to his speed (i.e. as the acoustical path length changes one complete wavelength P_T will describe a complete 360° rotation with respect to P_S). The interference signal P_I will thus contain both phase and amplitude modulation.

The frequency of this modulation is given by the following relationship:

$$F_M = \frac{\text{intruder path length velocity}}{\text{acoustical wavelength}},$$

where intruder path length velocity is the rate of change of the acoustical path length due to the movement of the intruder.

In this simple case there is a direct relation between the phase modulation in degrees and the amplitude modulation. As an example:

Assume $P_R = 1.0$ unit and $P_T = 0.035$ units. The amplitude modulation magnitude is $\pm 3.5\%$. The maximum phase displacement occurs when P_T is at right angles with P_I . This forms a right triangle whose base is 1.0 and height is 0.035. The angle formed is 2.0° . Hence 3.5% magnitude change is equal to 2° phase change.

It is obvious that when all of the multiple transmission paths contribute to the initial pressure wave P_R , and multiple paths to the intruder exist as well, the situation will produce a very complex modulation spectrum. The added effects of appendage movements further increase the complexity.

An additional result of the multipath concept is that the object is not required to produce a reflection for theoretical detection. Even if the object is an absorber of acoustical energy, the presence of the object interferes with some of the multiple transmission paths, and this absorption in turn produces a change in the standing wave pattern.

Any technique which measures these perturbations (either or both phase and magnitude) can provide detection of the intruder.

As with all measurements, the problem is to determine the signal of interest in the presence of noise. In this case noise (unwanted signal) arises from three distinct sources.

1.2.1 Ambient Acoustical Noise

Any acoustical energy present in the protected volume containing frequency components near the source frequency will produce interferences with the signals of interest. $N_A = \text{SPL}_{\text{AMBIENT}}/P_R$ where P_R is the sonification SPL and N_A is the relative noise produced by ambient acoustical energy. The most obvious solution to reduce the effects of this interference is to choose an operating frequency at which the background noise is minimal.

If this is impractical for other reasons, such as those discussed in the following section, an absolute solution is to increase the source levels such that the ambient energy becomes a smaller contribution to the total received energy. It should be noted at this point that given a detectable signal, the detection sensitivity is not related to source power, although the false-alarm rate may be expected to be. The measured quantity for detection is the change of the existing field pattern due to the introduction of the foreign object. Therefore, the source acoustical power required for an operational system is only related to the room volume and reflecting properties and the requirement to mask any existing acoustical energy present.

1.2.2 Noise Caused by Environmental Changes

Signal vector modulation can also result from changes in the local environment. All changes such as air motion, thermal gradient changes, temperature changes, wall vibrations, and in addition, small animals (mice) can modulate the SWP. Each source of modulation will produce its own effect, and the combination will produce a modulation frequency spectrum.

This noise is assumed to increase in magnitude with increasing source frequency. Additionally it is assumed that the frequency of this noise is maximum at or near zero Hz in the modulation spectrum, decreasing in magnitude with increasing modulation frequency. This assumption was made from the following hypothesis (for the purpose of this report):

$$N_{EN} = \Delta P_R / P_R,$$

where N_{EN} is defined to be the normalized environmental noise.

ΔP_R is produced primarily by the relative change in phase occurring in the vector summation of all signals contributing to P_R from all paths. As the source frequency increases (shorter wavelength), the environmental effects will have a proportionately larger phase change for a given environmental change. This would increase ΔP_R , hence increasing N_{EN} .

The modulation frequency of ΔP_R will be determined by the rate of change of those environmental effects which are taking place. For example, a rapid window vibration will produce a small change in the summation of P_R , while dimensional changes of the building due to outside temperature changes which affect the entire structure would be slow but rather large.

With respect to small animals such as mice which might be part of the environment (and which are a problem for ultrasonic systems), it was assumed that by using source sonification of relatively low frequency (less than 10 kHz) their scattering cross section would be made too small to produce significant reflections.

1.2.3 Equipment Noise and Sensitivity

In order that the detection sensitivity be limited to natural or background effects, the instrumentation used for this evaluation was either designed or selected to insure it did not become the limiting factor.

2.0 OBJECTIVE

The objective of this effort was to determine the inter-relationship of the parameters which affect the detection of an intruder. This work had the following goals:

1. Determination of the spectral distribution of the intruder signal.
2. Determination of the spectral characteristic of environmental noise as a function of enclosure types.
3. Analysis of the above for carrier frequency optimization.
4. Examination of the effects upon detectability of speaker-microphone physical position.
5. Measurements of area coverage by single units.

In order to accomplish these goals the following tasks were identified:

1. Determination of instrumentation requirements.
 - a. Ambient noise analysis.
 - b. Spatial characteristics of standing wave pattern.
2. Construction and/or purchase of instrumentation.
3. Preliminary tests to determine intruder signature as a function of carrier frequency.
4. Analysis of signal and noise for a variety of conditions.
5. Tests to determine volume coverage.
6. Final analysis and recommendations.

3.0 INSTRUMENTATION REQUIREMENTS

The purpose of this task was to provide the preliminary instrumentation specifications. Decisions based upon this work determined the selection of the discrete frequency to be used for intrusion tests. It would additionally provide receiver specifications. All references to sound pressure levels given in dB use the standard reference of $0.0002 \text{ dynes/cm}^2$ (hearing threshold). (Note: In some cases a reference is included which equates specific dB levels to environmental conditions. Generally a single frequency sounds louder to humans than the same sound pressure level in a broadband spectrum.) The following areas were evaluated for this purpose.

3.0.1 Ambient Noise Characteristics

The spectral distribution of ambient noise should suggest the most favorable carrier frequency ranges. The ambient sound pressure level (SPL) magnitude would, additionally, determine the minimum output acoustical power from the speaker for given signal-to-noise ratios at specific carrier frequencies.

3.0.2 Target Scattering (reflection coefficient)

Rayleigh scattering theory predicts that the normalized target scattering of a sphere is dependent upon carrier frequency when the ratio of circumference to wavelength is less than 10 [1].

By approximating the volume of an intruder as a sphere, Rayleigh theory was used as one of the guides for determining the lower test frequency.

3.0.3 Sound Pressure Level Field Patterns

The SPL field characteristic is important in determining the dynamic range of the instrumentation required to measure the signal levels encountered in a typical enclosed area.

3.1 Ambient Sound Pressure Level Measurements

As noted in section 1.2.1 the ultimate limiting factor in determining the minimum acoustical power level required for detection at a given carrier frequency is the ambient sound pressure level. Preliminary ambient spectral measurements were performed in a variety of locations using a sound pressure level meter equipped with an active filter. The bandpass of this unit is $\pm 1/2$ octave. This information provided one of the guides for selecting the carrier frequencies used in testing detection characteristics.

The results of these tests are presented in figure 3.1. With the exception of the Camco Building, the noise power slope was nominally 15 dB/decade from 100 Hz to 4 kHz. If we assume that the intruder interference spectrum is directly related to carrier frequency, we are justified in using a meter whose bandpass is a function of frequency. If this is incorrect, one must convert the noise to a per Hz noise power, thus increasing the slope of these curves. In Camco, a warehouse which contains no forced air ventilation or machinery, the noise appears to level off at frequencies below 1 kHz.

3.2 Target Scattering Calculations

No formal target scattering calculations were attempted, due to the highly irregular shape of the human body. Rayleigh's relationships of the effective acoustic scatter to geometric cross section of a fixed rigid sphere were used as a guide (see fig. 3.2) to determine the minimum lower test frequency. The following assumptions were made:

- a. Scattering is roughly omnidirectional.
- b. The impedance mismatch of air to the human body is large enough for the target to appear rigid.
- c. The human body volume is nominally 0.07 to 0.085 meters³.
- d. The human body to be a sphere of that volume; thus having a diameter of 0.51 to 0.55 meters.

AMBIENT SOUND PRESSURE LEVEL

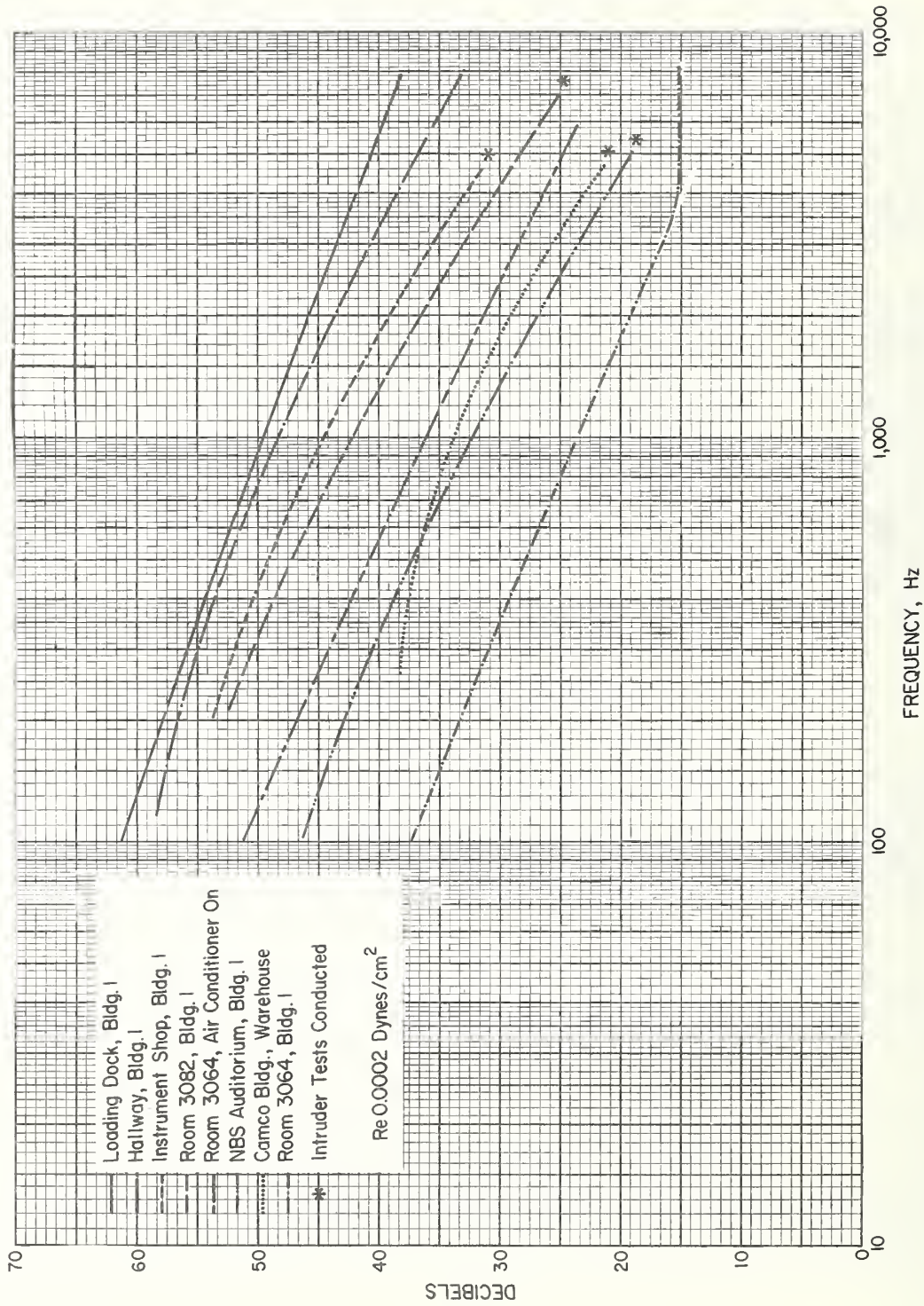
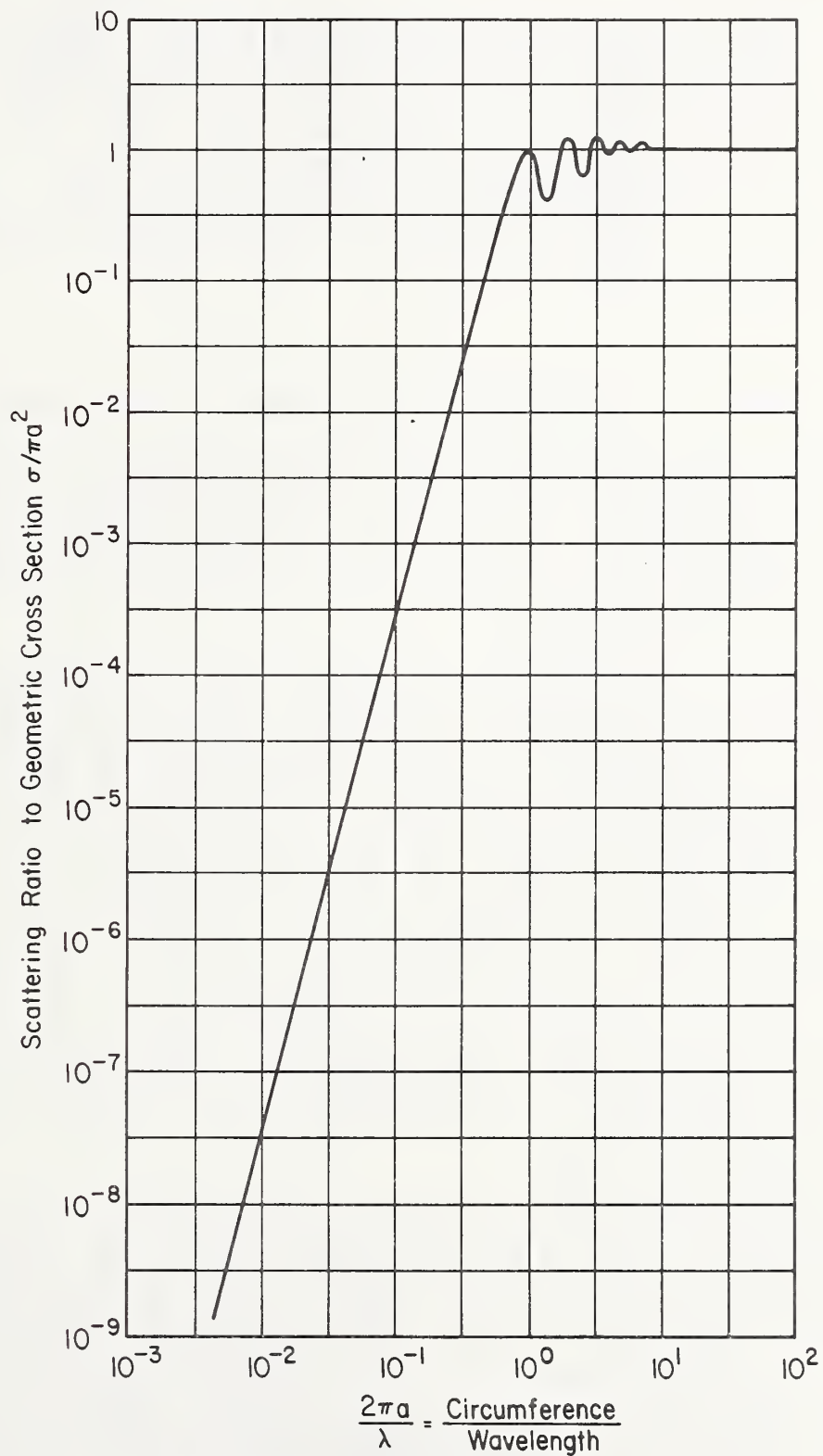


Figure 3.1

NORMALIZED SCATTER FROM A RIGID SPHERE



a = Sphere Radius
 σ = Scatter Cross Section

Figure 3.2

- e. The circumference/wavelength ratio to be 3.0 minimum for a non-oscillatory target return (fig. 3.2).

The wavelength thus required would be

$$\lambda = \frac{\text{circumference}}{3} = \frac{\pi}{3} 0.51 = 0.53 \text{ meters corresponding to a carrier frequency, } f = 331 \text{ meters/sec}/0.53 \text{ meter} = 625 \text{ Hz.}$$

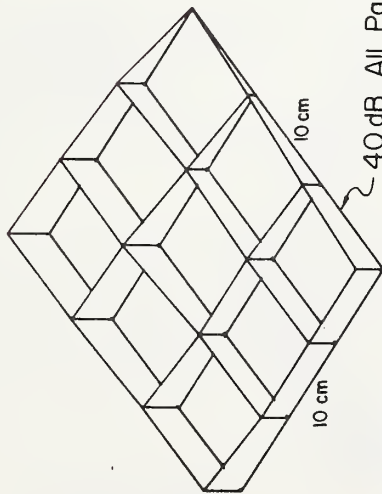
3.3 Sound Pressure Level Field Pattern Measurements

Despite the fact that detection does not depend upon absolute signal levels but rather upon the change of existing levels, instrumentation requirements dictate signal levels within finite values. Hence it is important to determine the range of sound pressure levels to be expected for random placement of the microphones.

A series of sound pressure field pattern measurements were conducted in two rooms. In each case the room was illuminated with acoustical energy at discrete carrier frequencies. The room was first investigated for general areas of low intensity. In all cases the fluctuations in SPL occurred over short distances (0.3 meters). Over larger volumes the general average appeared to be uniform. Two patterns were investigated. In the first pattern, the microphone was moved through a sixteen point grid in a vertical position. The microphone and speaker were separated by a room divider. In the second case the SPL meter was rotated in a horizontal circle (0.6 meter dia.). It is obvious that the presence of the rotating meter will alter the absolute SPL values. The purpose of these measurements is only to determine the variation in SPL with position of the sensing microphone. No individuals were in the enclosed area during the readings.

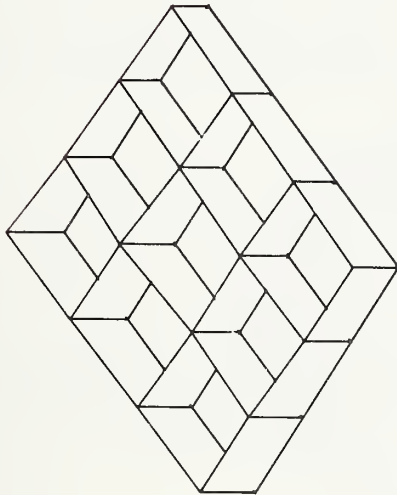
The field patterns in figures 3.3 and 3.4 are representative of all field pattern measurements conducted. No measurements were made in the larger rooms (> 100 sq. meters) because at the outset of the program, areas of that size were not considered feasible. The vertical grid measurements (fig. 3.3) were made over very small areas (10 cm sq.) and indicate a general change of 10-14 dB with location. The 1 cm microphone represents 10% of the total grid dimension and thus probably provides some averaging. The circular patterns (fig. 3.4) were judged more appropriate in that

TYPICAL SOUND PRESSURE LEVEL
SPATIAL DISTRIBUTION

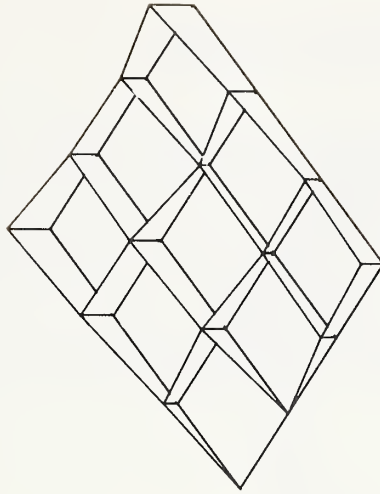


dB RANGE- 40 - 54
FREQUENCY - 500 Hz

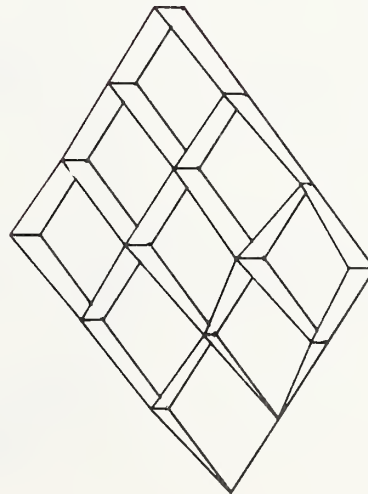
40 dB All Patterns



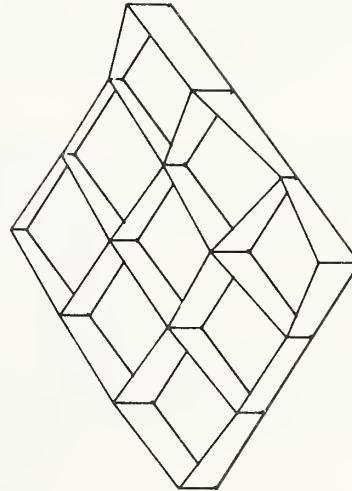
52-60
1 kHz



40-56
2 kHz



40-51
4 kHz



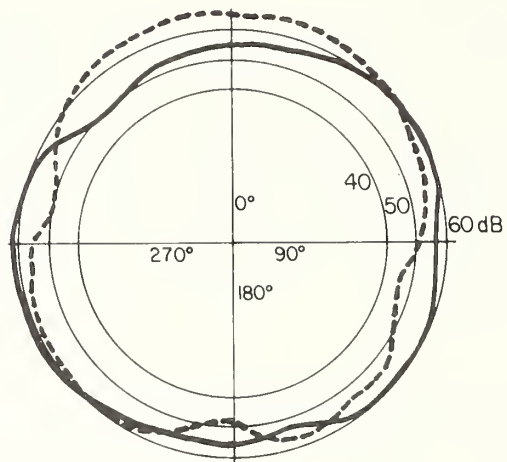
44-56
8 kHz

Room 3064 - Radio Bldg
Power - 20 mW Speaker

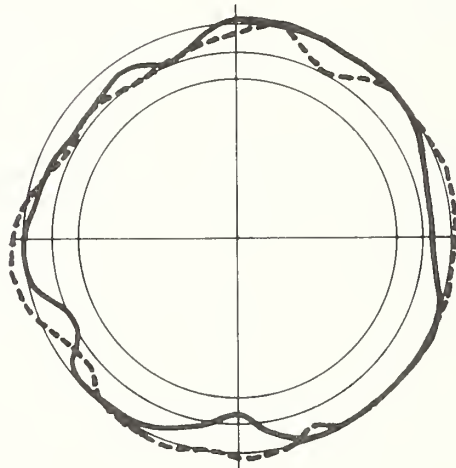
Room 3064

Figure 3.3

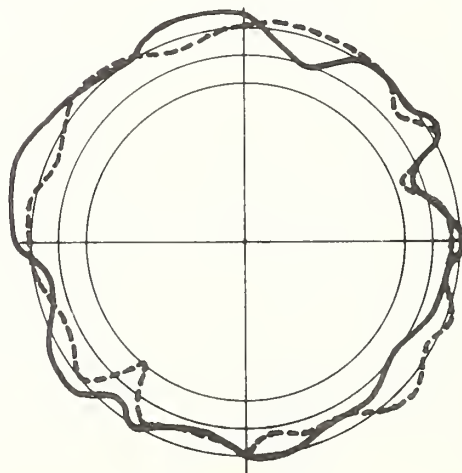
CIRCULAR SOUND PRESSURE PATTERNS



500 Hz



1 kHz



2 kHz

— No obstructions
- - - Speaker - Sound level
meter separated by
book case

Room 3064

Figure 3.4

there was a significant change as carrier frequency was increased. The circular path corresponded to 1.5 wavelengths at 500 Hz and 6 wavelengths at 2 kHz. The number of maxima and minima of the sound pressure, as well as the magnitude of the change, increase with frequency. Measurements attempted at 4 kHz were unsuccessful due to signal amplitude drift during the time interval required for the measurements. This type of drift is an example of environmental noise as defined in section 1.2.

3.4 Conclusions

The first parameter to be chosen was the carrier frequency which was to be used for the tests. The results of the ambient noise tests favor the use of higher frequencies (> 1 kHz) which would permit lower sonification levels for given detection levels.

The results of the crude examination of target scattering indicate a minimum test frequency in the vicinity of 500 Hz due to the oscillation of effective scattering cross section below 600 Hz. This minimum test frequency was left open to change pending the experimental results.

The results of the sound pressure field patterns indicate considerable signal instability would be encountered at frequencies in excess of 4 to 5 kHz, since the signal strength experienced considerable drift during the time period of the tests.

Based upon the above, the test carrier frequencies were chosen. It was concluded that the decade from 500 Hz to 5 kHz should be investigated. The following nominal frequencies were selected for investigation; 0.5, 1.0, 1.5, 2.2, 3.3, and 5.0 kHz. With the exception of 0.5 to 1.0 kHz they were chosen to provide 1/2 octave steps. Hardware constraints ultimately resulted in 1.5 and 3.3 kHz being changed to 1.7 and 3.4 kHz.

On the basis of these measurements, the receiver sensitivity specification was chosen to insure that the limiting factor in detection would be either the ambient or the environmental noise, and not the receiver sensitivity or noise characteristics.

Because environmental noise could not be determined until testing began, the ambient noise was initially chosen as a guide in determining the sensitivity specification.

A subjective evaluation of various sonification levels indicated that intensities exceeding 74 dB (1 ubar) were very uncomfortable when produced at a single frequency. The preliminary maximum sonification level was therefore chosen to be 66 dB (0.4 ubar). The minimum measured ambient acoustical noise in test areas occurred in the auditorium at 4 kHz (20 dB at 2800 Hz BW). For the receiver to resolve this level, the following analysis was used to determine minimum receiver sensitivity:

$$\begin{aligned} 20 \text{ dB} &= 0.002 \text{ ubar (2800 Hz BW)} \\ &= 0.00004 \text{ ubar (1 Hz BW)}. \end{aligned}$$

$$N_A = (\text{SPL}_{\text{AMBIENT}}/P_R) \times 100\% = \frac{0.00004 \text{ ubar}}{0.4 \text{ ubar}} \times 100 = 0.01\% \text{ (1 Hz BW)}$$

The receiver therefore should have a sensitivity adequate to resolve a power level change equivalent to 0.01% of a 1 Hz BW at a 66 dB sonification level.

At 1 kHz, in the instrument shop, the ambient noise was 46 dB (0.04 ubar) in a 700 Hz BW or .0015 ubar (1 Hz BW). Therefore the sonification level would have to be greater than:

$$P_R = \frac{\text{SPL}}{.01\%} = \frac{0.0015 \text{ ubar}}{0.01\%} = 15 \text{ ubar (97 dB)}$$

for the receiver to influence the detectability at 1.0 kHz carrier frequency.

The receiver total bandwidth was arbitrarily chosen to be 1-75 Hz based primarily on the difficulties in providing corrections to the phase servo at higher frequencies.

The dynamic range of the receiver was chosen by the following analysis:

At 500 Hz, the ambient noise \approx 60 dB (0.2 ubar) (350 Hz BW).

The receiver BW = 75 Hz

Receiver is a peak detector.

Ambient noise in the receiver BW is

$$N_A = \frac{0.2 \text{ ubar } \sqrt{2}}{\sqrt{350/75}} = 0.13 \text{ ubar}$$

At a sonification level of 66 dB (0.4 ubar).

$$N_A = \text{SPL}_{\text{AMB}}/P_R = 0.13/0.4 = 0.325.$$

The goal for the receiver dynamic range was therefore set at $\pm 35\%$ minimum. This specification assures that the receiver does not saturate due to ambient noise.

Following the preliminary operational tests the receiver response was changed from 1-75 Hz to 10-75 Hz due to unexpected target return levels in the 1-8 Hz range in room 3082. This change reduced the dynamic range requirements, but did, however, require frequency response corrections in all the data analysis.

4.0 INSTRUMENTATION

The following section describes the instrumentation which was either purchased or designed and constructed for use on the program.

4.1 Sound Source

4.1.1 Transducer

The primary sound source used for these tests was a 50 watt, 4-way, ducted-port, commercial speaker system (hereafter referred to as the speaker). The unit was capable of a 25-20,000 Hz response; however, the mid-range speaker alone covered the test frequencies used for our measurements. A second directional, exponential horn with a 600 Hz low-frequency cutoff was used for comparison tests (hereafter referred to as the horn).

Speaker input power is given for each test. The value is calculated from E^2/R (R = nominal speaker impedance). No correction for power factor is included, so actual power was probably somewhat less than that listed.

4.1.2 Amplifier and Oscillator

An NBS-designed battery powered audio amplifier was used to drive the speaker. The battery operation permitted easy movement and remote positioning without external cables.

A commercial variable-frequency audio oscillator was used for the source oscillator and gain control.

4.2 Microphones and Preamplifiers

Three commercial omnidirectional condenser microphones were purchased. Specifications are as follows:

Sensitivity -68 dB (re 0 dB = 1 V/uBar)
Frequency Response 30-15,000 Hz

Each microphone was provided with a broadband 46 dB battery powered amplifier (see appendix). Three additional 40 dB preamplifiers were available to provide extra gain when low power tests were conducted.

4.3 Acoustical Hardware Mounting

The microphones were equipped with adjustable stands. These stands were either taped to the walls or attached to available structures. The speaker was placed on the floor or a bench as selected for the tests.

4.4 Receivers

The receiver functions by automatically adjusting the phase and magnitude of the audio signal from the microphone preamplifier for a null with respect to a hard-wired reference signal from the source oscillator. The response time of the servo loops is faster than any modulation frequency of interest. By selecting a longer time delay for the servo for either quantity (phase or magnitude), the uncorrected perturbations will be present from the detector (i.e. if the phase servo is delayed to a response time of 1 Hz all phase perturbations occurring at a rate greater than 1 Hz will be present from the phase detector). The receivers are so equipped, with an optional time delay in both the phase and magnitude control circuits.

The upper frequency response is controlled by a low-pass filter in the output amplifier. Thus, the output band-pass of the receiver is controlled by two filters. The receiver sensitivity to phase and magnitude changes is constant, regardless of changes in the received signal, because the gain of that channel is continuously adjusted to match the fixed reference.

4.4.1 Functional Analysis

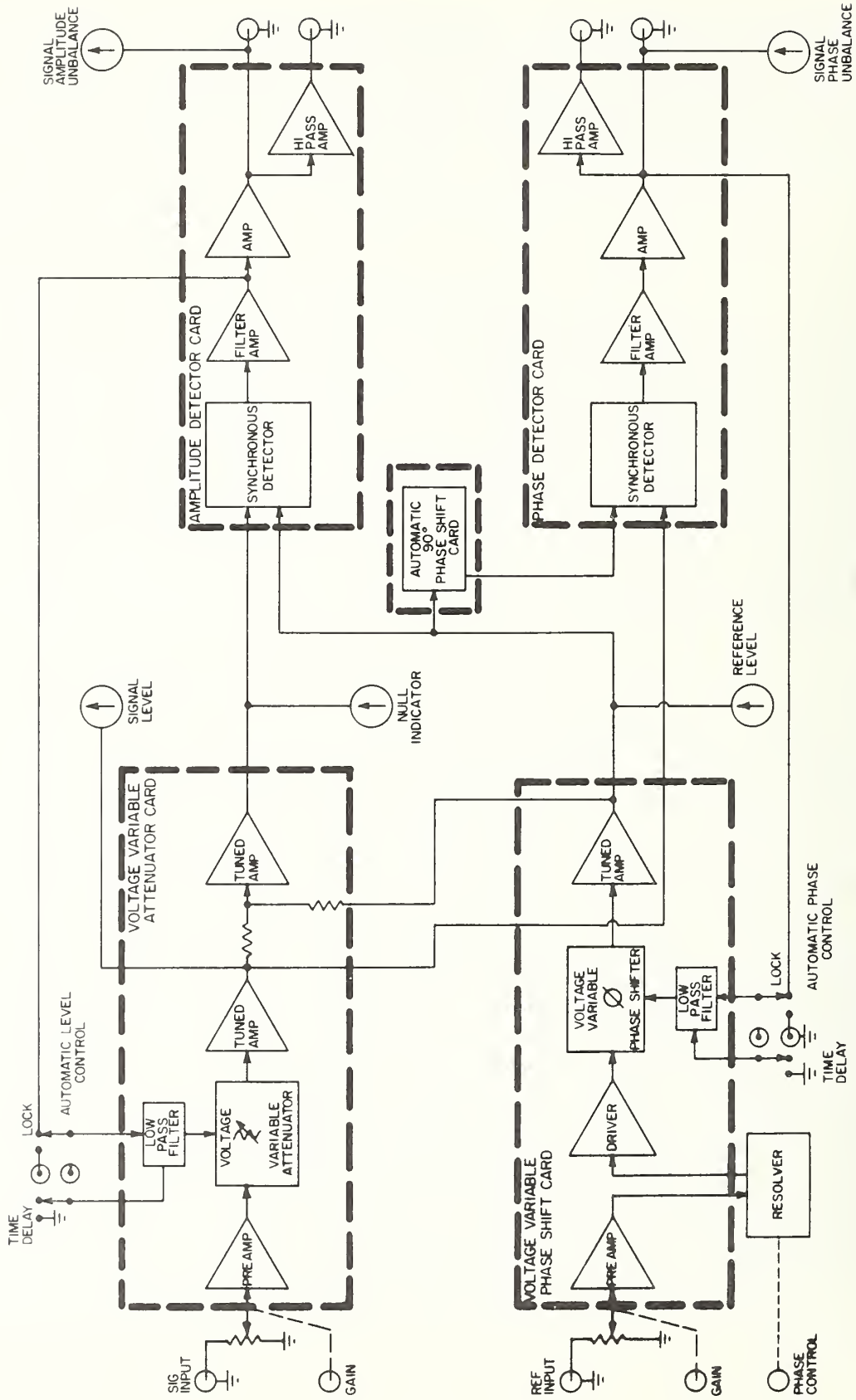
The receiver functions are shown in figure 4.1 .

The receivers are composed of five plug-in printed circuit boards mounted in a main frame which contains various switches, meters, and connectors. The two input cards determine the frequency of operation, while the remaining three are universal, covering the frequency range of 1 to 10 kHz. Five meters are provided for monitoring the operation:

- a. Signal Level Indicators (2) -- One each for reference and signal channel.
- b. Null Indicator -- Indicates the signal addition.
- c. Amplitude Unbalance -- Indicates the amplitude unbalance of the two signals.
- d. Phase Unbalance -- Indicates phase deviation from 180°.

The reference and signal voltages are applied to the input gain controls, which furnish manual gain adjustment. The reference signal amplifier is followed by a manual phase adjustment, achieved by a resolver which is continuously adjustable through 360°. Appropriate resistor-capacitor networks are furnished on each reference board for the specific frequency of operation. The resolver output is connected to a voltage variable phase shift network through a driver. This is followed by a tuned amplifier which reduces noise and any harmonics present. The control circuitry for the voltage variable phase shifter is selected for each carrier frequency to insure uniform response of the phase control servo. In the disable position of the phase lock switch, the control is connected to an external connector for calibration purposes. In operation, this jack is grounded by a shorting cap. This feature allows manual adjustments prior

AUTOMATIC NULL RECEIVER - BLOCK DIAGRAM



• FREQUENCY DETERMINED BY INPUT PC CARDS

Figure 4.1

to placing the servo in operation. As noted above, two response times are available for the control circuitry. In the fast mode, all perturbations up to 75 Hz are corrected by the servo. In the slow mode, the time delay switch adds an additional capacitor reducing the response to nominally 10 Hz (see response data in the appendix).

The signal channel is similar to the reference channel except that a voltage variable attenuator replaces the phase control circuitry, and the manual phase adjustment is eliminated.

The reference and signal channel outputs are combined in a resistive summing network. The output of this network furnishes the input to the null amplifier. The null amplifier is additionally tuned to further reduce harmonics.

Automatic level control is obtained from a synchronous detector whose inputs are the reference and null signals. The output is a polarity reversible voltage, proportional to the null magnitude. The polarity is determined by the phase of the received signal relative to the reference. The detector output is filtered to remove the carrier frequency components and connected through the lock switch to the voltage variable attenuator control circuitry. The detector output is further amplified and displayed on the amplitude unbalance meter. The receiver is provided with dual outputs from the amplifier, one direct, and the second through a 6 Hz high-pass amplifier. Each output contains a 75 Hz low-pass filter, thus limiting the receiver output to 75 Hz.

Automatic phase control is obtained from a similar synchronous detector. The synchronous detector provides a polarity-reversible output voltage, proportional to the phase displacement from 90° (for small phase angles). The voltage is 0 VDC at 90° and 270° .

The reference and signal voltages are 180° out of phase at null, so an additional 90° phase shift is required in the phase detector reference voltage. This phase shift is obtained from an automatic 90° phase shift card (quadrature hybrid). The automatic feature allows the units to operate over a wide frequency range while maintaining the 90° phase displacement.

The automatic 90° phase shift is accomplished by servoing a voltage variable phase shift network to 90° by use of a synchronous detector. All of this circuitry is contained on the printed circuit card.

The post-detector portion of the phase detector card is identical to the amplitude detector card with the exception of the absolute gain. Gain of the amplifiers is adjusted to provide equal output signal from either the phase or magnitude for a given input vector addition. This requirement was noted in section 1.2.

The following steps are followed to place the receiver in operation.

- a. Time delays out.
- b. Lock switch out.
- c. Adjust reference level to 3 VRMS.
- d. Adjust signal level to 3 VRMS.
- e. Adjust resolver for null on null indicator.
- f. Lock switches to lock.
- g. Time delay to delay for parameter of interest.

The high-pass amplifiers are provided to allow additional signal compression if the low frequency components of the noise below 6 Hz are large with respect to the higher frequencies. The magnetic recorder used in these tests had a dynamic range limited to 40 dB. If the range of signal magnitude exceeded the recorder capabilities, the higher frequency information would be lost without this provision. This feature was not required for the tests.

Six receivers were constructed. As noted, the receiver frequency is determined by the input printed circuit cards. Three sets of input cards at 2.2 and 3.4 kHz were available for simultaneous triple tests. In addition, one set at 1.0, 1.7, and 5.0 kHz were used for single tests. A set at 500 Hz was fabricated, but we experienced problems with the voltage variable phase shifter. Early intruder tests indicated that 1.0 to 5.0 kHz covered the frequencies of interest, so no further effort was expended on this unit.

Measured receiver specifications:

Dynamic tracking range
Phase $\pm 50^\circ$
Amplitude (nominally ± 10 dB)

Dynamic range
Phase $\pm 20^\circ$
Amplitude $\pm 35\%$

Bandwidth 75 Hz

Minimum detectable change (1 Hz BW)
0.01%
0.07°

4.5 Recording Capabilities and Signature Analysis

All tests were monitored in real time with a dual channel high speed strip chart recorder. In addition, the outputs were magnetically recorded on a four-channel FM tape recorder. Following each test, the recording was replayed on the strip chart recorder to insure that an accurate recording had been obtained. Variable active filters were available during the tests to examine portions of the frequency spectrum when required.

The primary data analysis for spectral examination of both the noise and the intruder signature for this program was accomplished by fast Fourier transform calculations with the computer. The analog data from the magnetic tape was first digitized, and then individual power spectral density plots were computed. These were then integrated into a three dimensional presentation (see fig. 6.1) which displays power vs. time and frequency.

Time is plotted from left to right, frequency from back to front at .997 Hz per interval, and log amplitude of the signal is plotted vertically. These displays enable a rapid evaluation of the spectral content of both noise and of the intruder disturbance. A short section of the noise "floor" is visible on the right side of each plot and may be used to estimate the signal-to-noise ratio of each test. A better estimate may be obtained from the correlation plot.

After the completion of the computer spectral analysis, the primary analysis technique used was single frequency correlation. The correlators used for this work consist of an internal two-phase oscillator, analogue multipliers, and filters. The correlator output is a slowly varying dc voltage proportional to the total signal-plus-noise power in a 0.2 Hz band centered at the oscillator frequency. Five correlation frequencies, 2, 4, 10, and 15 Hz, were available for this analysis. These units provided an additional benefit in that they could be used in real time to monitor the intrusion.

For all displays showing correlated data, the gain of the correlators was compensated to correct for the frequency response of the receivers.

5.0 TEST LOCATION DESCRIPTIONS

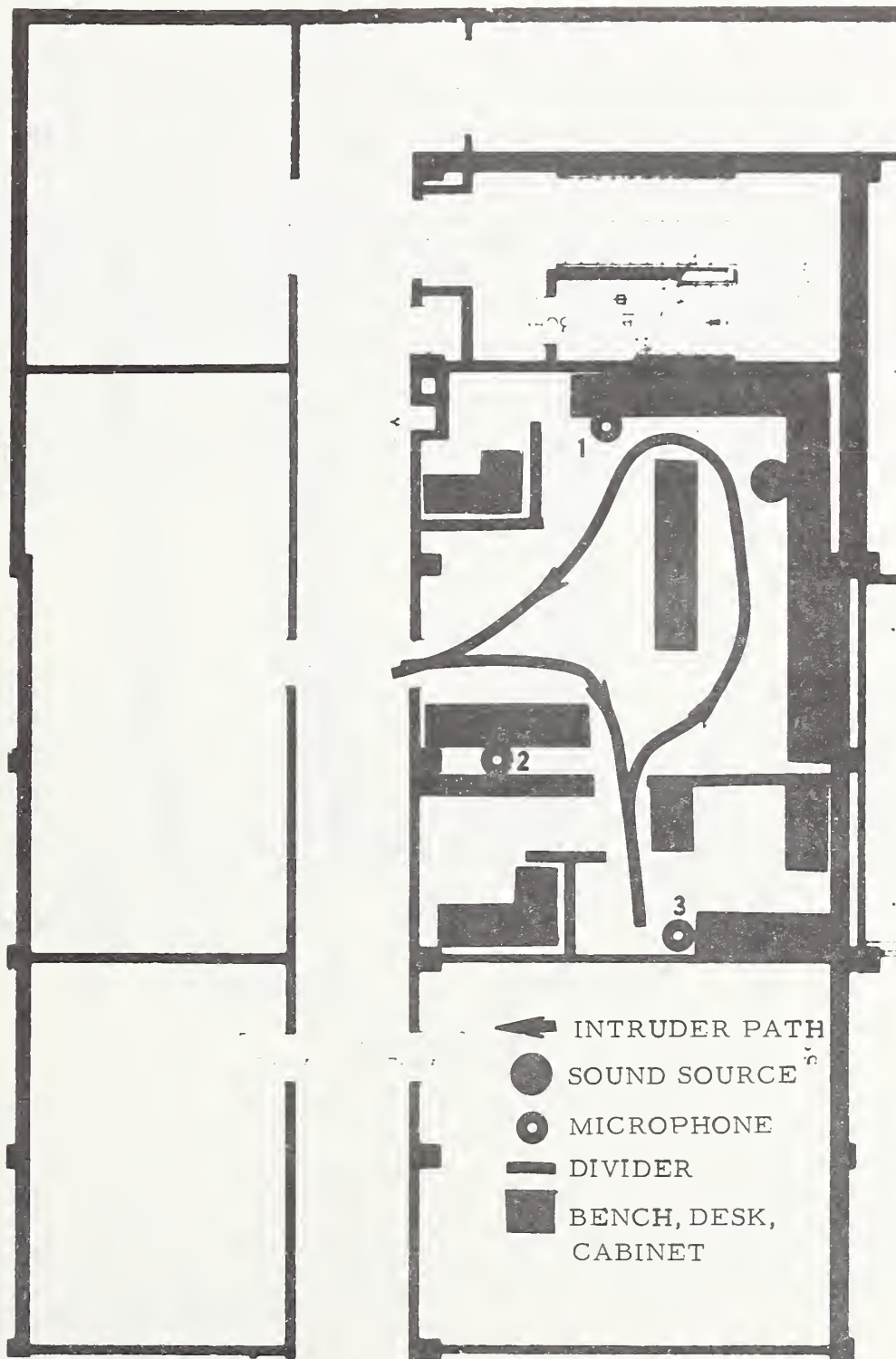
The following is a description of the test areas used for the intruder perturbation analysis. The intruder path is shown in each figure. Microphone position and speaker locations are shown in the figures. Exceptions will be noted separately. The term "geometry" is used to indicate relative microphone and speaker location throughout this report.

5.1 Room 3082, Radio Building

See figure 5.1. This 83 sq. meter (890 sq. ft.) laboratory was chosen for the initial test. It is slightly larger than what is normally considered to be the effective coverage of ultrasonic Doppler units (60 sq. meter). The ceiling and walls are copper foil over gypsum board with a concrete floor. Ceiling height is 3 meters. The room contains no windows but has a forced air ventilation system which ran continuously during the tests. Considerable air is flowing at all times. There are several room dividers and benches. The ducts for the ventilation system were suspended from the ceiling, and extended downward 0.75 meter, to produce a highly irregular volume.

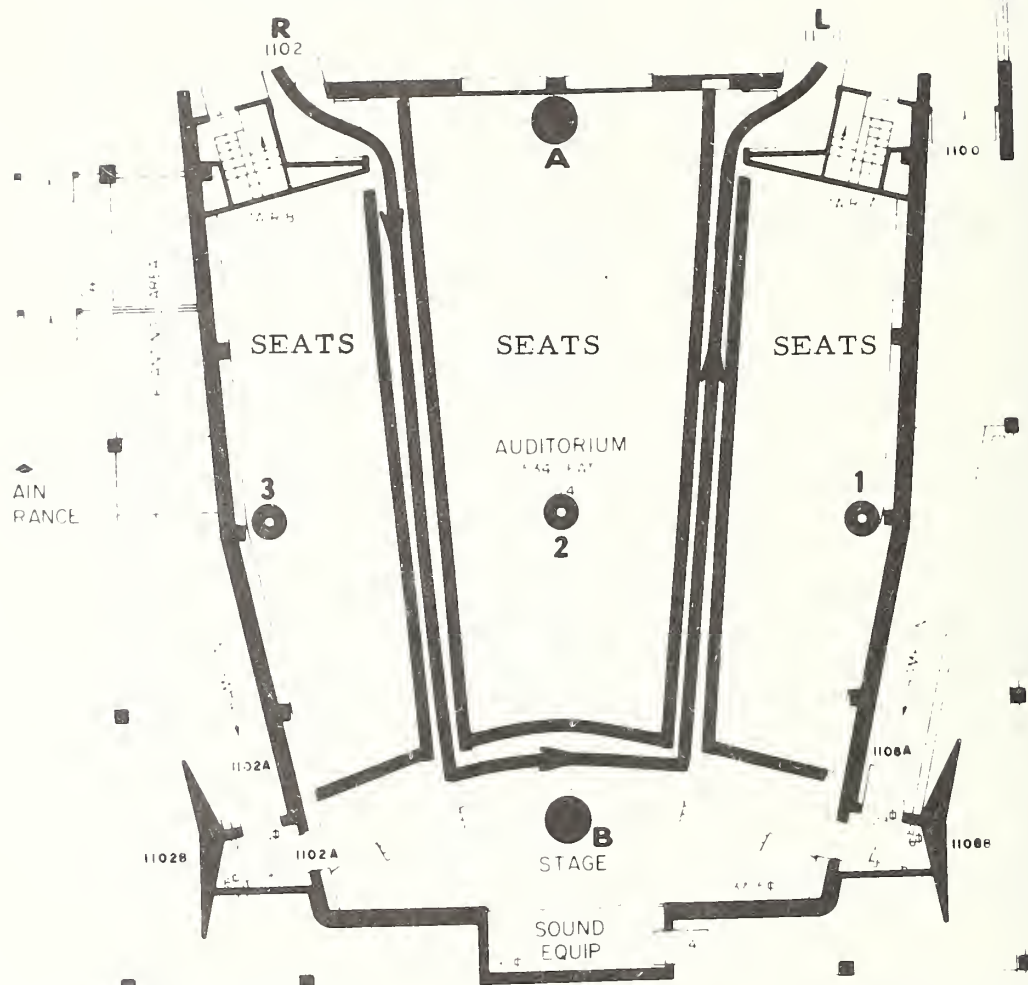
5.2 NBS Auditorium

See figure 5.2. The NBS auditorium is a conventional auditorium of 345 sq. meters (3705 sq. ft.). The walls and floor are concrete, and the only obstructions are 534 seats and the stage. The walls are covered with wood paneling. The equipment was set up in the projection booth so the intruder action could be observed. The ceiling is approximately 6 meters high, thus producing a rather large volume. Ventilation is provided by forced air through overhead vents. Considerable air movement was present during the tests.



Room 3082

Figure 5.1



- ← INTRUDER PATH
- SOUND SOURCE
- MICROPHONE

NBS Auditorium
Figure 5.2

5.3 NBS Instrument Shop

See figure 5.3. This shop is located in wing 3 of the main Radio Building. It contains a floor space of 600 sq. meters (6456 sq. ft.). The length is about three times the width. It is very crowded with large machinery (see figure 5.3 for placement). The outside wall has windows for the entire length, from approximately 1 meter above the floor up to the ceiling. The ceiling is at two levels, divided by the center line of the length and is formed of concrete beams. The outside half is about 3.5 meters high, while the inside section is 5.5 meters. Several large double doors result in rather unstable reflecting surfaces. Heating is provided by baseboard steam heat. The speaker location, shown midway in the plan drawing, is a tool crib with large counters. The equipment was set up in room 3332 at one end. This room has windows so that the intruder could be viewed during his traverse.

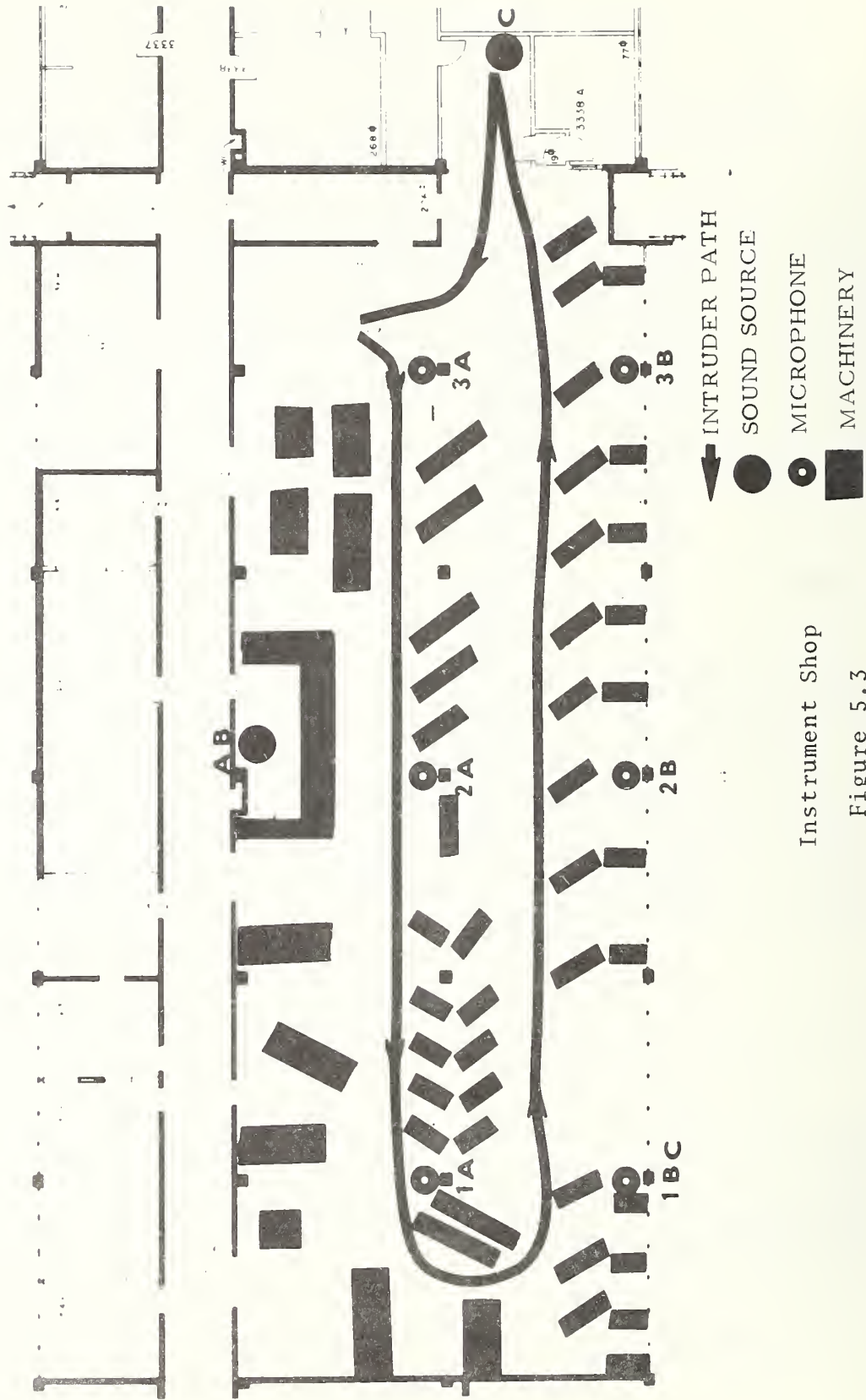
5.4 Camco Building #5

See figure 5.4. The Camco Building is a frame warehouse with corrugated steel roof used to store surplus equipment. The room has a floor space of 487 sq. meters (5241 sq. ft.) and a distance of 12 meters from the floor to the base of the roof. The room is full of shelves and racks. A large steel roll-up door was of very loose fit. Chirping birds were present inside and were flying during the first part of the tests. Forced air overhead heaters were present, but it is not known if they operated. Outside temperatures were in the range of 50-60°.

6.0 PRELIMINARY EVALUATION, ROOM 3082

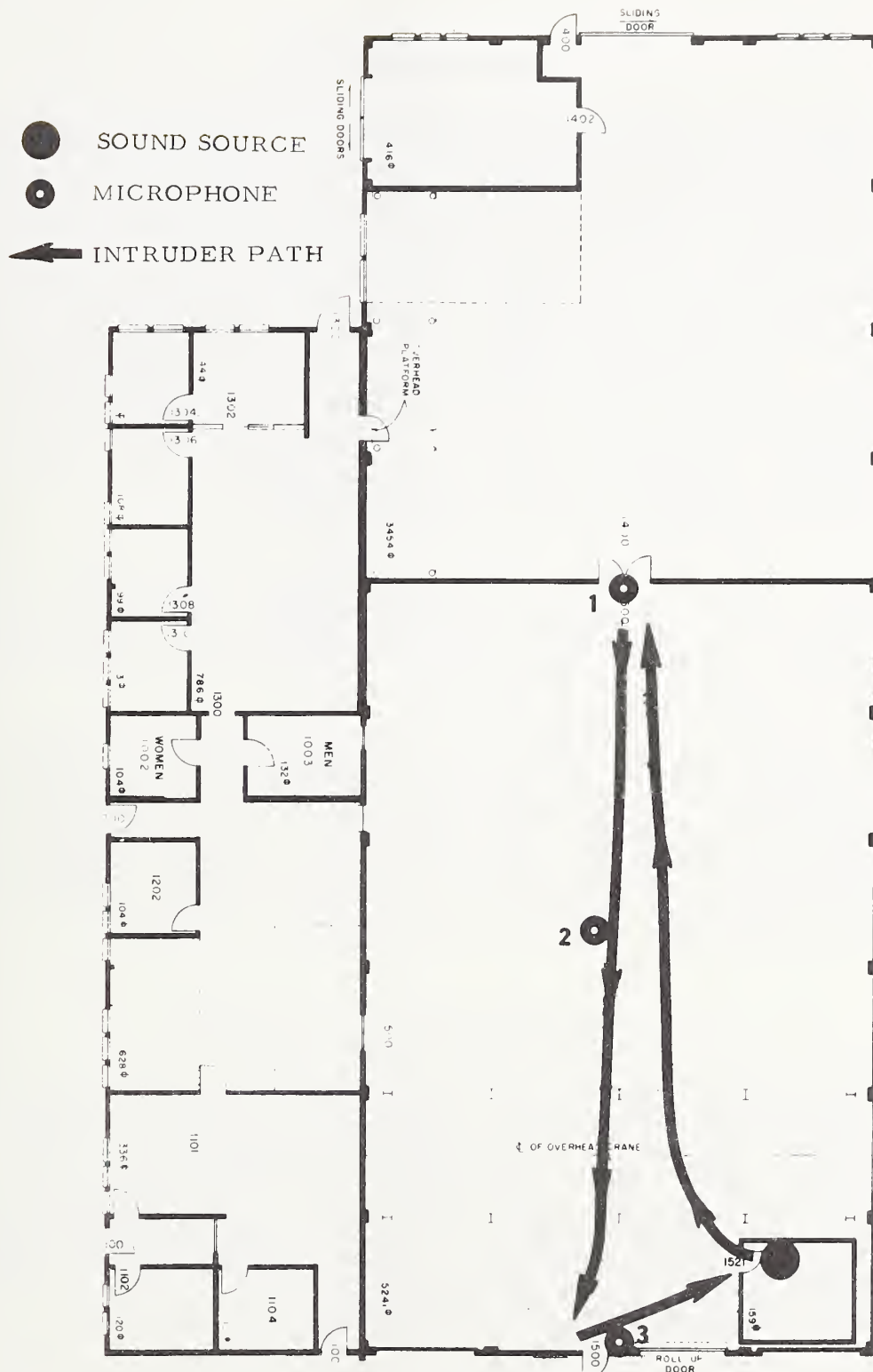
SPECTRAL DISTRIBUTION OF INTRUDER SIGNATURE AND NOISE

This initial intruder test series was designed to investigate the spectral characteristics of both the background noise and the intruder signature. (In this report background noise refers to all noise from the receiver.) The results also provided a basis for the determination of target strength (intruder scattering).



Instrument Shop

Figure 5.3



Camco Building

Figure 5.4

6.1 Test Description

These tests were performed in Room 3082 (fig. 5.1). The room was chosen because it was somewhat larger in size than the typical Doppler ultrasonic area of coverage for a single unit. Three microphones were placed as shown, and the intruder path was selected to provide some detection from each unit. No pretesting of locations was conducted. All test equipment was set up outside in the hallway. In each test, the intruder opened the door, stepped in, and closed the door, remaining motionless for 5 seconds before proceeding along the path. The intruder again halted for 5 seconds before exiting the room. The intruder path was practiced for several runs before the tests to insure as nearly identical intrusions as possible. Electrical power to the speaker was 22 mw, and typical sound pressure levels ranged from 0.07 to 0.2 ubars. This level is typical of a business office.

Tests were conducted at the following five carrier frequencies: 1.0, 1.7, 2.2, 3.4 and 5.0 kHz. Originally 500 Hz was to have been included, but difficulties were experienced in producing exact calibration, so preliminary tests were conducted without that frequency.

A minimum of one test from each microphone at each carrier frequency was conducted. In addition, several tests were performed to insure repeatability from test to test. Also, three tests using the output jack from the sound pressure level meter in place of the microphone-preamplifier were conducted to determine if any unanticipated effects from the microphone might be encountered. None were.

6.2 Test Results and Analysis

The spectral displays of the intruder interference from each position at each carrier frequency (except 5.0 kHz) are presented in figure 6.1. The results from the tests at 5.0 kHz were very poor because of considerable phase and amplitude fluctuations during the tests. This condition was noted as a potential problem in section 3.0 in discussions concerning the field patterns. The receivers did not have sufficient dynamic range and made operator corrections necessary during the tests at 5.0 kHz.

SPECTRAL DISPLAYS
INTRUDER SIGNATURE VS. CARRIER FREQUENCY

POSITION 3

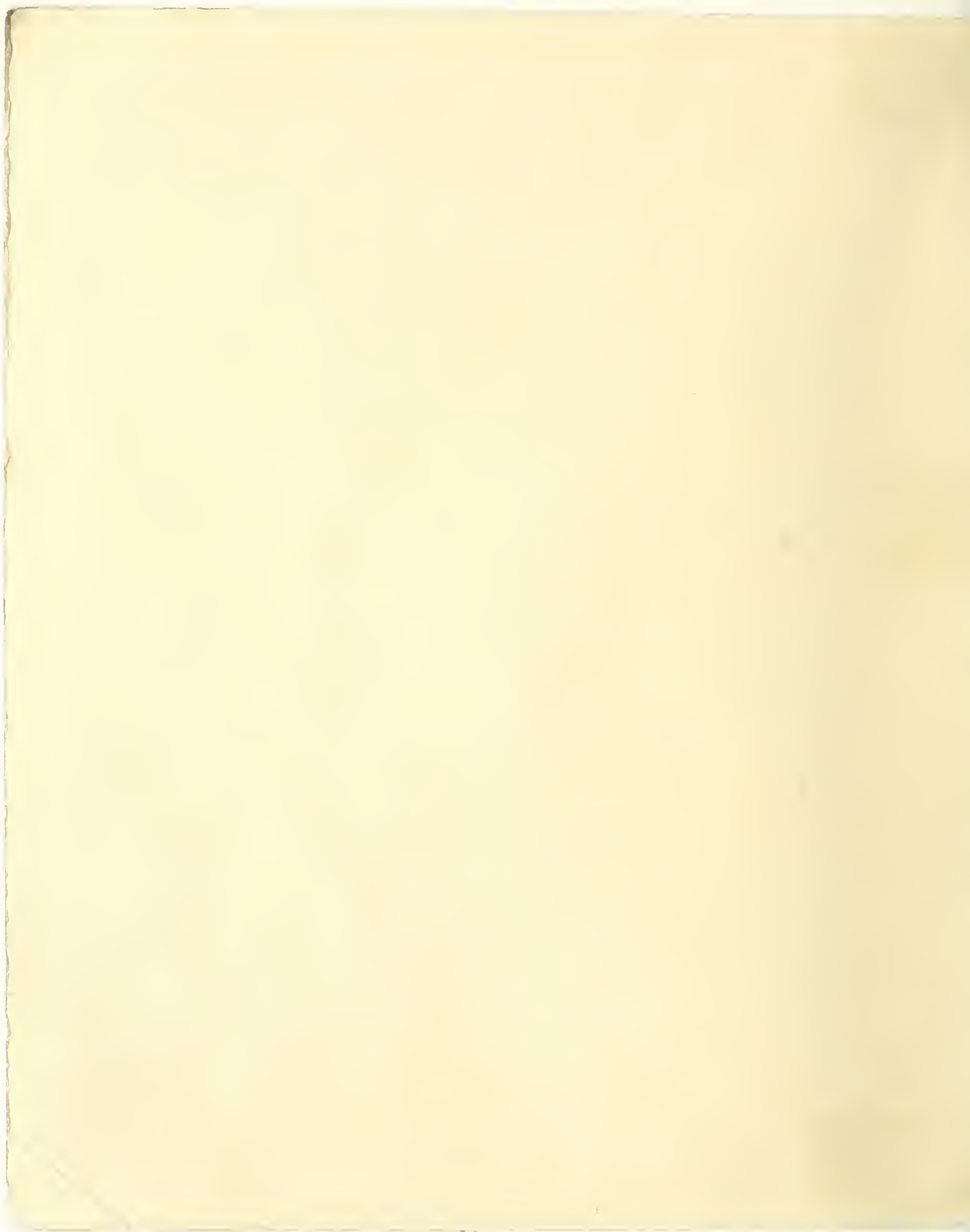
POWER - 22 mW
INTRUDER A

POSITION 2

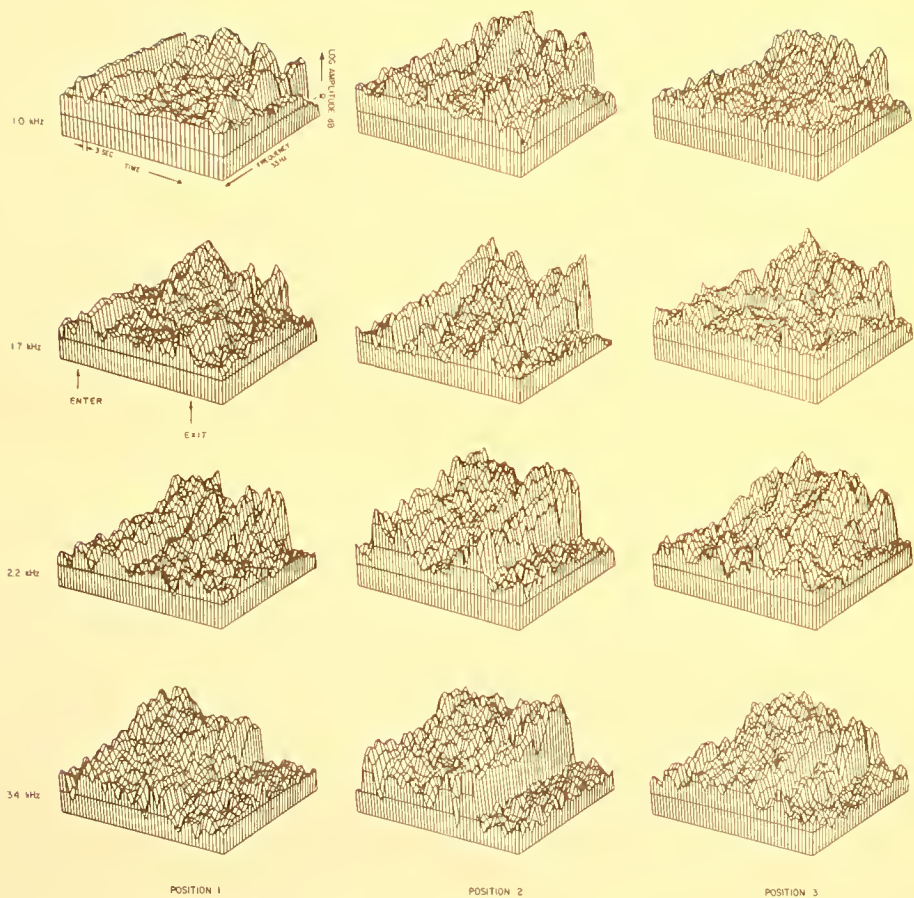
Room 3082

Figure 6.1

POSITION 1



SPECTRAL DISPLAYS
INTRUDER SIGNATURE VS CARRIER FREQUENCY



POWER: 22 mW
INTRUDER: A

Room 3082

Figure 6.1

As noted in the instrumentation section, the presentations display time from left to right, perturbation frequency from back to front, and log amplitude of the signal in the vertical direction. In addition, the 10 Hz low-pass response of the receivers reduces the output by 17 dB at 1 Hz, thus reducing the low frequency magnitude. At a later date, a correction was added to the computer program which produced displays of absolute response. See figure 6.2 for a comparison of this effect.

The intruder entry and exit in which the door was opened (including the additional acoustical energy from the closing) is quite evident in all displays. In particular, position 2, which was next to the door, resulted in very large impulse energy during the door closure. This should be ignored when analyzing the data for intruder signatures.

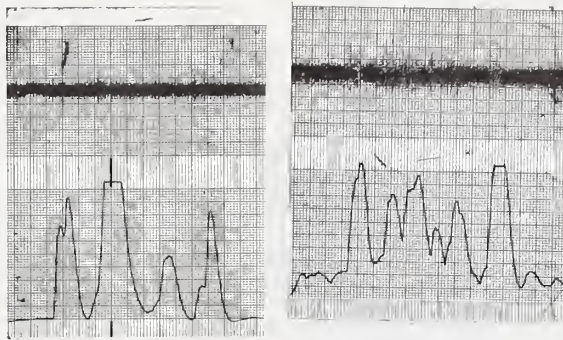
The most remarkable result of these tests was the wide area of coverage. Detection was literally 100% from any position in the room during the entire time the intruder was moving in the room. It should be remembered that this room is 1.5 times the size normally covered by an ultrasonic unit.

The second unexpected effect was the exceptional sensitivity of position 3, located on the far side of the room on top of a file cabinet 2 meters high. Position three appears superior to number one at all frequencies. Position three is nearly as good as position two which was centrally located, and thus being, on the average, closest to the intruder.

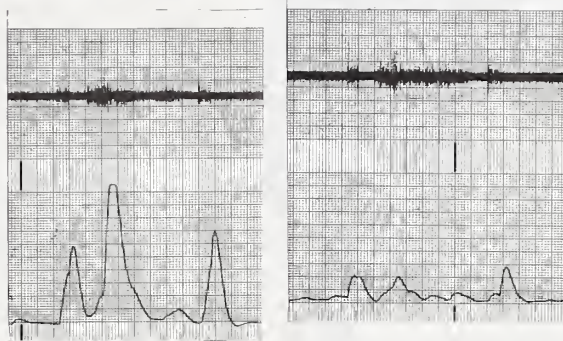
The spectral distribution is generally broadband, with increasing slope as the carrier frequency decreases, thus supporting the hypothesis that the intruder signature spectrum is roughly proportional to carrier frequency.

Since the general character of the signature was broadband, the same data was analyzed with the correlators (see section 4.5) to determine if they could provide an effective substitute for the spectral displays. Spectral displays are quite expensive (nominally \$35 each). In addition, correlation is available either in real time or immediately after the test was conducted. Computer analysis required the services of extra personnel and several days of elapsed time. The correlations are presented in figure 6.3.

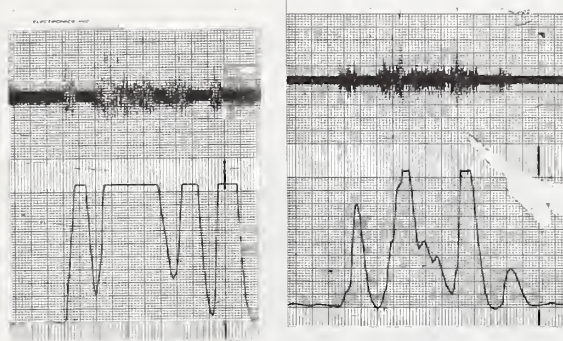
1.0 kHz



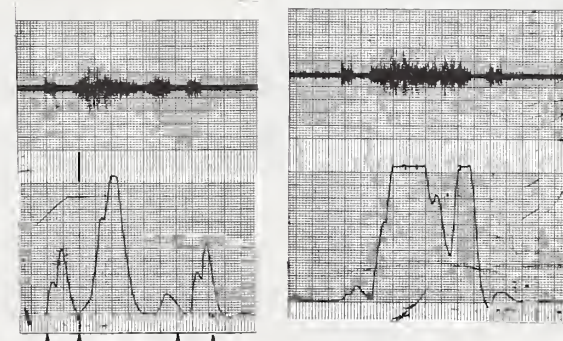
1.7 kHz



2.2 kHz



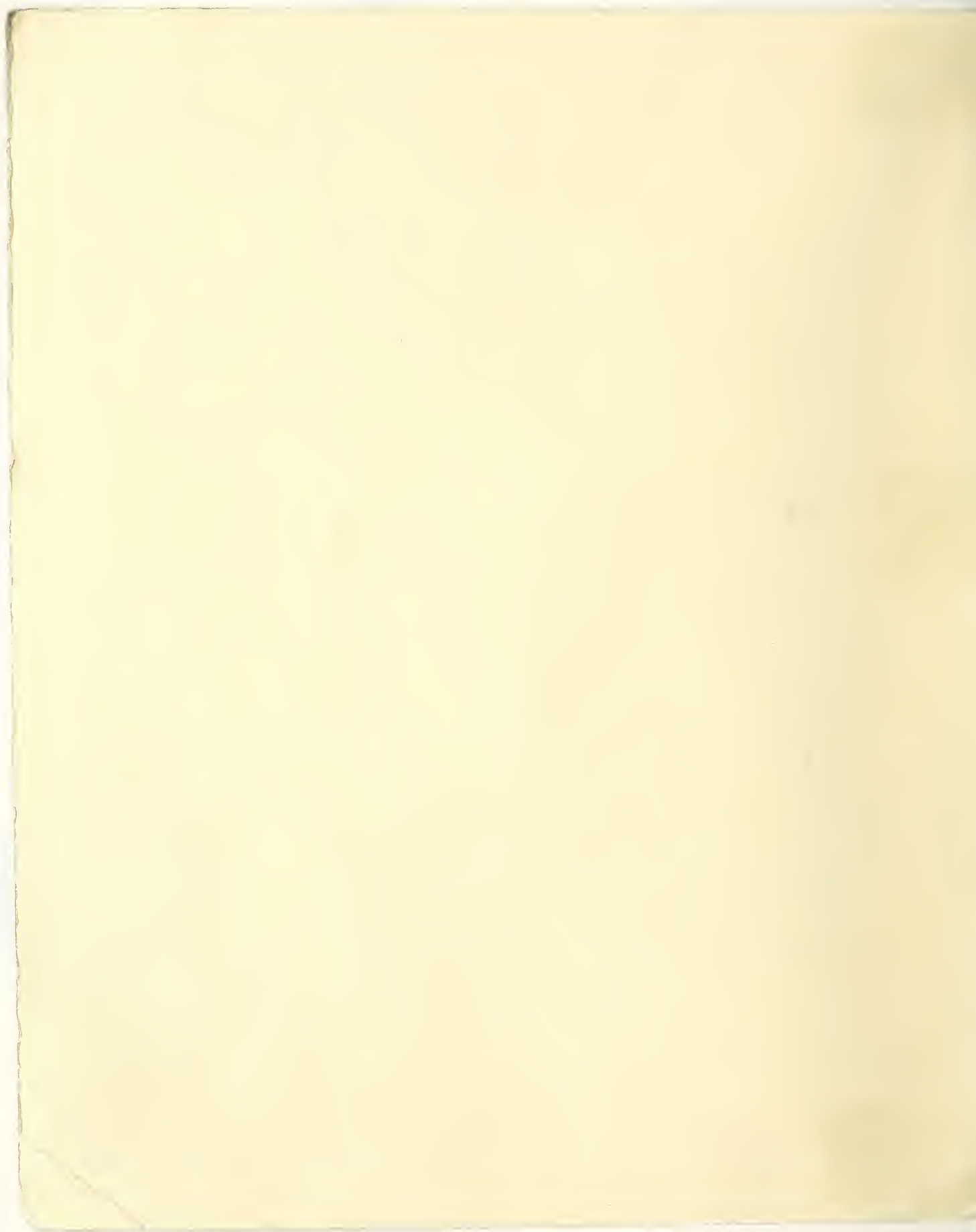
34 kHz



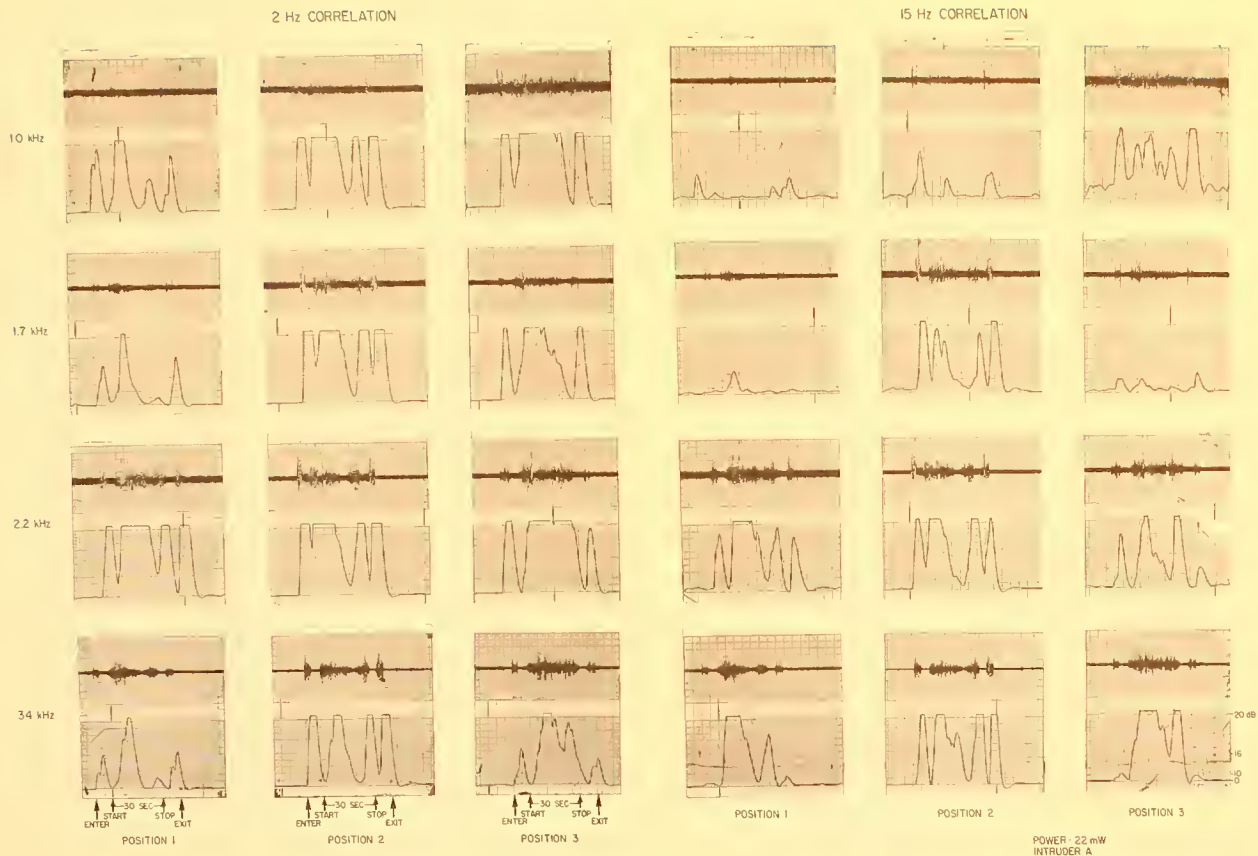
ENTER START 30 SEC STOP EXIT

POSITION 3

POSITION 1 - 22 mW
ER A



RECEIVER OUTPUT VS. CORRELATION

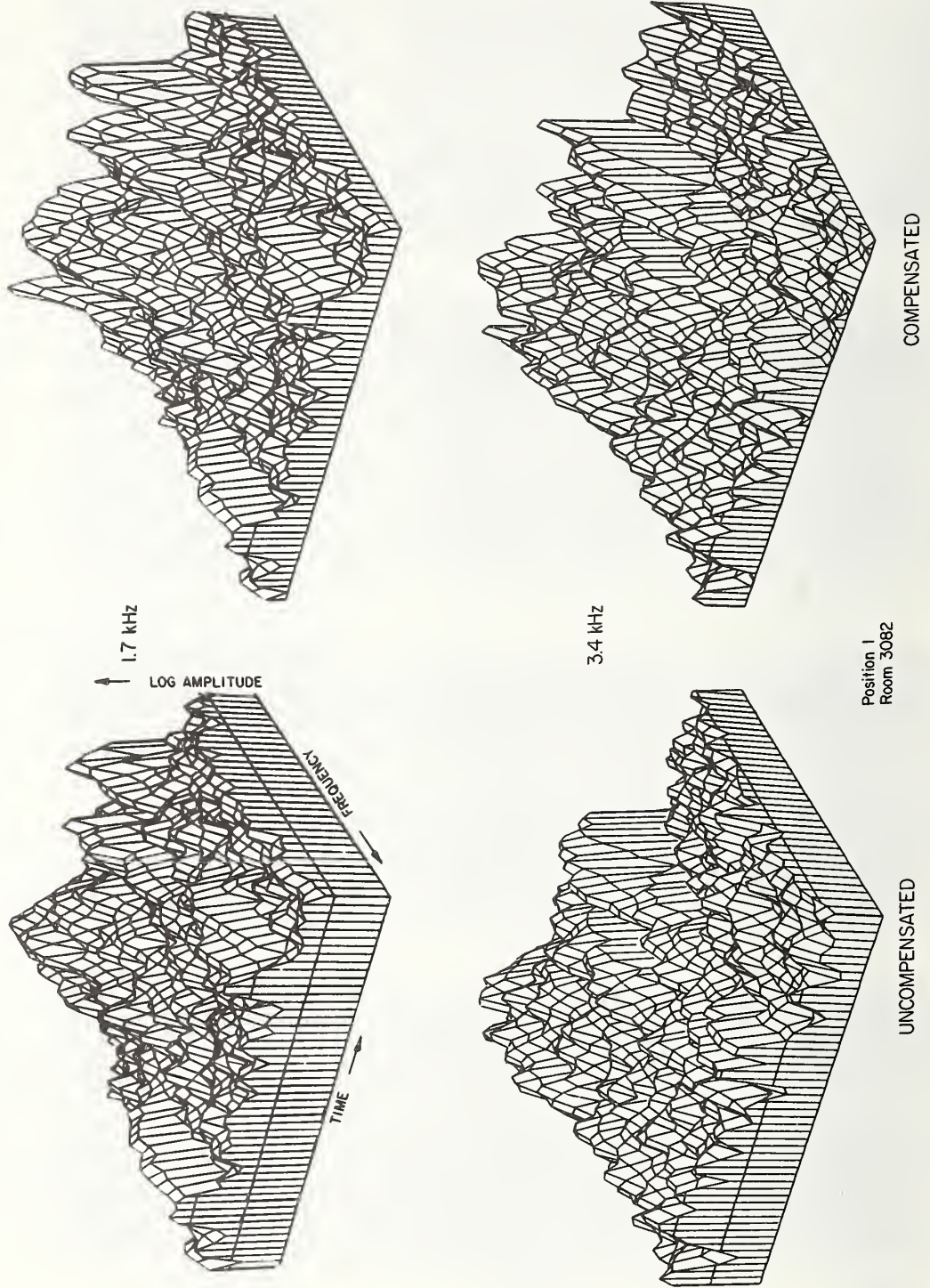


POWER - 22 mW
INTRUDER A

Room 3082

Figure 6.3

CORRECTED SPECTRAL DISPLAYS



Room 3082

Figure 6.2

It is apparent that correlation provides an adequate method of investigating the signatures and noise of all the tests. In fact, signal to noise ratio may be more easily determined from the correlations than from the spectral displays. This conclusion was confirmed by making the same comparison with tests conducted in the shop and auditorium.

An evaluation of the background noise supports the assumptions of section 1.2 describing the spectral composition of the noise. See the right-hand side of the displays in figures 6.1 and 6.2.

Note: If the limiting noise is ambient noise, the spectrum will be flat over the very narrow bandwidth of the receiver. If the limiting background noise is produced from environmental effects, the lower frequencies contain more power (see section 1.2.2).

During the tests, the ambient SPL was 14 dB at 1.0 kHz and 0 dB at 3.4 kHz (1 Hz BW). The 3.4 kHz spectral displays indicate a low frequency (< 3 Hz) response of about +10 to +15 dB with respect to the general spectrum response, thus indicating environmental effects. The noise spectrum at 1.0 kHz is nearly flat, indicating that any environmental effects have been swamped by the additional 14 dB ambient noise. The relative effect of ambient as opposed to environmental effects is examined further in later tests.

Both the spectral displays and the correlations indicate superior signal to noise ratio at the two higher frequencies. In order to determine if this was due completely to increased ambient noise at the lower frequencies, an analysis of the intruder signature magnitude was performed.

Intruder signature magnitude as a function of perturbation frequency with a 20% BW was measured for each carrier frequency and position.

Note: Throughout the remainder of this report the intruder signature magnitude is referred to as target strength. This value is the maximum Δ SPL produced by the presence of the intruder. Because the intruder signature is broadband, this parameter is listed for a specified bandwidth.

These data were corrected for receiver response and for the difference in microphone SPL to average room SPL (the receiver output is Δ SPL/SPL). The received SPL at the microphone will normally be different than the room average. All values from each carrier frequency were averaged, and the response

for each carrier frequency plotted in figure 6.4. Due to the corrections required, and the variations in SPL with which the intruder interferes as he traverses the room, this is not a precise measurement. It does, however, produce a general average with which to judge the validity of the assumptions concerning the effects of carrier frequency upon target strength.

The results of these measurements produced a peak of 6% modulation for carrier frequencies from 1.7 kHz to 5.0 kHz. This corresponds to a $\Delta\text{SPL}/\text{SPL}$ of -25 dB. The response at 1.0 kHz is nearly -5 dB with respect to the other frequencies. This loss of target return is attributed to a loss of effective scattering cross section as the acoustical wavelength approaches the dimensions of the target (see section 3.3). The cause of the increased target return at 0.25 Hz for 1.7 and 3.4 kHz while both 2.2 and 1.0 kHz drop is unknown at this point. It is suspected to be related to the particular intruder velocity and wavelength since similar response occurs at nominal harmonics.

Note: The target strength value at 0.25 Hz required a receiver correction factor of +27 dB. This, in addition to the problems of recording and analyzing these low frequencies, reduces our confidence in this data point.

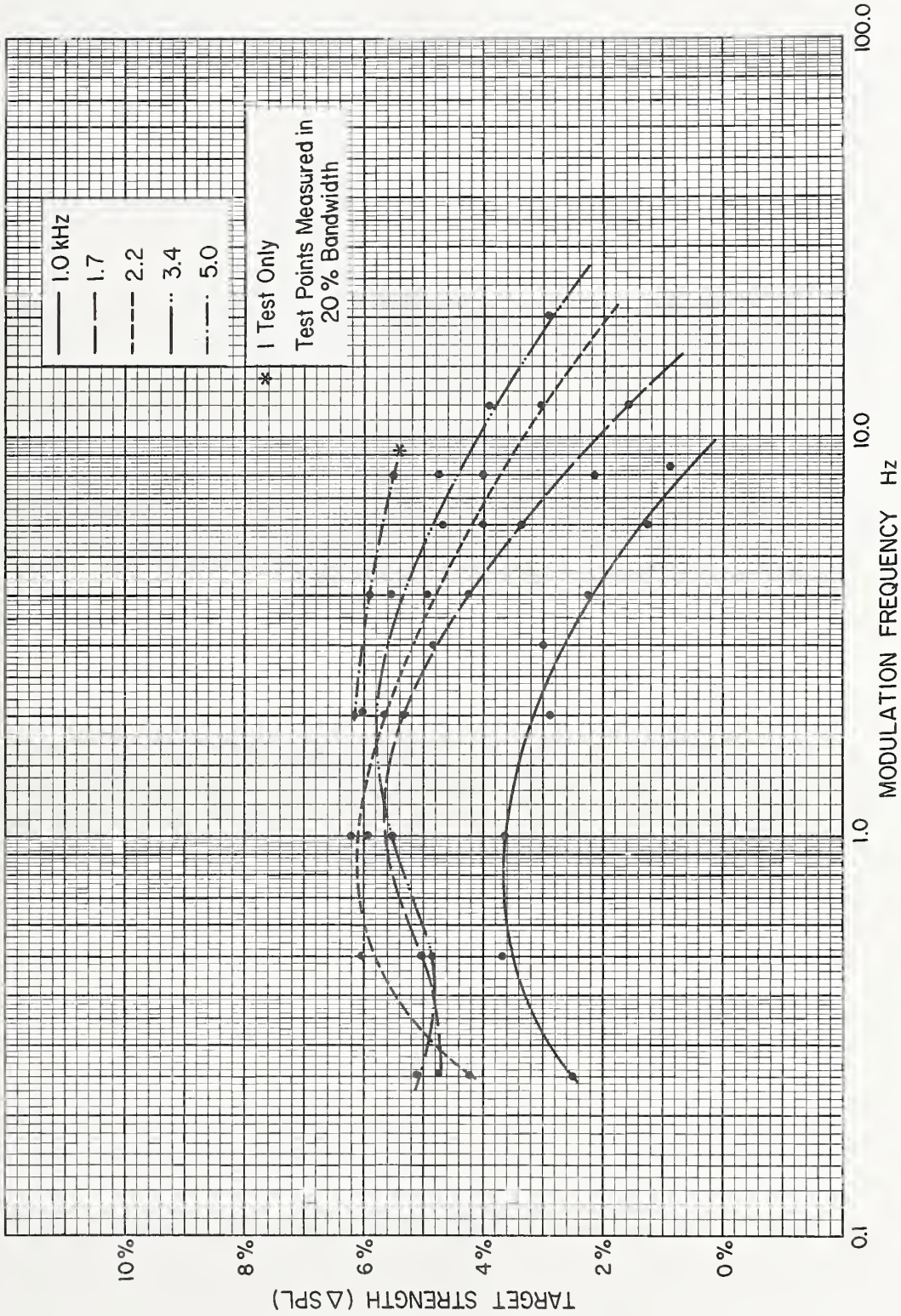
The assumed spectral dependence of the signature upon carrier frequency was shown in both the spectral and correlation displays (figs. 6.1 and 6.2). Very little high frequency response (except for the door operation) is indicated at 1.0 kHz, while all microphone positions show increasing high frequency response with increasing carrier frequency.

Note: Spectral plots display log power in 1 Hz bandwidth while target strength is plotted as voltage in 20% BW so direct comparisons cannot be made.

6.3 Conclusions

The goals of this test series was satisfactorily achieved. The intruder signature was identified as broadband, peaking at relatively low frequencies (1-8 Hz). The intruder signature frequency response is roughly proportional to carrier frequency.

TARGET RETURN VS. CARRIER FREQUENCY



Room 3082

Figure 6.4

The noise spectrum agreed completely with the hypotheses stated in section 1.2. The environmentally produced noise spectrum is highest at very low frequencies and decreases with increasing frequency. If the ambient noise becomes the limiting factor, the receiver output noise spectrum is flat over the range of interest.

The validity of using a correlator as a general data analysis tool was confirmed. This allowed a larger number of tests for a given time and fund restriction.

The most significant result of the test series was the absolute detection from all microphone positions throughout the entire room. All subsequent tests were planned for larger volumes to enable a more detailed comparison.

The analysis of the intruder target strength indicated that the 500 Hz tests were not required. Target return at 1.0 kHz was nearly -5 dB with respect to the other four frequencies. Adding to the reduced target return is the increased ambient noise which further reduced the signal to noise ratio.

7.0 INTRUDER TESTS, NBS AUDITORIUM

A total of 67 intrusion tests were conducted at five carrier frequencies on five separate occasions. These tests examined the spectral content of both the intruder signature and the noise, with respect to carrier frequency. Ambient and environmental noise were examined in detail for their individual effects. In addition, the effects of intruder velocity, sonification source, geometry, intruder size, and multiple intruder actions were investigated.

7.1 Test Description

All tests which are analyzed in this section were conducted in the NBS Auditorium. The microphones and speakers were placed as shown in figure 5.2. Microphones one and three were taped to the walls 2 meters from the floor, while microphone two was taped to the back of a seat with the sensing portion approximately 15 cm above the seat back. Two speaker positions were used; in geometry A the sound source was placed upon the seat arms while in geometry B the sound source was set on a box about 2 meters above the stage floor. No pre-selection of speakers or microphones was used for any test.

The instrumentation was set up outside the auditorium for the first test series. It was placed in the projection booth in the remaining test series so that the intruder action could be observed.

Unless noted differently, each intrusion consisted of the following: the intruder entered the right auditorium door, waited 5 seconds, walked down the right aisle, paused 5 seconds at the stage, walked across the front, paused again for 5 seconds, walked up the left aisle, waited 5 seconds and then exited.

Two intruders were used: intruder A, weighing 70 kgm, and intruder B, weighing 100 kgm. Intruder velocity was nominally 0.9 m/sec.

This test area provided a nearly unobstructed volume which would, in theory, produce a minimum of standing wave fluctuations due to the lack of reflecting surfaces. It is extremely large in volume due to the high ceiling. The room also provided an area with few non-rigid surfaces such as windows and doors. The ability to conduct a large number of tests at 3.4 kHz can be attributed to the latter feature.

7.2 Test Results and Analysis

The various types of tests are separated into individually headed sections.

7.2.1 Intruder Signature Analysis

The intruder signature spectrum was analyzed as a function of carrier frequency to determine if the spectral character exhibited in room 3082 would be confirmed in an entirely different test area. Several intrusions were conducted at 1.0, 1.7, 2.2 and 3.4 kHz. Tests at 5.0 kHz were attempted on several occasions but signal stability was poor, and the results were not repeatable.

A spectral analysis of the signature from position 2, geometry B, of these tests is presented in figure 7.1. The signature frequency response shows a clear carrier frequency dependence. In geometry B the intruder passes directly between the speaker and position 2 when passing in front of the stage, so the two aisle traverses are most representative



of the response. At 3.4 kHz the response shows very little decrease for the four correlated frequencies (2, 4, 10, 15 Hz), while at 1.0 kHz no response is indicated at 10 or 15 Hz. The response at the two intermediate carrier frequencies is approximately proportional to the carrier frequency ratio.

An examination of the noise from these tests clearly supports the hypothesis presented in section 1.2 and the results from room 3082. At 1.0 kHz, the noise level is nearly the same at all correlated frequencies indicating that ambient noise is the predominant limiting noise source. At 3.4 kHz, the noise at 2 Hz is approximately 3 dB greater than the 2 Hz noise at 1.0 kHz. At 15 Hz, the noise from 3.4 kHz is at least 3 dB less than that observed at 1.0 kHz. The higher noise at the lower frequencies implies that the environmental effects produced the noise.

7.2.2 Sonification Level vs. Noise and Intruder Signature Magnitudes

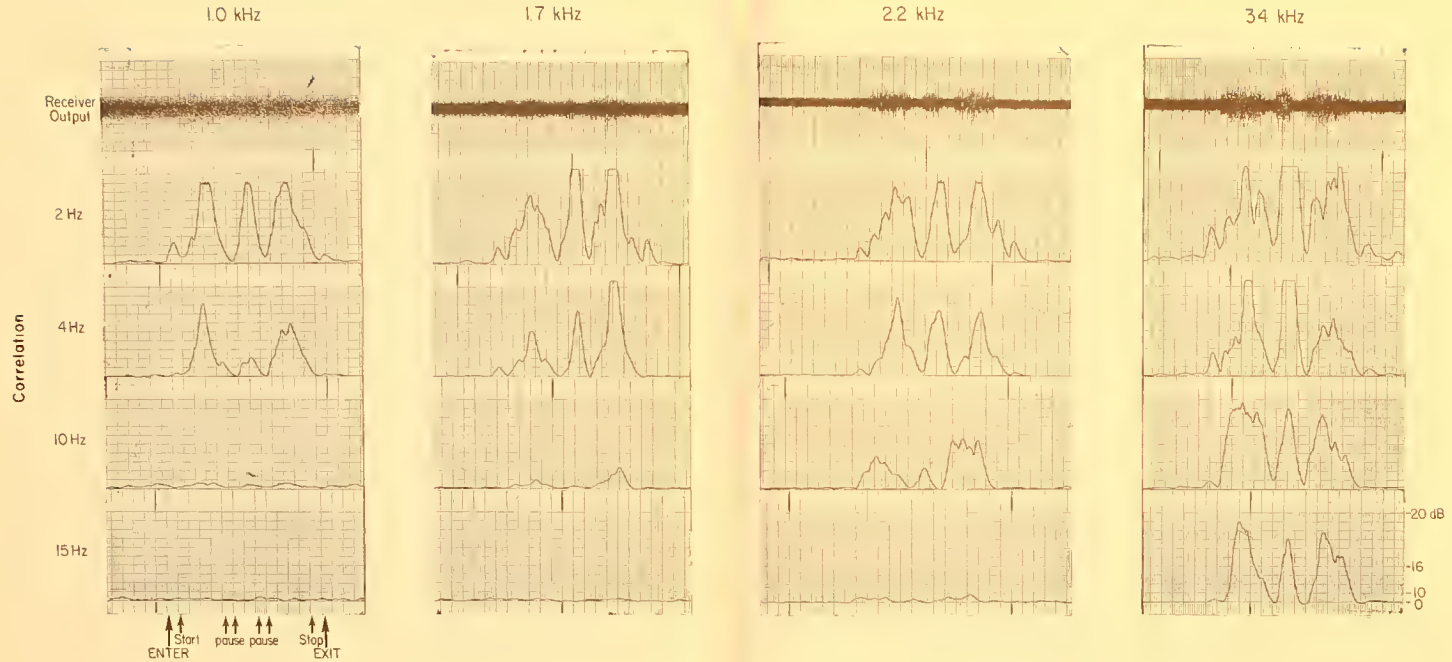
These tests were conducted to verify that the effect of ambient noise could be reduced while that produced by environmental effects would be unaffected by increasing the source level. A second purpose was to establish the independence of intruder magnitude with respect to source levels.

The results of the tests are shown in figure 7.2. Three source levels were used for the tests at 3.4 kHz. The results at 3.4 kHz are used to provide environmental noise levels sufficient to demonstrate the principle.

Very little increase in noise level is evidenced when reducing the input electrical speaker power from 60 to 15 mw. Independent measurement of the noise indicated nominally 2 dB change at 4 Hz with no change at all at 2 Hz. When the power was further reduced to 9 mw, a significant increase in the noise is encountered at all correlated frequencies. The results of the environmental noise are still evident at 2 Hz indicating that the ambient noise has not become the total limiting source of noise. The correlator output is the summation of all signal energy present.

An independent noise analysis was also performed to determine the agreement of measured and calculated noise levels. Tests were conducted at 2.2 kHz with four power levels. The results are as follows:

INTRUDER SIGNATURE SPECTRAL DEPENDENCE VS CARRIER FREQUENCY



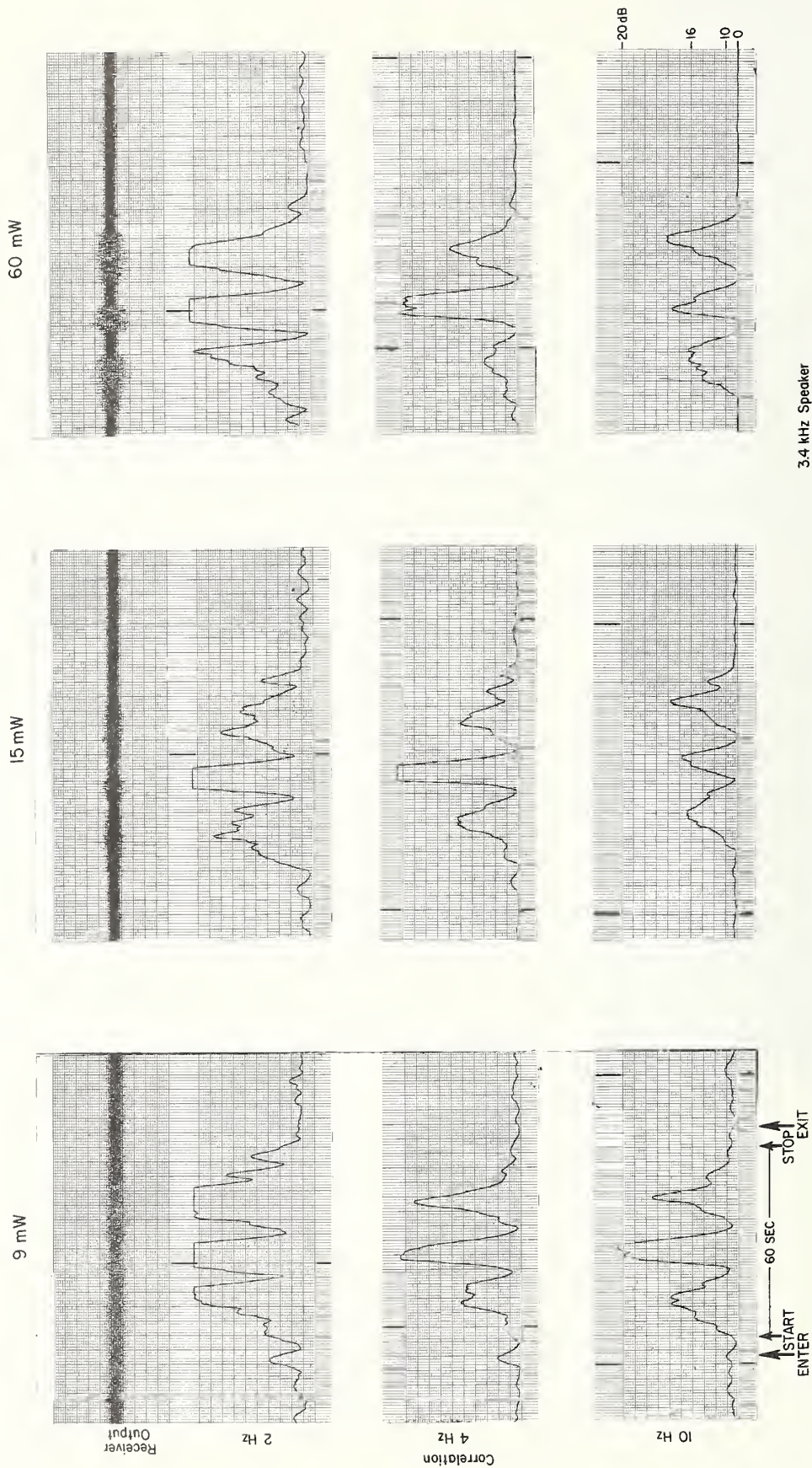
NBS Auditorium

60mW Speaker
Position 2 - Geometry B
Intruder A - 70 kg
1Sec/Division

Figure 7.1



SONIFICATION VS. NOISE AND INTRUDER SIGNATURE



3.4 kHz Speaker
 Geometry B - Position 2
 Intruder B

NBS Auditorium

Figure 7.2

Speaker Input Power	SPL	Indicated Noise (1 Hz BW) From the Receiver	
		10 Hz	2 Hz
960 mW	70 dB	40 mV PP	200 mV PP
240	65	50	200
60	58	100	240
15	51	175	280

Note: The receiver output sensitivity is 1 volt for each 3.5% change in the ratio of $\Delta\text{SPL}/\text{SPL}$, which in this case is N_A . Thus, for constant ambient noise, the indicated noise will decrease as the SPL produced by the source is increased.

Ambient noise level was 29 dB or 0.0055 ubar in a 1400 Hz BW (0.00015 ubar in 1 Hz BW). At 15 mW the sonification SPL was 51 dB or 0.07 ubar. From section 1.2.1, $N_A = \text{SPL}_{\text{AMB}}/\text{SPL}_{\text{SONIFICATION}} = 0.00015/0.07 \times 100 = 0.21\%$. The receiver-indicated noise was 175 mV PP, or 62 mV RMS. The receiver sensitivity is 3.5%/V. Indicated noise is therefore $3.5\%/V \times .062 = 0.22\%$

No attempt to justify the close agreement is offered, due to the multiple corrections and assumptions required to perform this calculation. These include the record levels, receiver calibration, and the assumption for calculation purposes that the measured ambient noise was flat over the bandwidth. If the calculations are compared at 60 mW there is an error of about 3 dB.

The noise at 10 Hz dropped approximately 6 dB for each 6 dB increase in power, except for the final increase. This indicates that environmental effects have become predominant at 70 dB. At 2 Hz there is very little noise level change with increasing power, indicating that the environmental effects are predominant.

The intruder signature magnitude shows negligible changes at each of the three source levels considering that they are the results of three separate intrusions. As expected, the 9 mW signature magnitude is somewhat higher, again due to the correlator indicating the summation of both signal and noise.

Intruder signature is again shown as a function of source level in figure 7.3 with the horn as the source in these tests. Two input power levels are shown, and no change in the intruder signature is demonstrated. The noise level did not change, indicating that environmental noise is predominant at these levels.

7.2.3 Intruder Signature as a Function of Source and Receiver Characteristics

The absence of change in the intruder signature with respect to the sonification source and the type of microphone preamplifier are shown in figures 7.4 and 7.5.

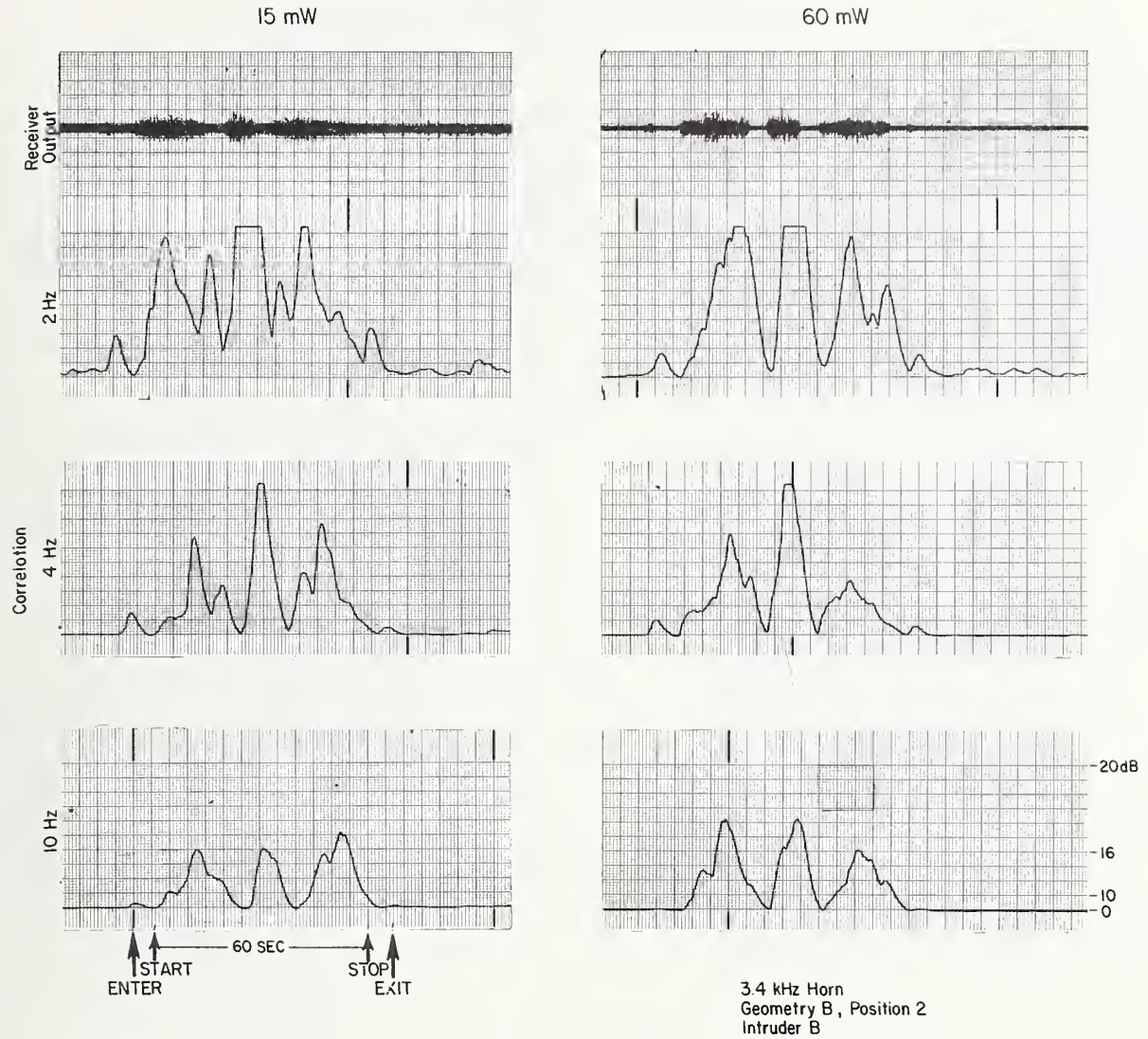
A comparison of the intruder signature and noise when the sound level meter was substituted for the microphone and preamplifier is shown in figure 7.4. The sound level meter was substituted for the microphone and preamplifier and the recorder output was used as the receiver input. Duplicate intrusions were conducted. No significant change in the signature is indicated, while the noise actually increased slightly. The increase was not evidenced in other comparisons and is attributed to a change in the environment for that test.

The results of the direct substitution of the exponential horn for the speaker are shown in figure 7.5. The horn consistently produced higher sonification levels for equal electrical input, so the input power was adjusted for nominally the same acoustical levels as measured with the sound pressure level meter. Some differences were expected from the directional effects of the horn, but little is indicated.

The computer-produced spectral display does indicate a higher 1 Hz peak from the horn at the instant the intruder passed directly in front of the source.

This lack of change in signature when the directivity of the source is changed radically is attributed to the multiple reflections producing an extremely complex standing wave pattern. The standing wave pattern probably becomes somewhat independent (in average magnitude and complexity) of the source characteristics when examined at points remote from the source position.

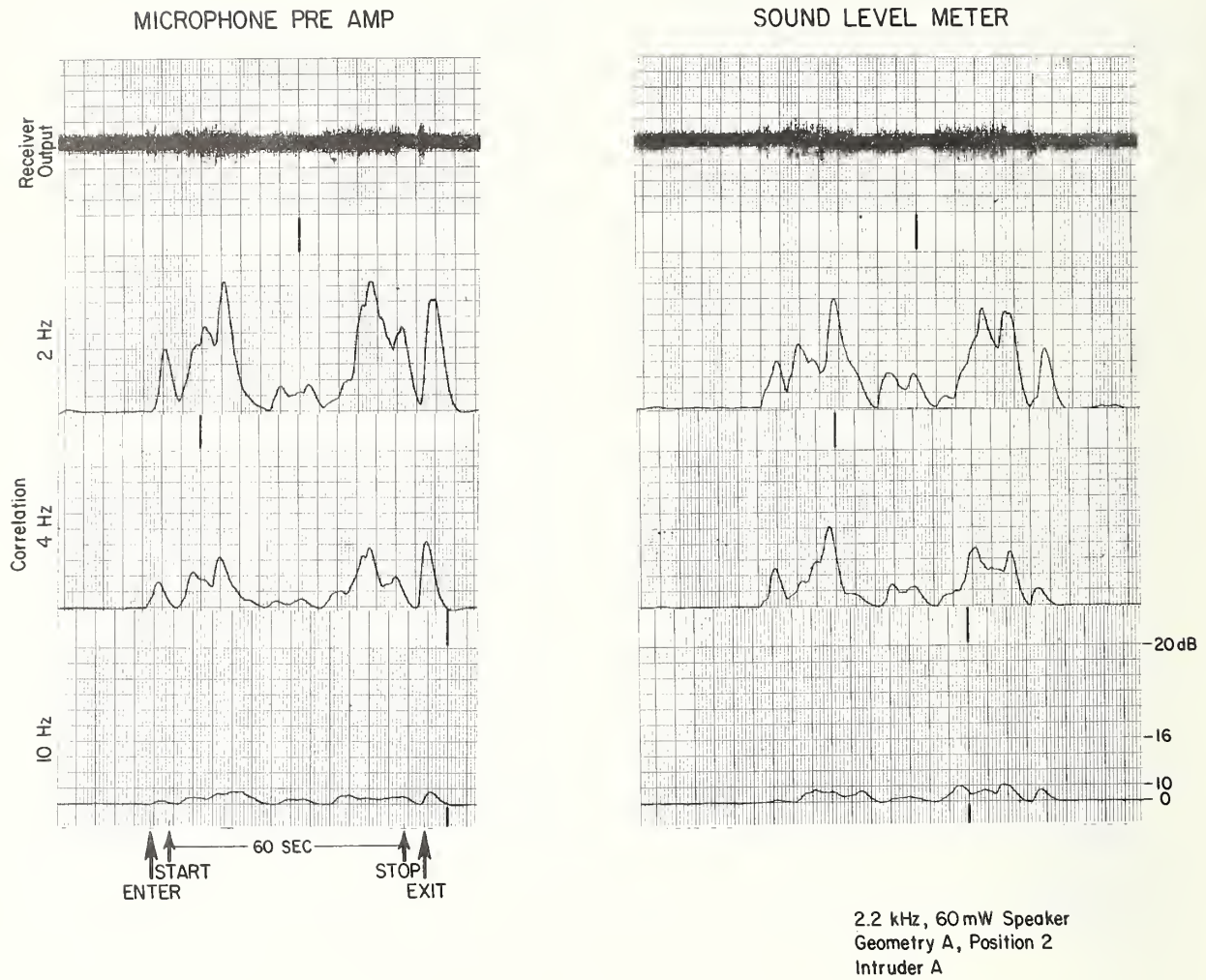
SONIFICATION VS. NOISE AND INTRUDER SIGNATURE



NBS Auditorium

Figure 7.3

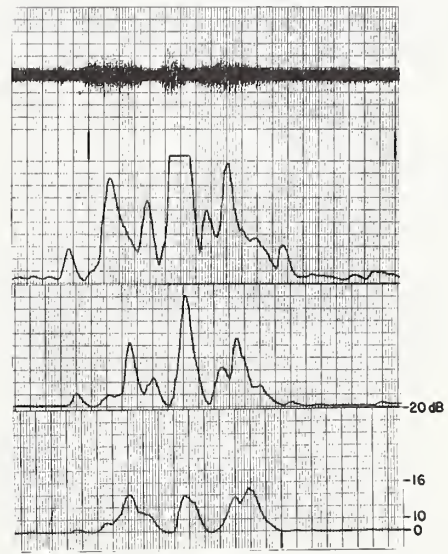
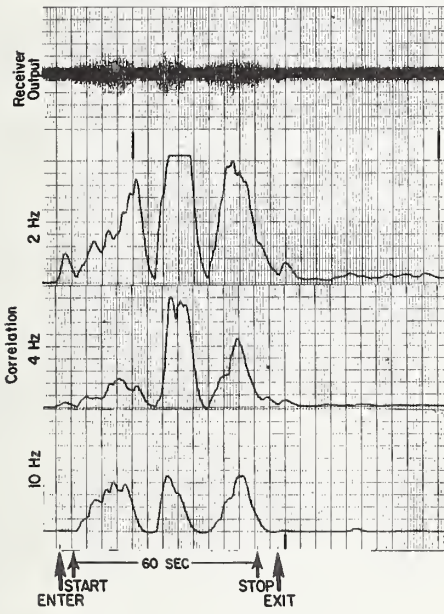
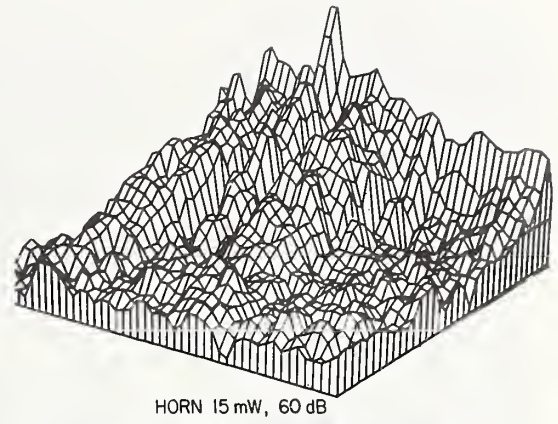
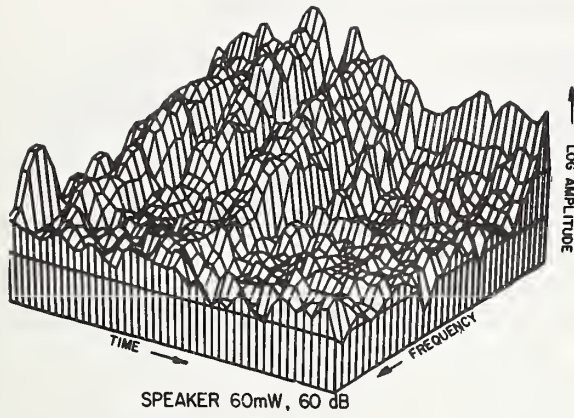
INTRUDER SIGNATURE
MICROPHONE PRE AMP VS. SOUND LEVEL METER



NBS Auditorium

Figure 7.4

INTRUDER SIGNATURE - SPEAKER VS. HORN



34 kHz, Intruder B
Geometry B, Position 2

NBS Auditorium

Figure 7.5

7.2.4 Detection as a Function of Geometry

The effects of the microphone and speaker placement are shown in figure 7.6. In each of the tests, the results from these microphone positions are compared. Three tests are shown: in the first two a common geometry was used and two frequencies were compared; while in tests two and three, the effect of changing the source from geometry A to B is compared.

In each test, the results from position two were nearly symmetrical. This was expected, since the geometry is symmetrical with the room. In positions one and three, the maximum detection occurred when the intruder was traversing the aisle closest to the respective microphone. The difference in detection from one side to the other for a given intrusion was not large, nominally 3-4 dB.

There appears to be a small detection improvement using geometry A, which can be attributed to the fact that the auditorium acoustics are designed for minimum reflections when the sound source is in front. The reduced number of reflections should reduce the standing wave complexity, and hence, the intruder signature. Most tests were conducted in geometry B so as not to take advantage of this fact.

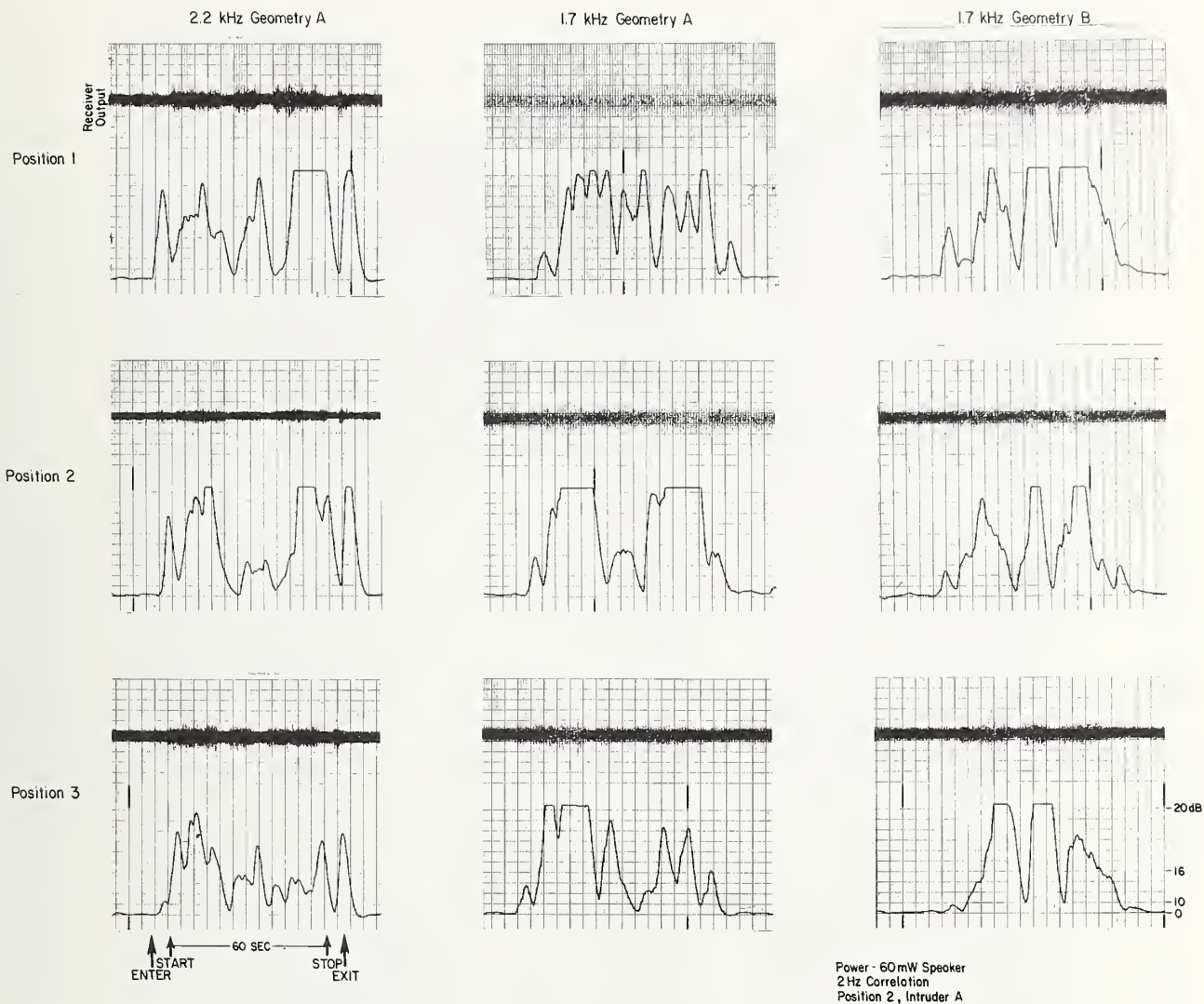
7.2.5 Spectral Distribution vs. Intruder Velocity

Tests were conducted to determine if there is a direct dependence of the intruder spectrum upon the intruder velocity. The results of one of these tests are shown in figure 7.7. The intruder velocity was reduced to 0.4 meters/sec and compared directly with a standard intrusion of 0.9 meters/sec. At the reduced velocity, the response at 10 Hz was nearly nonexistent. The response at 2 Hz was approximately the same, and detection occurred for the entire intrusion. The response at 4 Hz was slightly reduced.

7.2.6 Intruder Size Comparison

The effect of the intruder size upon effective target return was investigated in 6 tests. The results of two of these tests are shown in figure 7.8.

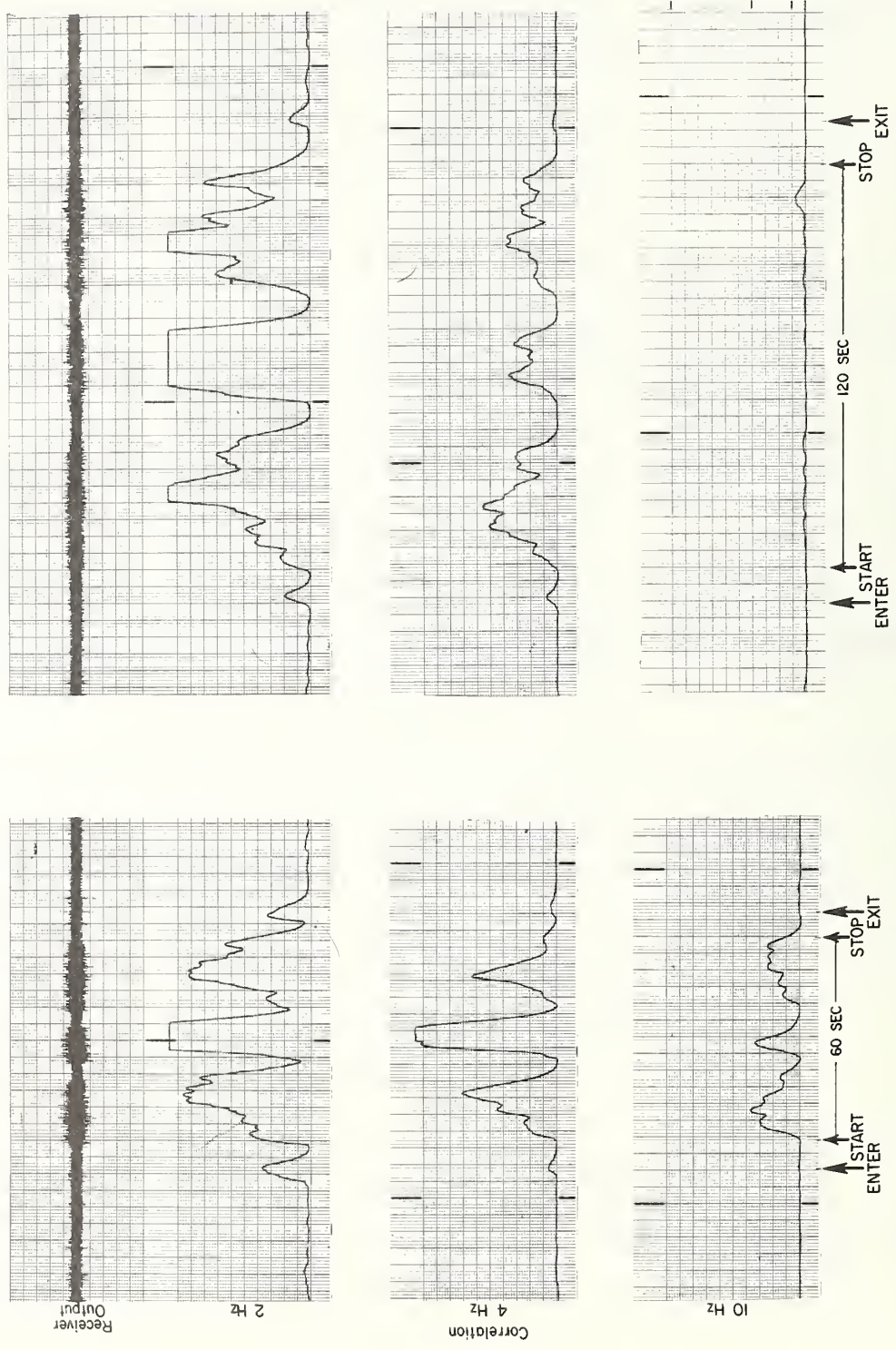
DETECTION VS. GEOMETRY



NBS Auditorium

Figure 7.6

INTRUDER SIGNATURE VS. INTRUDER VELOCITY



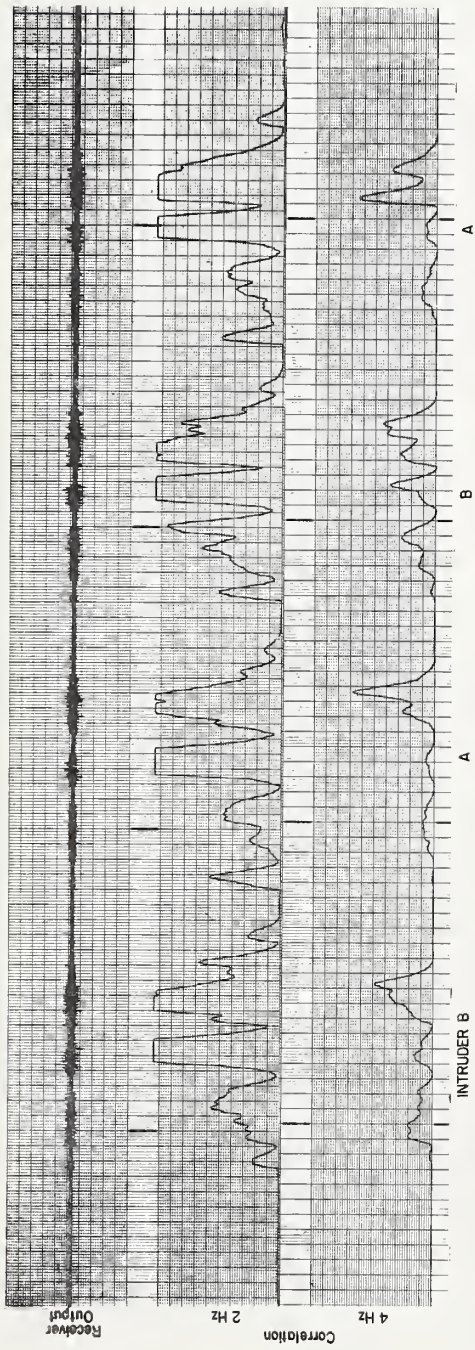
2.2 kHz, 60mW Horn
Geometry B, Position 2
Intruder B

NBS Auditorium

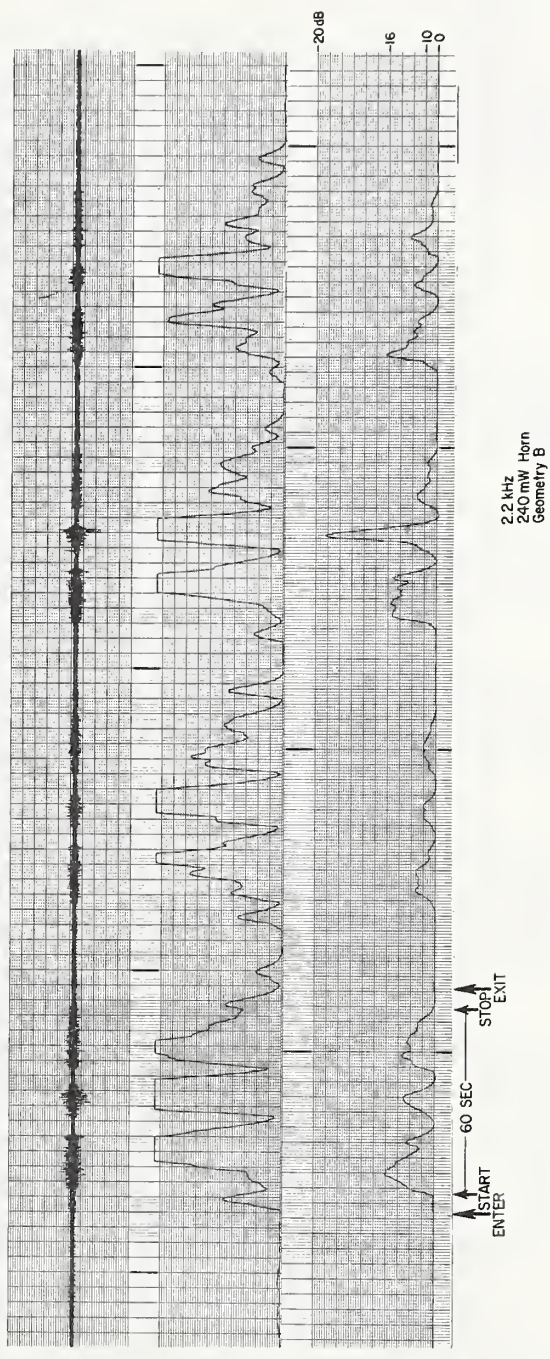
Figure 7.7

INTRUDER SIGNATURE VS. SIZE COMPARISON

POSITION 1



POSITION 3



NBS Auditorium

Figure 7.8

In each, the intruder conducted two intrusions to test repeatability. The repeatability was very good at 10 Hz for all comparisons. Some small variations in the 2 Hz response occurred.

At 10 Hz, there appears to be about a 3 dB increase in target return from the large intruder. There is a definite increase in target return at 2 Hz also; however, it does not appear to be as large. Integration of all the energy under the curve would be required to provide a precise answer.

7.2.7 Additional Exploratory Tests

In addition to the tests required to satisfy the goals of the program, several additional tests of a feasibility nature were conducted.

Four tests were conducted in which a radio was turned on and the spectral content of the receiver output examined. The radio was -6 dB with respect to the sonification level (broadband) as measured with the sound pressure level meter.

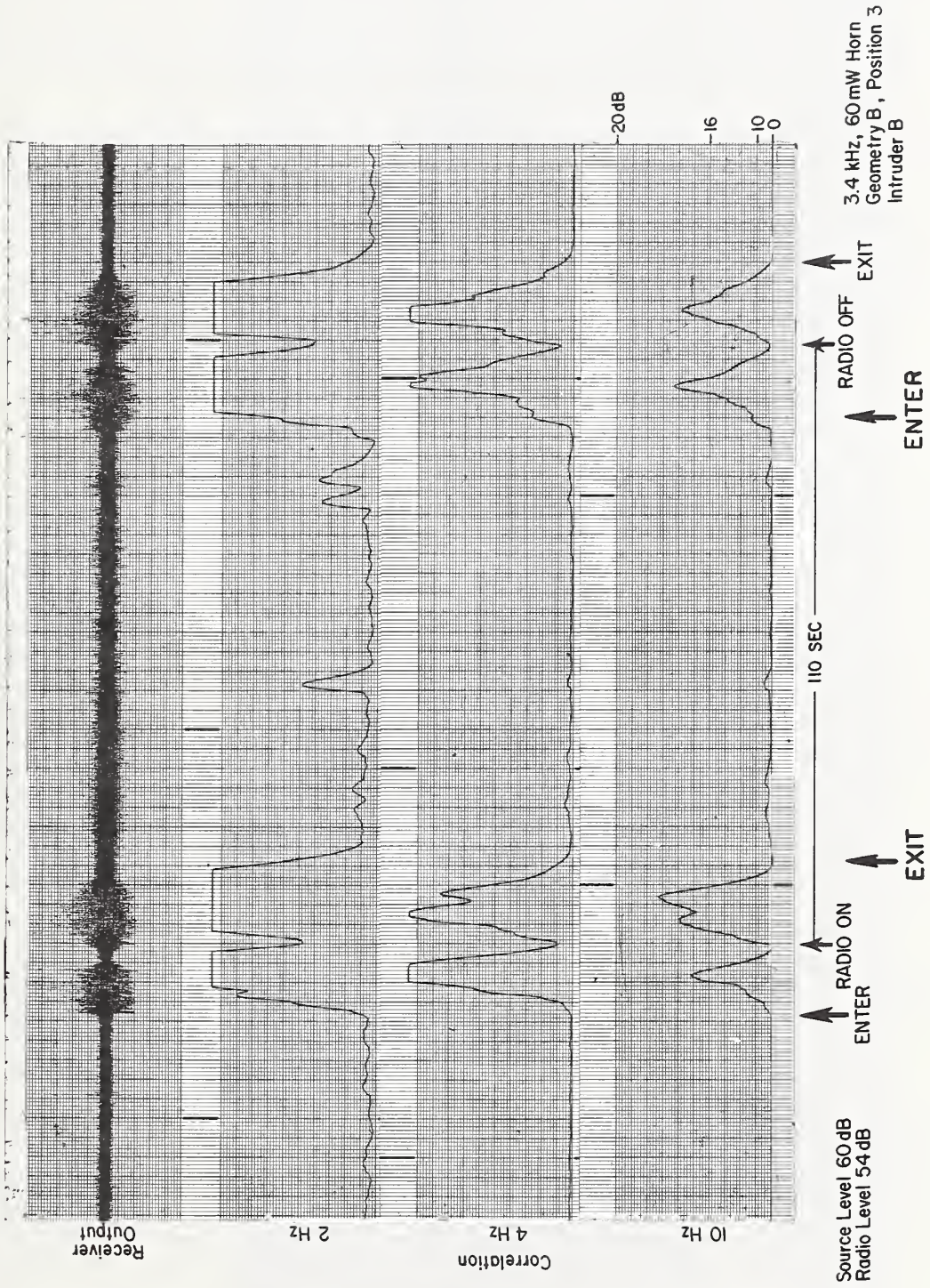
The effects of one test are shown in figure 7.9. The intruder entered the auditorium, walked to the front, and turned the radio on and then exited. After 110 seconds he returned, shut the radio off, and again exited.

The purpose of the test was twofold. If exterior broadband noise were coupled into the protected area, it could produce false alarms. The results of this test, however, indicate a minimal increase in noise level and certainly not of the same character as that of an intruder.

The second purpose was to investigate the possibility of masking the sonification energy for producing a nominally covert system. Even in this test, in which the radio spectrum was not filtered at the source frequency, it appears likely that a system could be produced in which the sonification energy would go unnoticed by a casual intruder. That is, if desired, a radio could be used to prevent the intruder from being aware of the alarm system.

A second test is shown in figure 7.10 in which the intruder performed a random pattern of movements. The horn was used for a sonification source. The intruder action is noted and will not be discussed except to comment on the

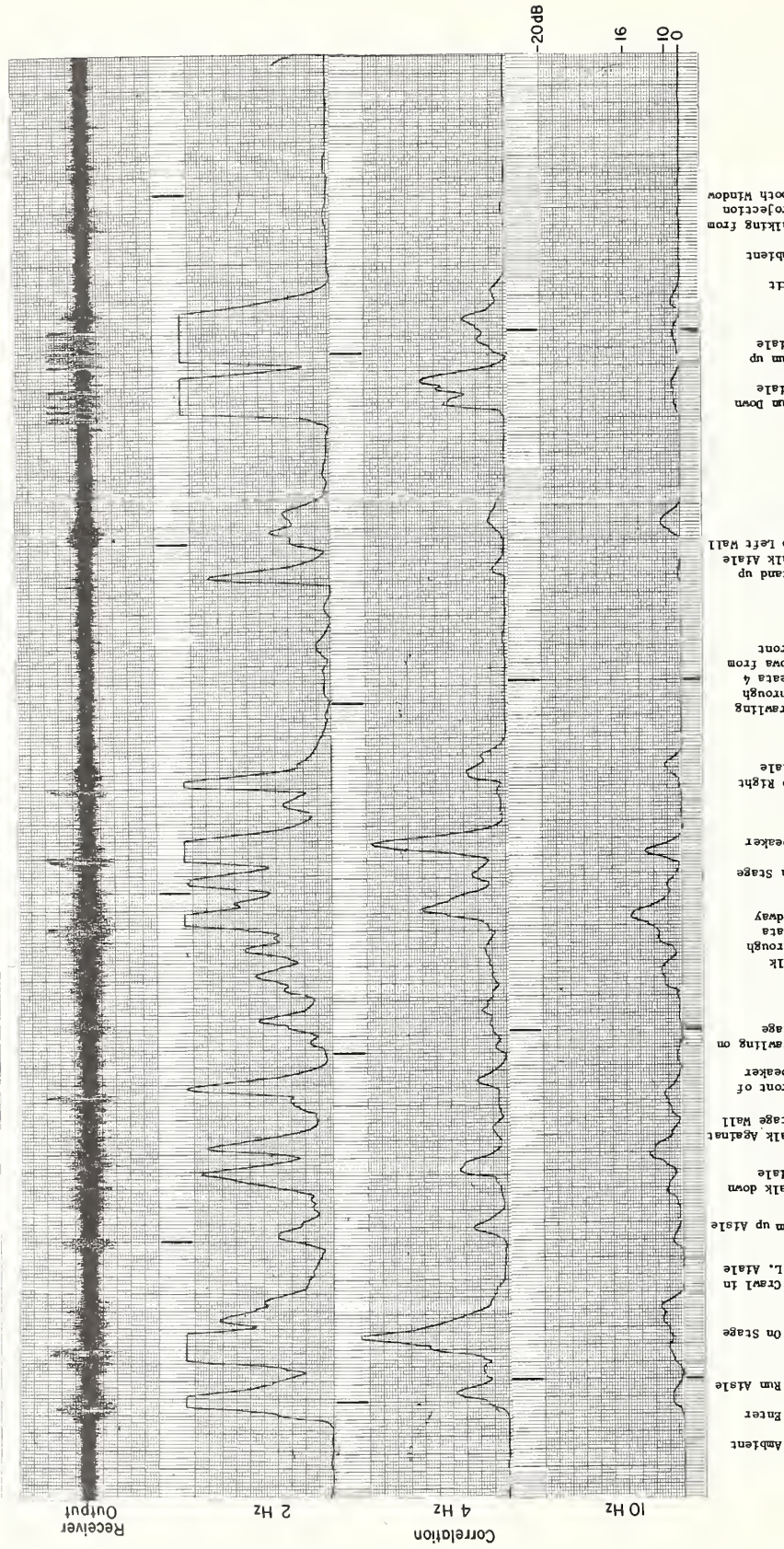
RADIO EFFECTS UPON INTRUDER DETECTION



NBS Auditorium

Figure 7.9

RANDOM INTRUDER ACTIONS



2.2 kHz, 60mW
Position I, Geometry B
Intruder B

NBS Auditorium

Figure 7.10

section in which the intruder was crawling between the seats. Although the signal to noise ratio during that part of the test was low (3-4 dB), the equipment was not designed to detect low frequency modulation which is a characteristic of slow movement. A low frequency correlator would be desirable to take advantage of the reduced velocity.

In addition to these tests, an experiment was conducted in which an arm was extended through the projection booth window and waved. No effect was observed at 1.7 kHz, minimal at 2.2 KHz, but was quite noticeable at 3.4 kHz. The susceptibility to small object movement indicates that for any environment with small animals such as mice, rats, or cats, lower operating frequencies would be more desirable.

7.3 Conclusions

The results of these tests provided data which supported all of the initial concept described in section 1.2 and the analysis. The spectral dependence of the intruder signature agreed completely with the measurements from room 3082. However, no loss of target strength at 1.0 kHz was found in the auditorium as had been the case in room 3082. No tests were conducted at 500 Hz, which was selected in section 3.2 to be the probable lower limit for uniform target return. Target return magnitude measurements are rather difficult to perform because the receiver measures Δ SPL of the standing wave pattern. In this case, P is the SPL measured at the microphone position. It is unlikely that this value will equal the SPL average for the room. A correction for this difference must be added when calculating absolute target return values. The accuracy of the average room SPL measurements is estimated to be no better than 3 dB.

Reliable receiver operation at 3.4 kHz occurred in the auditorium. This is attributed to a solid and unobstructed room, where environmentally produced signal changes were relatively small.

The results of the noise tests indicate that the factor limiting detection will be environmental noise, even with reasonably low sonification pressure levels. No significant increase in noise was detected in the auditorium at 3.4 kHz until the electrical power to the speaker was reduced to 15 mW, which produced a SPL of about 54 dB.

The analysis at 2.2 kHz also indicates that sonification levels of 60-66 dB provide adequate power to mask ambient conditions.

8.0 INTRUDER TESTS, NBS INSTRUMENT SHOP

Four test series were conducted in the instrument shop consisting of 57 intrusions. The general parameters examined were the same as for those tests conducted in the auditorium (section 7.0).

8.1 Test Descriptions

These tests were conducted to determine the effects of a very complex environment. This room was considered likely to be a difficult area to protect, because its 3:1 length to width ratio and, because of the presence of a number of very sizable machines. In addition, the entire length of outside wall consists of windows, which provides a flexible surface. Three large double doors are also subject to vibration and provide little attenuation path to the noise occurring in the hallway. The instrumentation was set up in a small room at the far end of the shop area. The small room is enclosed with windows, thus allowing the operator to view the area.

The microphones and speakers were placed as shown in figure 5.3. Three geometries were used; in A the microphones were placed on the center posts while in B and C they were attached to the outside wall 3 meters from the floor. In geometry A and B, the speaker was placed on a cabinet 1.5 meters from the floor, but it was moved to the far end for geometry C. No preselection of speakers and microphones was used prior to the tests.

In each test the intruder exited the small room, waited 5 seconds, began the traverse as shown, pausing 5 seconds prior to reentering the room. The intruder made a complete trip from one end of the shop to the other.

The same two intruders were used, A at 70 kgm and B at 100 kgm.

8.2 Test Results and Analysis

The following sections describing the test results in the instrument shop are divided into sections containing similar tests.

8.2.1 Intruder Signature Analysis

The intruder signature spectrum was again analyzed as a function of carrier frequency in geometry B, position 1. The results of these tests are shown in figure 8.1. which includes both computer spectral displays and individual correlated frequencies. Tests at 5.0 kHz were attempted on several occasions but none were even completed, due to signal instability. The tests at 3.4 kHz were also difficult to perform for the same reason. The effects of the environment in this area were much more pronounced than those encountered in the auditorium.

The results of the spectral analysis support the previous results of both the auditorium and room 3082. The response is nearly proportional to the carrier frequency. As in the auditorium, there is no clear evidence of target return loss at 1.0 kHz. However, a comparison made in geometry A (fig. 8.2) indicates a loss of about 3 dB. As noted in section 7.0, the measurement is difficult to perform. An added problem is evident from the oscillatory nature of the response as shown in figure 3.2. Small changes in the circumference/wavelength will produce changes of 3 dB in the effective scatter.

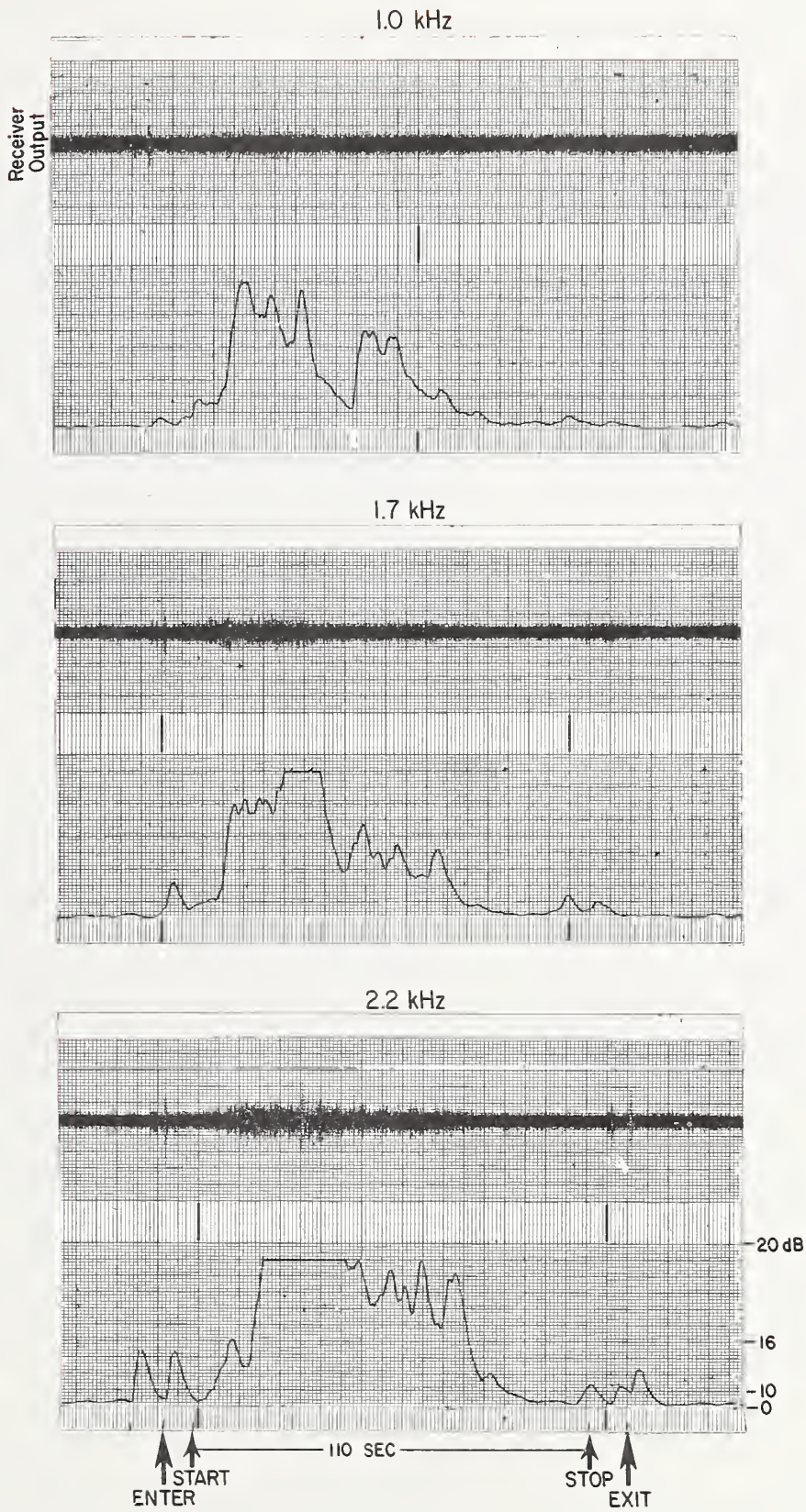
The background noise is very similar to that encountered in the auditorium with the exception of an increase in environmental noise at 3.4 kHz which would be expected from the large window area. Ambient noise was measured at microphone position #1 and found to be +26 dB at 3.4 kHz, somewhat lower than the general results in section 3, but very near that of the auditorium. Noise at microphone position #2 was 34 dB and at position #3 was 37 dB.

8.2.2 Sonification Level vs. Noise and Intruder Signature Magnitude

Tests were again conducted to verify that the effects of ambient noise could be reduced by increasing the sonification level. The results of these tests are shown in



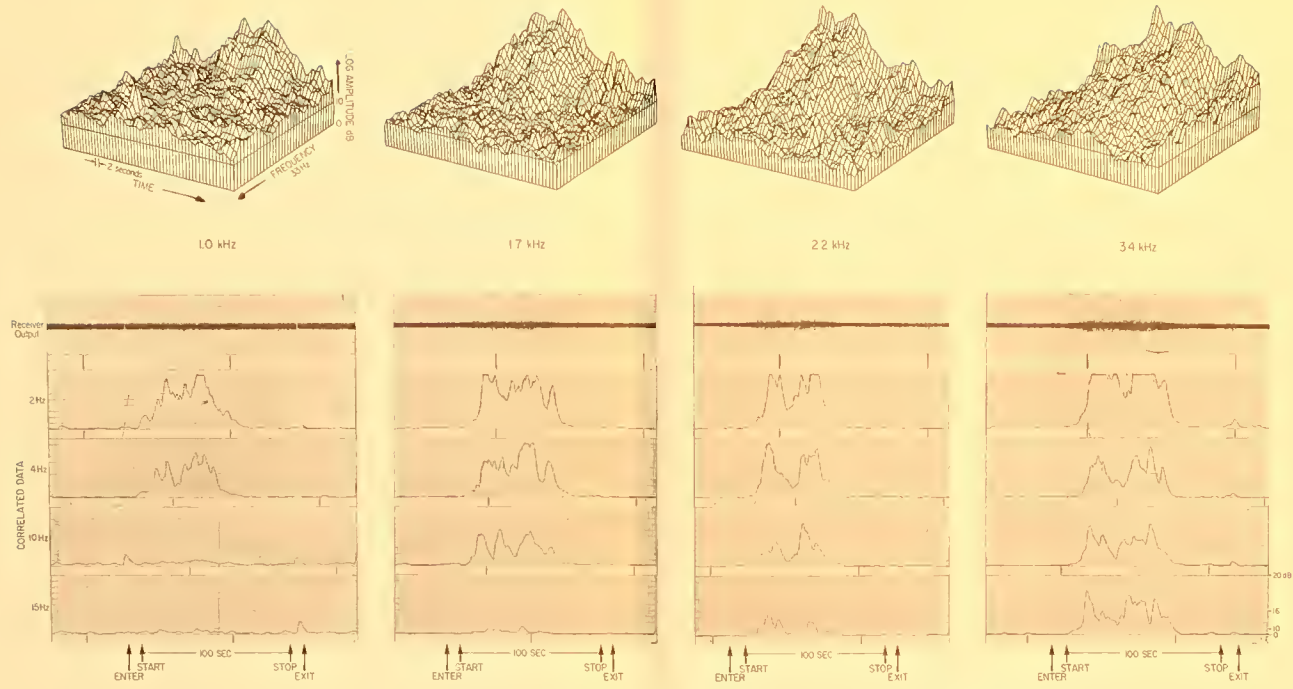
TARGET STRENGTH AS A FUNCTION OF FREQUENCY



Instrument Shop

Figure 8.2

INTRUDER SIGNATURE SPECTRAL DEPENDENCE VS. CARRIER FREQUENCY



Instrument Shop
Figure 8.1

Correlator adjusted to compensate
for receiver bandwidth
Intruder B - 100 kg
Electrical power - 62 mW
Average acoustical level - 55 dB

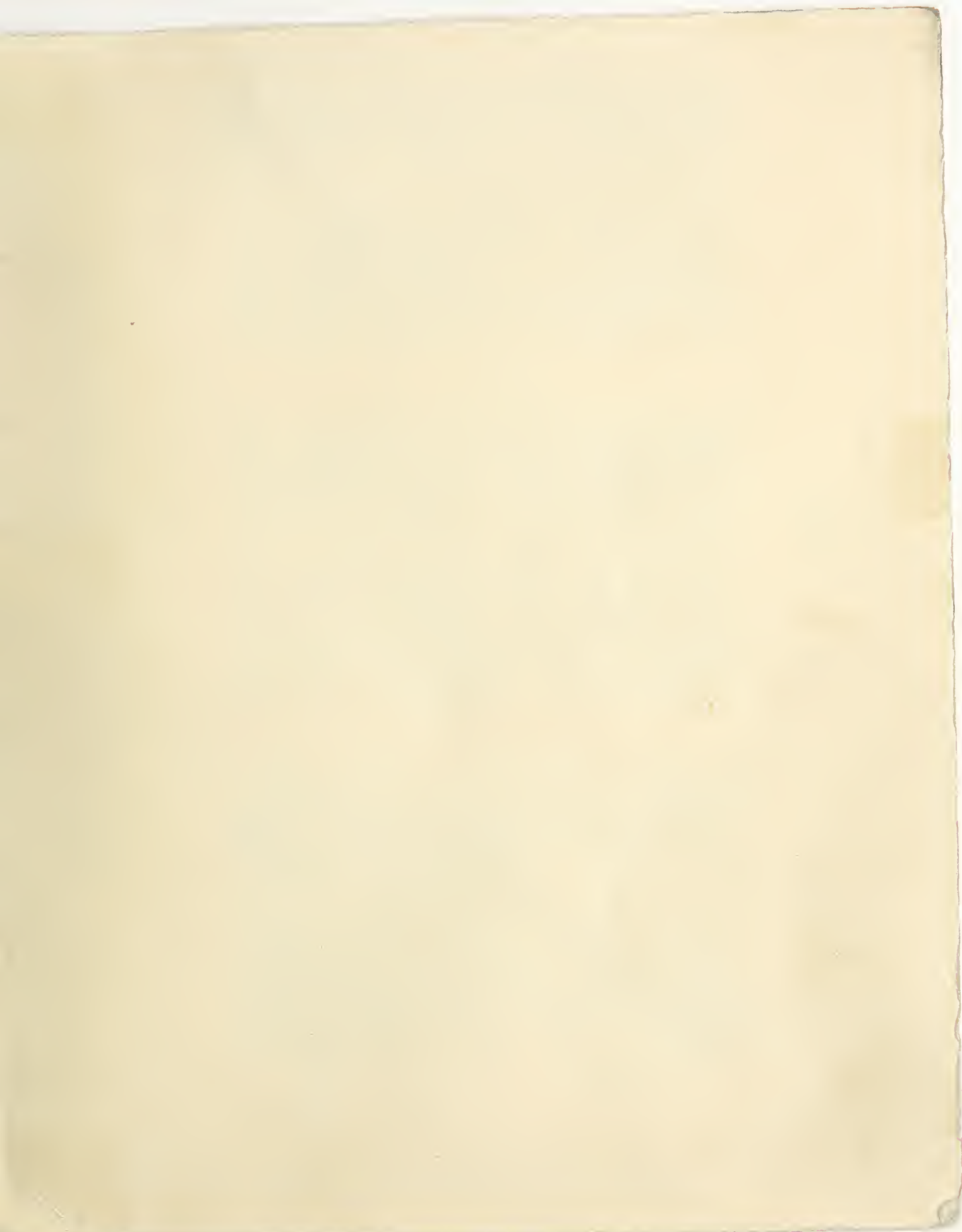


figure 8.3a. The power level was increased 6 dB with no apparent change in the target strength. An independent measurement of the noise power for these two tests produced the following results.

<u>Speaker Input Power</u>	<u>SPL</u>	<u>10 Hz</u>	<u>2 Hz</u>
240 mW	60 dB	80 mV PP	200 mV PP
60	53	150	320

The ambient noise at position 1 was 26 dB or 0.005 ubar. Converted to a 1 Hz BW it is 0.00013 ubar. At 60 mW the SPL was 53 dB or 0.09 ubar. From section 1.2.1,

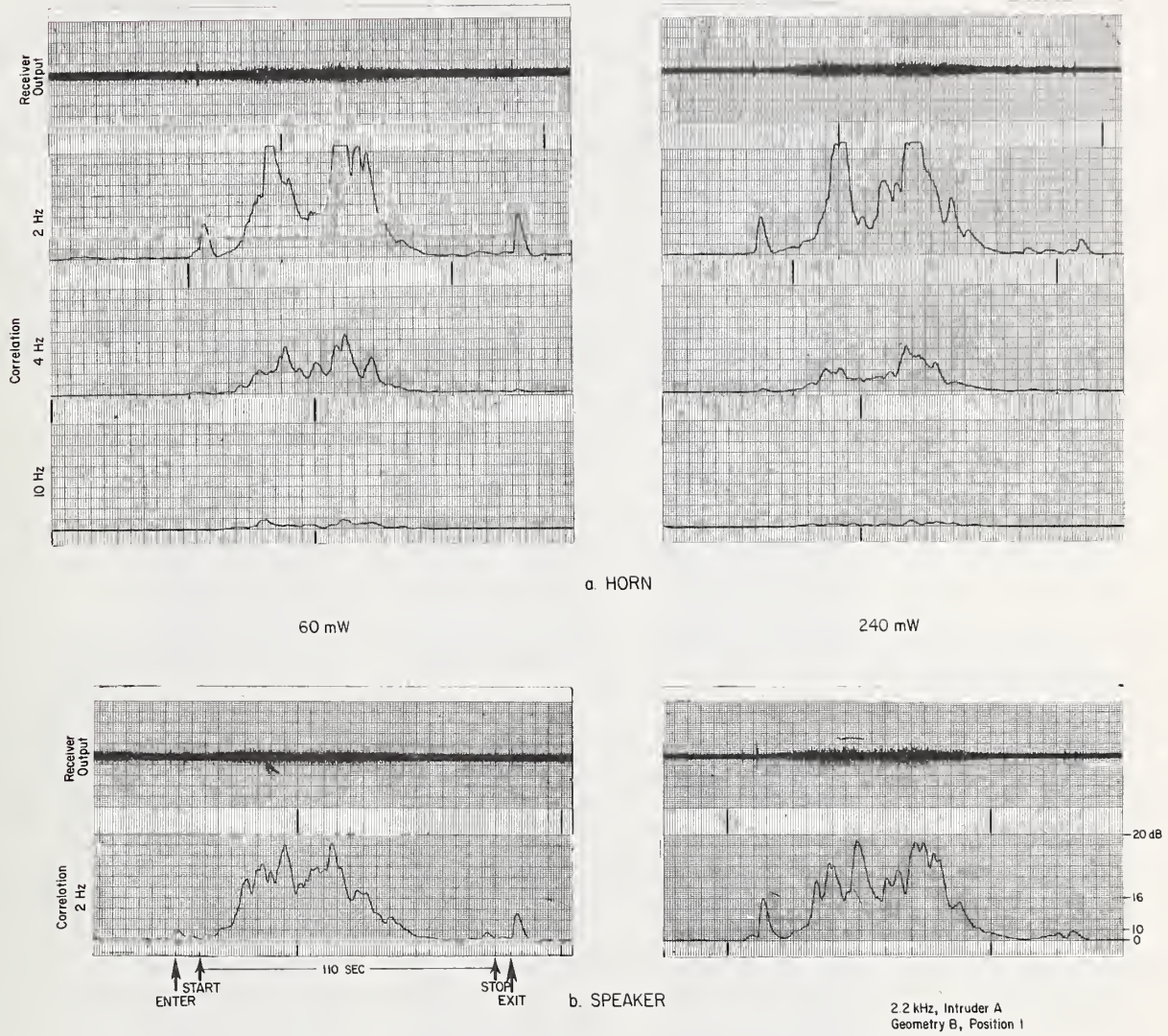
$$\text{Noise} = N_A = \frac{\text{SPL}_{\text{AMBIENT}}}{P_R} = 0.00013/0.09 \times 100 = .14\%.$$

The receiver-indicated noise is 150 mV PP, or 53 mV RMS. The receiver sensitivity is 3.5%/V. Indicated noise is therefore 3.5%/V x 53 mV = 0.18%; a variation of only 2 dB. A comparison of the 10 Hz noise levels shows a drop of about 6 dB for a 6 dB power increase while at 2 Hz the noise decreased 3 dB. This indicates significant environmental noise present at the lower frequencies. Again, the intruder signature magnitude remained the same for either power level.

8.2.3 Intruder Signature as a Function of Source Characteristics

A comparison was again made of the effects upon detection produced by changing the sonification source. In figure 8.3b, the horn was replaced with the speaker. When comparing the 2 Hz response of the intruder for the two sources (fig. 8.3a to fig. 8.3b), some differences appear. The signature produced with the horn has two high points which occurred as the intruder passed the source position. His route brought him past the source twice. The directionality of the horn would be expected to produce this type of reaction because a greater portion of the energy is transmitted directly in front of the horn. No other significant differences were observed.

INTRUDER SIGNATURE
AS A FUNCTION OF SOURCE



Instrument Shop

Figure 8.3

8.2.4 Detection as a Function of Geometry

The effects of microphone location upon detection at four different carrier frequencies are shown in figure 8.4. Very little difference in the detection sensitivity as a function of frequency is seen. It is apparent that a combination of only positions one and three would produce a detection level of greater than 10 dB for any point in the shop which the intruder passed.

Figure 8.5 shows the results of operating the system with the speaker at one end and using microphone position one only (geometry C). In this configuration detection at greater than 10 dB occurred for the entire time the intruder was in the shop. Positions two and three were also tested but provided no additional detection capability.

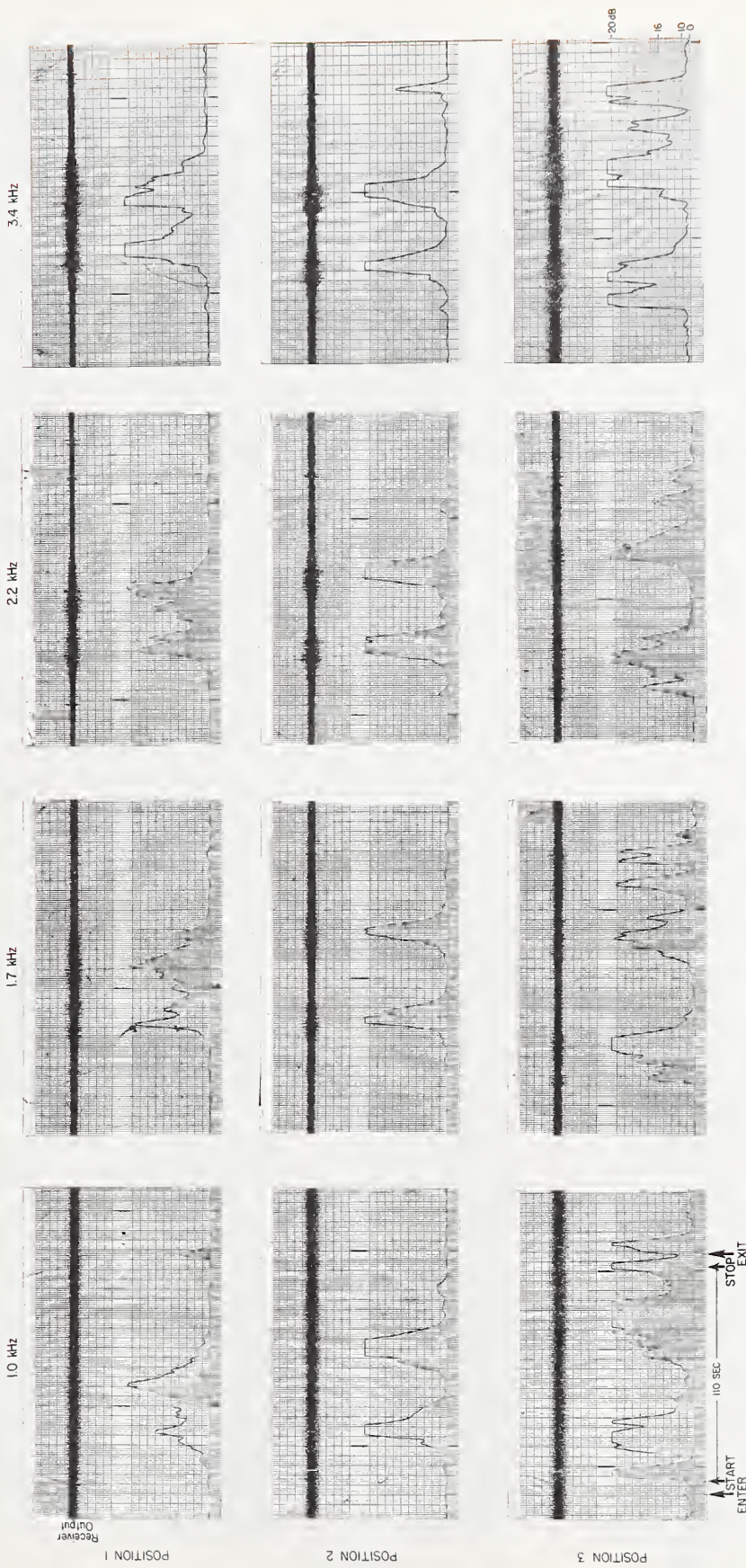
8.2.5 Intruder Signature as a Function of Intruder Velocity and Size

The effect of intruder velocity upon the signature was investigated in the shop to compare with the analysis from the auditorium (fig. 8.6). The spectral shift appears to be virtually the same as that which occurred in the auditorium indicating that the type of enclosure is not a factor in determining the spectrum. The only difference observed was the loss of 10 Hz energy in the intruder signature during the return portion of the intruder path. An examination of the recorded data indicates a probable recorder saturation at this point, which can destroy the higher frequencies. It appears that the absolute magnitude of the target return is not affected, but only the spectral distribution. This spectral distribution can provide a powerful discrimination technique.

The results of an intruder size comparison are also shown on figure 8.6. A reduction of signal magnitude is shown at all three correlated frequencies. The reduction appears to be approximately 3 dB, in general agreement with the results in the auditorium. This coincidentally corresponds to the weight ratio of the two individuals.

A computer spectral display is included for the first two intrusions. The frequency responses of the signatures appear to match very well. However, the reduction in magnitude does not show up well on the three-dimensional log scale.

DETECTION VS. MICROPHONE POSITION

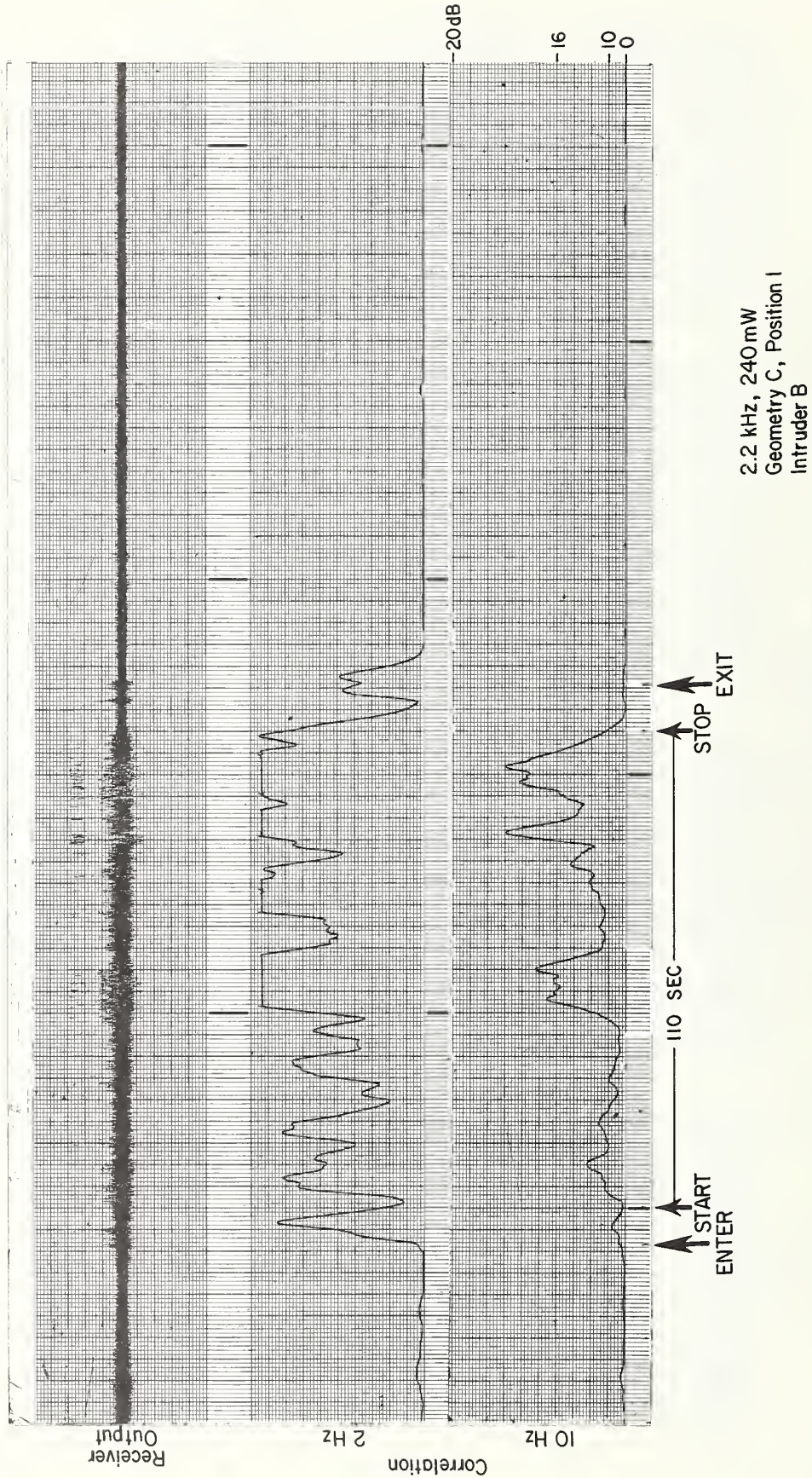


Power - 60 mW Speaker
 Geometry B, Intruder B
 2 Hz Correlation

Instrument Shop

Figure 8.4

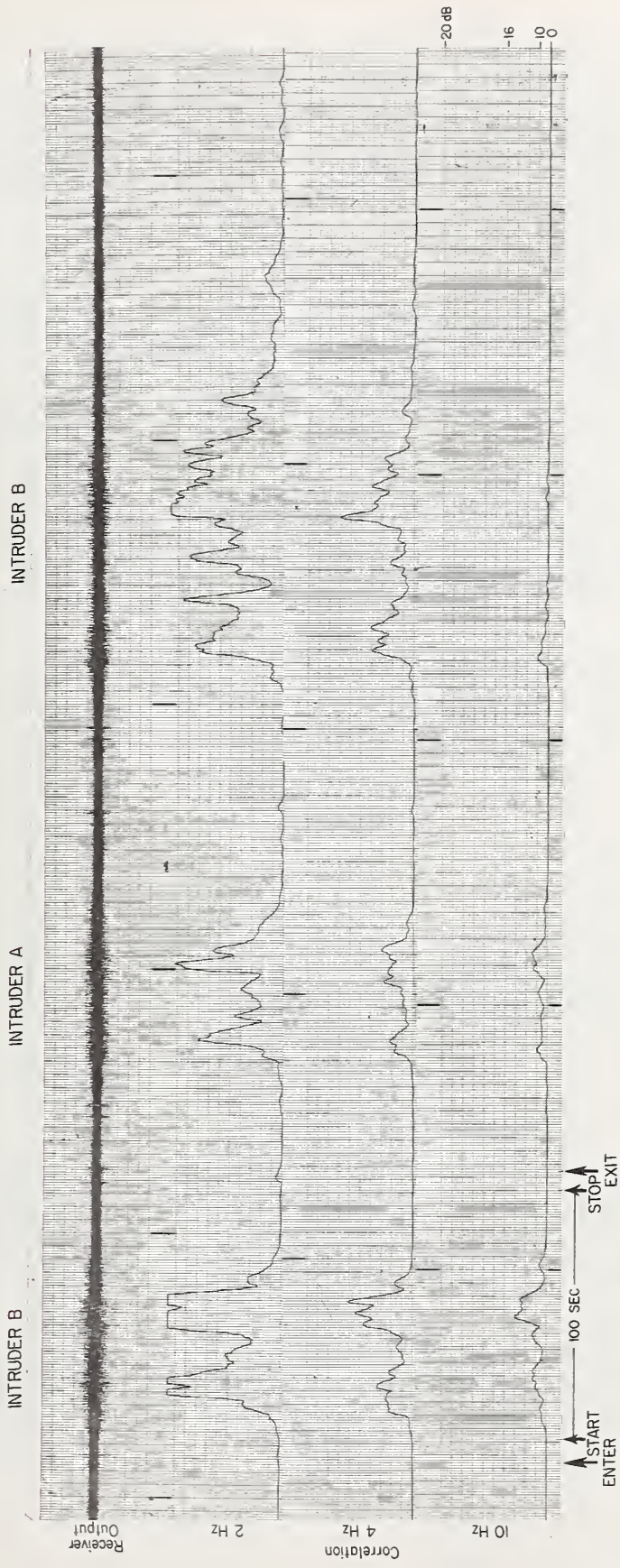
SINGLE SPEAKER/SINGLE MICROPHONE DETECTION



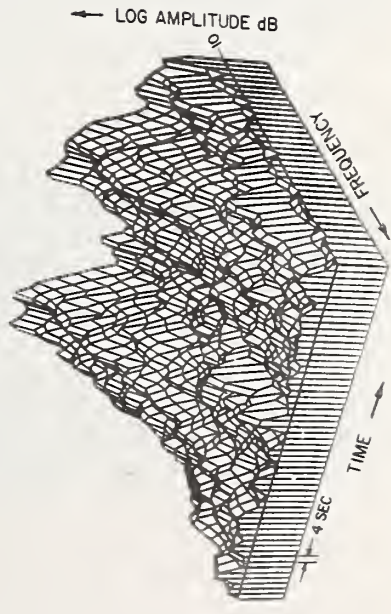
Instrument Shop

Figure 8.5

INTRUDER SIGNATURE AS A FUNCTION OF SIZE AND VELOCITY



2.2 kHz, 240 mW Horn
Geometry B, Position I



First Two Intrusions Only

Instrument Shop

Figure 8.6

8.3 Conclusions

The tests conducted in the machine shop closely duplicate the tests performed in the auditorium. These two diverse areas produced nearly identical results with regard to the spectral properties, velocity effects, noise analysis, and sonification level and directivity effects.

Altering the geometry produced some excellent unexpected results. The test conducted in geometry C (single microphone, single speaker) produced detection throughout the entire intruder traverse. This indicates a detection coverage increase of an order of magnitude with respect to ultrasonic Doppler systems.

The inability to even test 5.0 kHz, coupled with difficulties at 3.4 kHz, support the assumption that the natural vibrations of the enclosure will limit the use of the upper carrier frequencies to mechanically rigid confines.

No clear determination was established with regard to target strength as a function of carrier frequency. One test indicated lower returns from 1.0 kHz, while another did not.

9.0 WAREHOUSE FEASIBILITY TESTS

See figure 5.4. One set of tests was conducted in the Camco Building. These tests were conducted to determine if this technique is feasible in an enclosure constructed of very loose fitting, highly flexible material.

9.1 Test Descriptions

As noted in section 5.4, the Camco Building is a warehouse for surplus equipment. The construction is not rigid, vibrates in the wind, and has several openings which allow birds to enter and roost. Considerable wind was blowing during 9 of the 16 tests conducted. This provided considerable ambient noise from the rattle of the sides and the roll-up door. Microphones 1 and 3 were attached to the wall 3 meters from the floor, while microphone 2 was attached at 4 meters up on a center support column as shown in figure 5.4.

The speaker was set (3 meters high) on top of the office shown in the corner of the building. All instrumentation was assembled in the office. The intruder path is as shown in figure 5.4. As with all other tests, the intruder entered, waited 5 seconds, proceeded through the traverse, and paused for 5 seconds prior to exit.

9.2 Tests Results and Analysis

The tests described in this section will not be broken down into types, because it was a feasibility study. It should be noted that some of the tests attempted could not be conducted because of general signal instability; however, tests were successful at all four frequencies (1.0, 1.7, 2.2 and 3.4 kHz). As would be expected, microphone position 3, which is near the roll-up door on the outside wall, produced the most problems. Position 2 was always usable, while position 1 on the inside wall produced some problems.

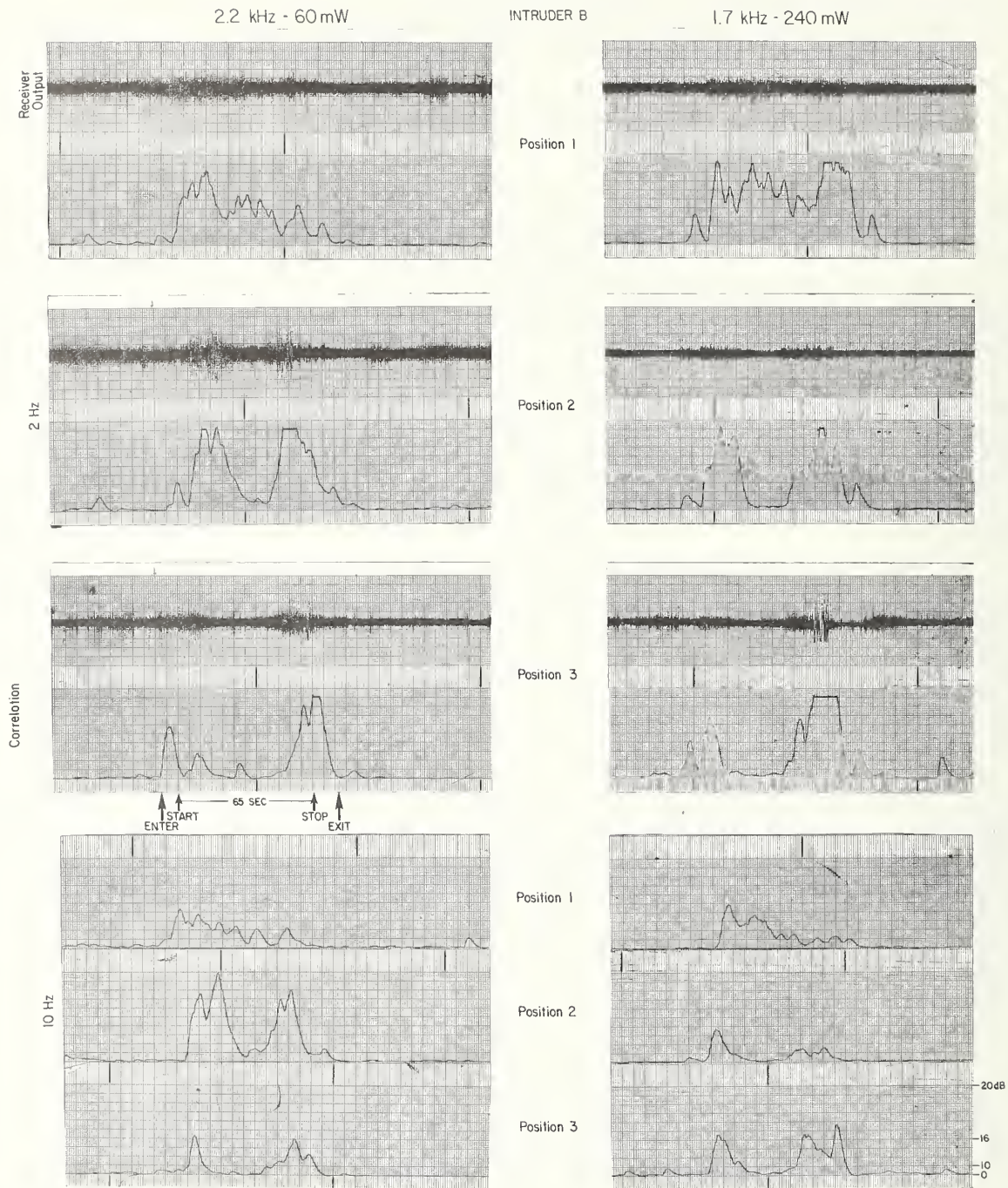
The results of the microphone position test are shown in figure 9.1. Two carrier frequencies were tested and indicated no significant differences. Position 1, in which the microphone and speaker were separated by the maximum distance, provided the best detection. The intruder produced signal to noise ratios in excess of 15 dB for the entire traverse at 1.7 kHz.

The noise background is considerably better at 1.7 kHz, due to the increased power levels in that test. The wind velocity had increased considerably during the 1.7 kHz test and increased power was needed to overcome the increased ambient noise conditions. The number 3 position on the outside wall indicates higher noise levels at both carrier frequencies and both correlated frequencies as a result of the increased noise.

A complete spectral analysis as a function of carrier frequency was not attempted in this area; however, the 10 Hz response for each test is shown in figure 9.1. The ratio of the 2 to 10 Hz responses is nearly the same as that found in the spectral comparison from prior work.

A target strength measurement shown in figure 9.2 was conducted for three frequencies. They are of a feasibility nature and not as rigorously controlled as those in the other areas. The test at 1.7 kHz shows an increase in power of

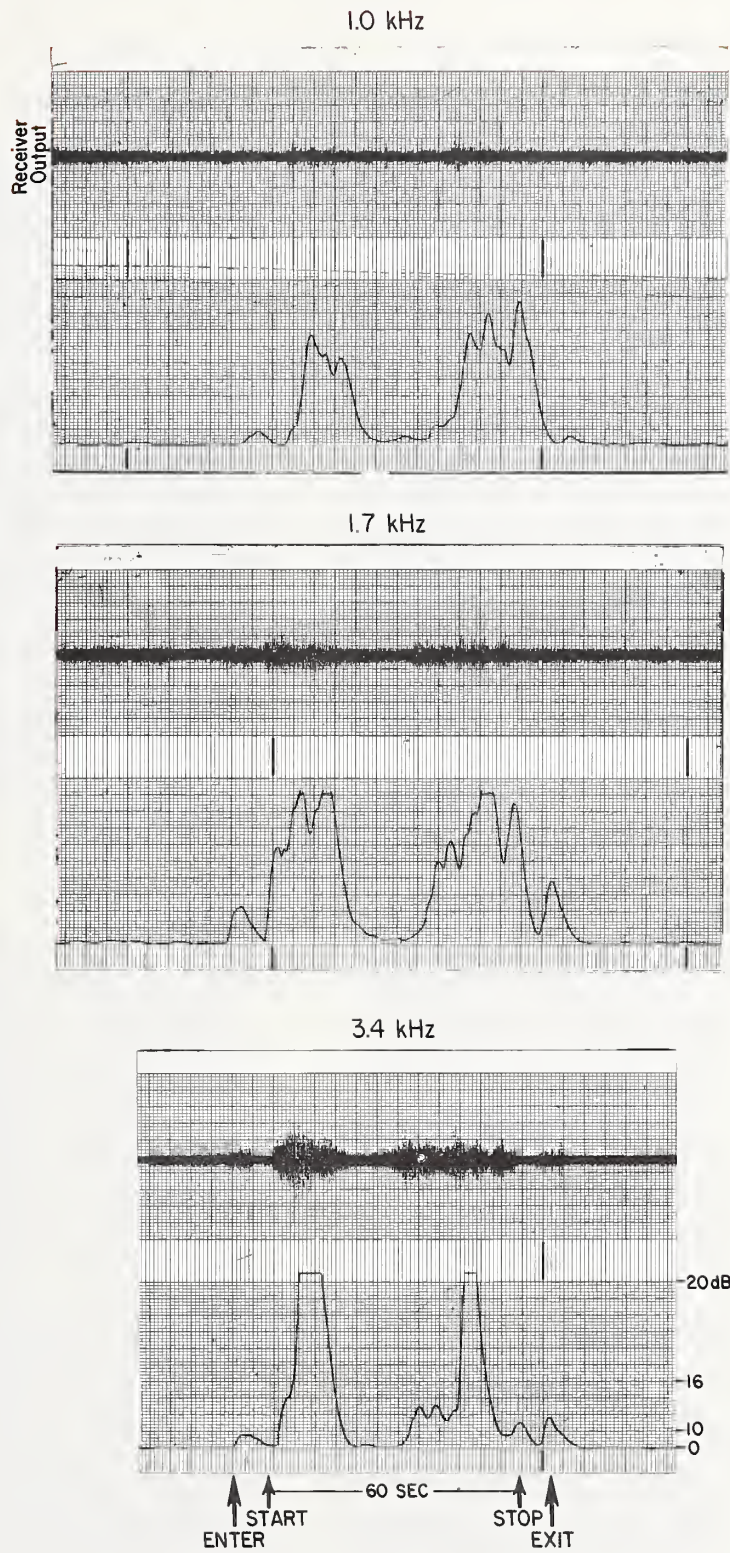
INTRUDER SIGNATURE VS. GEOMETRY



Camco Building

Figure 9.1

TARGET STRENGTH VS. CARRIER FREQUENCY



Power - 240 mW Position 2
2 Hz Correlation
Intruder A

Camco Building

Figure 9.2

about 3-4 dB over that at 1.0 kHz. The result for 3.4 kHz is peculiar in that the peaks were considerably higher than for 1.7 kHz, but the overall average does not appear to be as great. It is possible, in this area, that the higher frequency exhibits greater shadowing from the sections created by the shelves.

Sonification level tests were conducted at 1.7 and 2.2 kHz after the wind had subsided. Two power levels, 60 and 240 mW, were used, and the results are shown in figure 9.3. The relative noise level decreased at the higher power level as expected, while the intruder signature remained approximately the same. (Some increase in the magnitude of the indicated signature is to be expected due to the display of signal plus noise as noted earlier.)

9.3 Conclusions

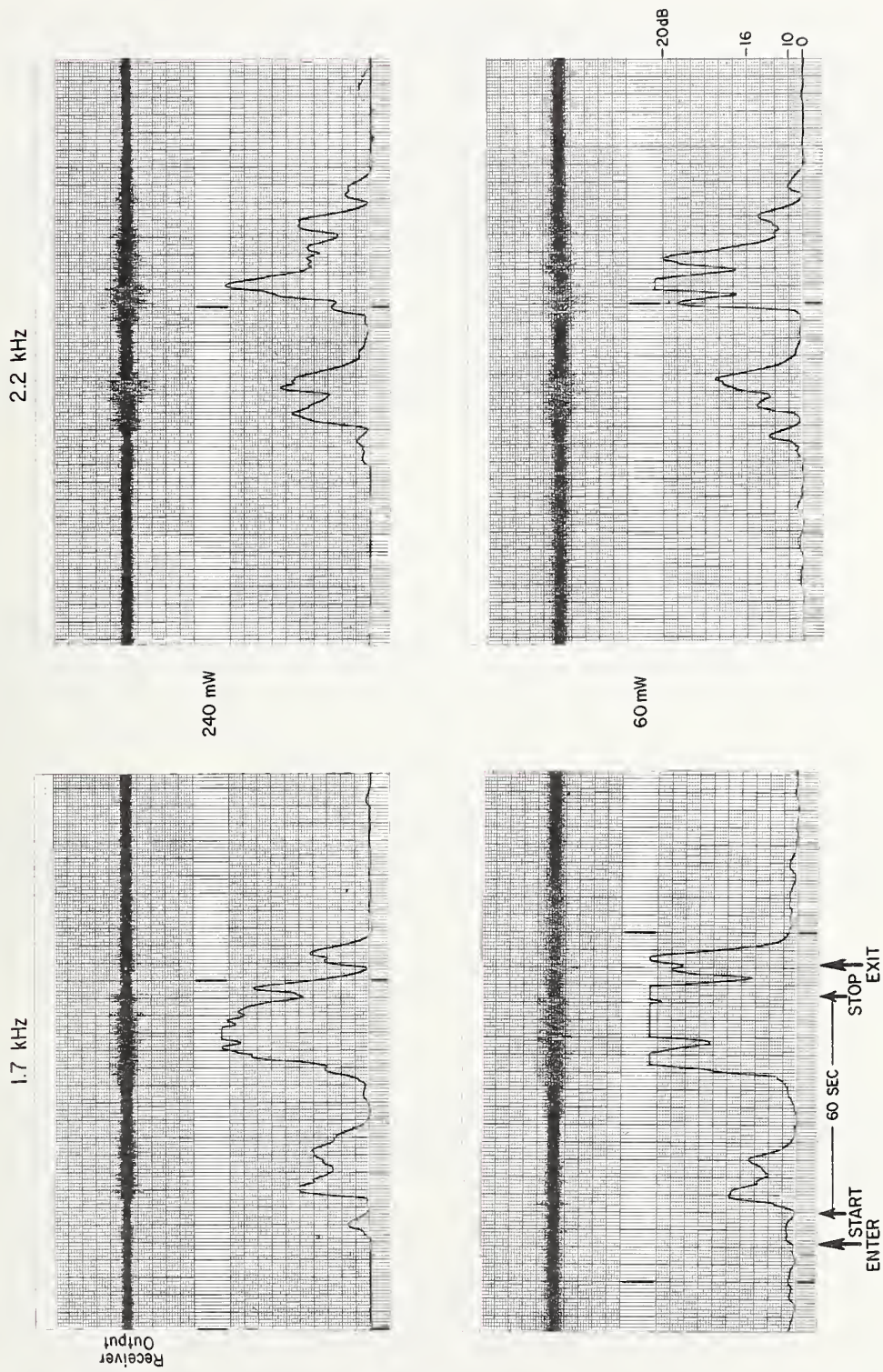
The results of this single feasibility test series were exceedingly encouraging. The intruder signature appears to be virtually the same as that of all other areas. The basic noise assumptions were supported in this area also. An interesting hypothesis concerning possible shadowing of the higher carrier frequencies in large partition buildings was suggested by the tests conducted at 3.4 kHz. This type of area should be investigated in greater detail in follow-on work of interferometric detection techniques.

10.0 LONG TERM FALSE ALARM TESTS

During a demonstration of the work to Mr. Jack Hinde of Sandia Laboratories, he suggested a long term (8-24 hour) false alarm test.

The receiver for this measurement series was designed primarily for laboratory measurements which would provide a maximum of calibration stability, linearity, and sensitivity. Long term tracking of the phase and magnitude of the received signal vector was not a design requirement. The limited phase correction rendered the units unsuitable for this type of test. It was, nevertheless, mutually agreed to attempt a test series. Two ten-hour tests were conducted.

SONIFICATION VS. NOISE AND INTRUDER SIGNATURE



Position 2
Intruder A
2 Hz Correlation

Camco Building

Figure 9.3

10.1 Test Descriptions

The tests were conducted at 2.2 kHz and used the 2 Hz correlator only for a detector. No multiple correlators or decision making logic were used to improve false alarm rates. The 2 Hz correlator output was recorded on a strip chart. Test 1 was conducted in room 3082 at 20 mW with the microphone at position 2. Test 2 was conducted in the NBS auditorium at 120 mW using geometry B and position 3 (figs. 5.1 and 5.2).

In each case, the signal to noise ratio was established before and after the false alarm test was run. It was greater than 20 dB in both tests. Both tests were conducted overnight and unattended.

10.2 Test Results and Analysis

As noted, the receivers were not designed for long term operation. As such, they provide only a finite phase correction, of $\pm 50^\circ$, without compromising the receiver operation. The receivers will remain phase locked up to about $\pm 80^\circ$ (depending upon the particular unit), but beyond $\pm 50^\circ$ the receiver output contains considerable noise.

Given this operational constraint, it was feared that phase lock would be lost completely during a period of several hours, thus invalidating the test. Loss of phase lock did not occur during either test.

The strip chart recording produced during these tests is 2 meters long, making it impractical to include the recording in this report.

In both tests, the phase of the received signal apparently approached the maximum dynamic range of the control circuit. We assume this to be true because with the test unattended, an absolute certainty could not be established.

In the test conducted in room 3082, the output from the correlator showed three 6-minute periods occurring over 30 minutes of the 4th hour of the test in which the noise level was 10 dB. The signal-to-noise ratio still remains greater than 10 dB. The phase servo was purposely offset to greater than 50° to observe the result on the correlator. The correlator output was identical to that produced during the tests.

It is difficult to speculate regarding types of disturbances other than phase drift that would cause a constant level of the type seen. Ambient noise is generally more erratic over 6-minute time periods.

During the test in the auditorium, similar outputs from the correlator occurred. During the first 2.5 hours of the test, seven 5 to 7 minute periods of +10 dB noise occurred. In addition three other outputs exceeded +16 dB during the 2.5 hours; however, none reached the level of the intruder. The remaining 7.5 hours indicated stable noise conditions.

As noted, the tests were unattended and intrusions were conducted both before and after to insure intruder signature levels, without any readjustments.

10.3 Conclusions

These test results exceeded our expectations. Since signal phase stability is considerably better than had been anticipated, hardware design requirements can be kept simpler than originally anticipated. Of course, the above results will have to be positively determined during the hardware development stage.

If further tests confirm that the perturbations experienced proved to be a phase drift rather than a false alarm caused by the test area, it appears that the low frequency interferometric technique may not be subject to some of the false alarm problems that occur in systems that are sensitive to air currents, window shake, etc.

11.0 CONCLUSIONS

The results of the program positively confirm the applicability of the low frequency acoustical interferometric technique for detection of human intruders into protected areas.

11.1 Conclusion by Parameter

The particular conclusions drawn from the results of this program are stated below.

11.1.1 Intruder Signature

The intruder signature frequency response is directly proportional to the carrier frequency for a walking velocity of 0.9 meters/sec. The response is nominally 0-15 Hz at 3.0 kHz and 0-5 Hz at 1.0 kHz. At 2.2 kHz the slope of the response is approximately 20 dB/decade for the 1-10 Hz range.

Target strength for the intruder is -26 to -30 dB with respect to the sound pressure level in a 1 Hz bandwidth at all frequencies tested in the larger test areas, except for 1.0 kHz, which on some tests produced an additional -3 dB.

Though not positively confirmed, a carrier frequency higher than 1.0 kHz is required for consistent average target return.

The spectrum from the intruder signature varies with intruder velocity. Reducing the velocity by half translates the frequency spectrum downward.

Intruder signature is proportional to intruder size at least within the range of test intruders used, roughly in the ratio of their weight.

11.1.2 Background Noise

Noise is produced from two sources: ambient acoustical energy and environmental changes which alter the multiple transmission paths thus producing unstable signal levels.

The ultimate limiting factor for signal to noise ratio is the environment. The effects of ambient noise can be overcome by increasing the source level. Environmental noise is related to carrier frequency and building structure. Increasing carrier frequency increases environmental noise. Tests show that the more rigid the structure, the less the environmental noise is present. For the areas tested, 3.4 kHz appears to be the upper frequency for reliable operational use.

Tests conducted to determine the limiting effect of ambient noise indicate that the sonification sound pressure level should be about 50-60 dB above the ambient noise in a 1 Hz bandwidth. At this level the ambient noise effects are reduced to the threshold of the environmental noise in typical enclosures.

11.1.3 Geometry of the Source and Receiver

In general, the maximum perturbation from the intruder occurred when the source and receiving microphones were separated by the maximum distance. With the exception of the single Camco test in which shadowing was suspected at 3.4 kHz, the results indicate that detection coverage and magnitude for a given geometry is not a function of carrier frequency (from 1.0-3.4 kHz). Of course, as noted in section 11.1.1, the spectral character of the signature is different but this is independent of geometry.

11.1.4 Area of Coverage

Areas of up to 600 sq. meters (6456 sq. ft.) were tested. Even in the largest volume, signal-to-noise ratios of +10 dB for intruders anywhere in the area were recorded for a single source and single receiving microphone in fixed locations.

In unobstructed rooms signal-to-noise ratios of +10 dB detection level were produced by any of the source and receiver geometries tested. Detection signal-to-noise ratio is generally better than +16 dB, and in a majority of the tests was better than +20 dB. Exceptions, of course, occurred during low sonification tests conducted to measure ambient noise effects.

11.1.5 The Effects of Source and Microphone Characteristics

Tests were conducted using both a "high-fi" speaker and a directional exponential horn. Except in the area immediately in front of the source, no changes in the intruder signal could be determined between the two.

The replacement of the microphones with a high quality sound level meter as a receiving sensor and preamplifier indicated no difference in the detection characteristics. It is probable that low cost microphones can be used for detection hardware.

11.1.6 General Comments

Detection signal-to-noise ratios remained high (+10 dB) even when the test area was flooded with acoustical energy from a radio. Tests conducted with a radio operating at -6 dB (broadband) with respect to the source level still provided excellent detection.

Detection at extremely low intruder velocities and low profiles appears probable from limited exploratory tests conducted by slow walking movement and crawling. However, a somewhat more sophisticated detector logic than that required for normal detection would probably be needed.

11.2 Recommendations

The following recommendations are offered for future efforts in the detection by low frequency interferometric techniques.

11.2.1 Minimum Velocity Effects

Additional tests should be conducted to determine the practical lower limit for intruder velocity which still permits detection. These tests could be accomplished by modifying the present receiver and correlators to determine the intruder spectrum below 1 Hz.

11.2.2 Additional Evaluation of Sound Pressure Fields

The sound pressure level variations for a wide variety of test areas should be thoroughly investigated to provide engineering specifications for hardware construction prior to a prototype engineering model detector.

11.2.3 Design and Construction of Prototype Engineering Model Detectors

Based upon the information in this report and that obtained by completing the efforts described in sections 11.2.1 and 11.2.2, engineering prototype detectors should

be designed and constructed. These units would provide adaptive circuitry for variable sound pressure levels, automatic phase tracking, and would allow for the incorporation of changes as the test program suggests improvements, such as variable logic alarm systems.

11.2.4 Detection Capability and False Alarm Tests

The engineering prototype detectors should be tested in a large number of environments.

They should be evaluated for various intrusion techniques, including minimum velocities, minimum profiles (crawling), sound absorbent covers, intruder size, and other techniques suggested by security personnel.

In addition, long term tests should be conducted to determine false alarm causes and rates of occurrence. Improvements suggested by these tests should be incorporated into the engineering prototype models for further tests.

11.2.5 Engineering Model Detector and Test

Based upon the knowledge that has been acquired from our testing program and the developmental improvements suggested by the prototype detectors, several engineering model detectors should be designed and constructed. The units would probably be of more than one type in order to meet particular requirements. They would then be assigned to security testing laboratories for evaluation.

ACKNOWLEDGMENTS

The author is indebted to Messrs. Robert Adair and Douglas Kremer for their enthusiastic and dedicated efforts which included working nights and weekends to successfully complete this program.

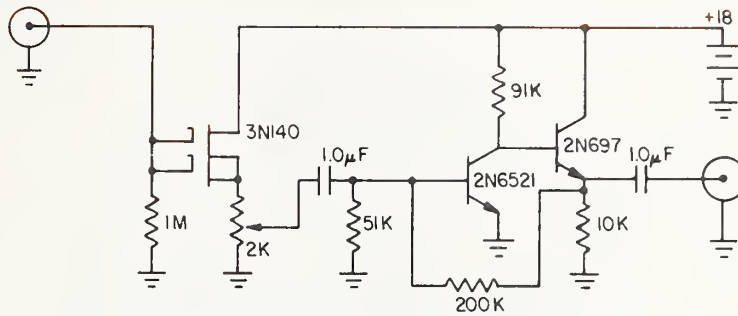
REFERENCE

- [1] Robert J. Ulrick, Principles of Underwater Sound for Engineers, McGraw Hill Book Company, New York, 1967, Section 9.

APPENDIX

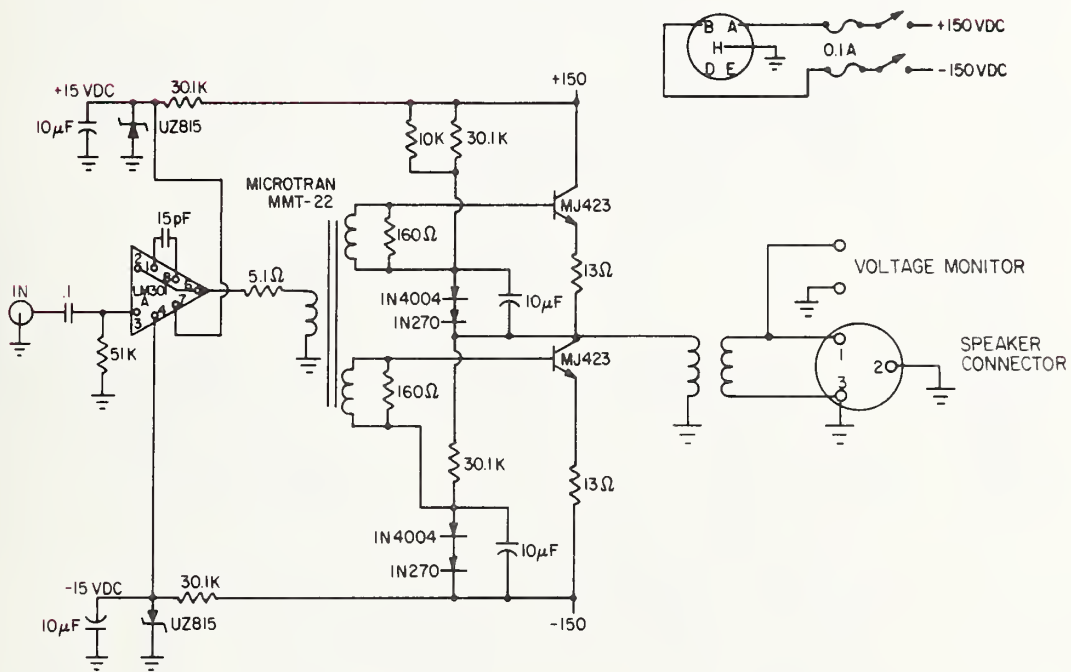
Certain commercial components and materials are identified in this report in order to adequately specify the equipment. In no case does such identification imply recommendation or endorsement by the National Bureau of Standards, nor does it imply that the material or equipment identified is necessarily the best available for the purpose.

MICROPHONE AMPLIFIER



≈ 50 dB GAIN
ADJ FOR 46 dB

SPEAKER AMPLIFIER



DC-DC CONVERTER

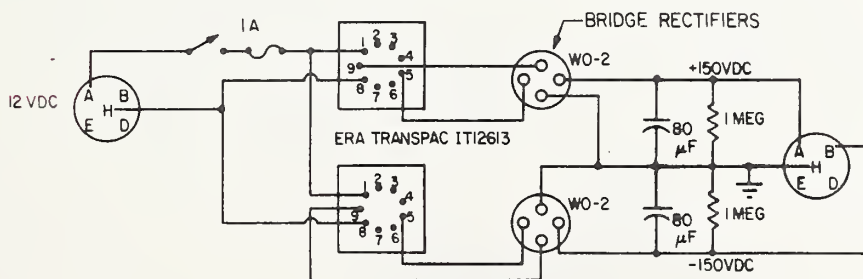


Figure A.1
Microphone amplifier, speaker amplifier,
and DC-DC converter schematics.

AUTOMATIC NULL RECEIVER
WIRING DIAGRAM

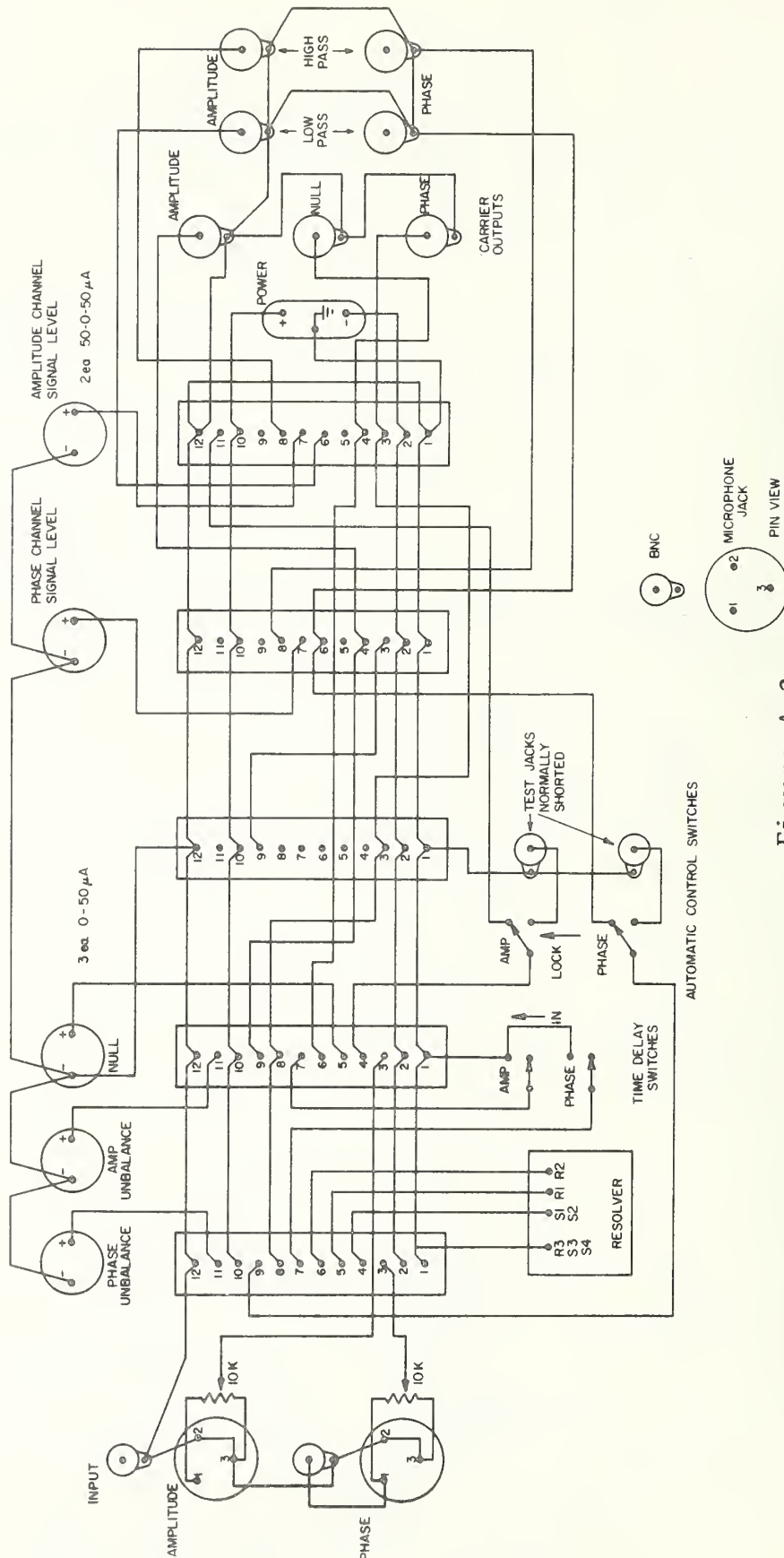
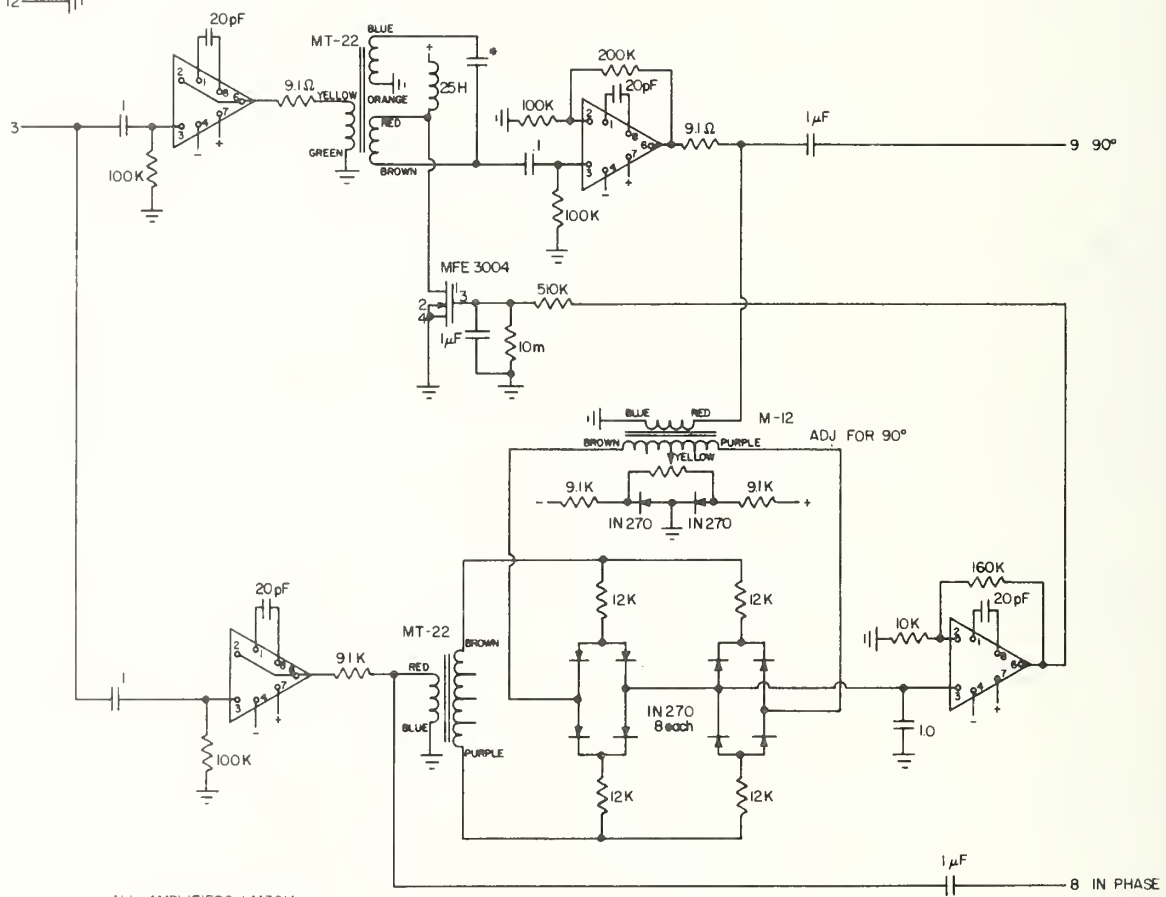


Figure A.2



QUADRATURE HYBRID

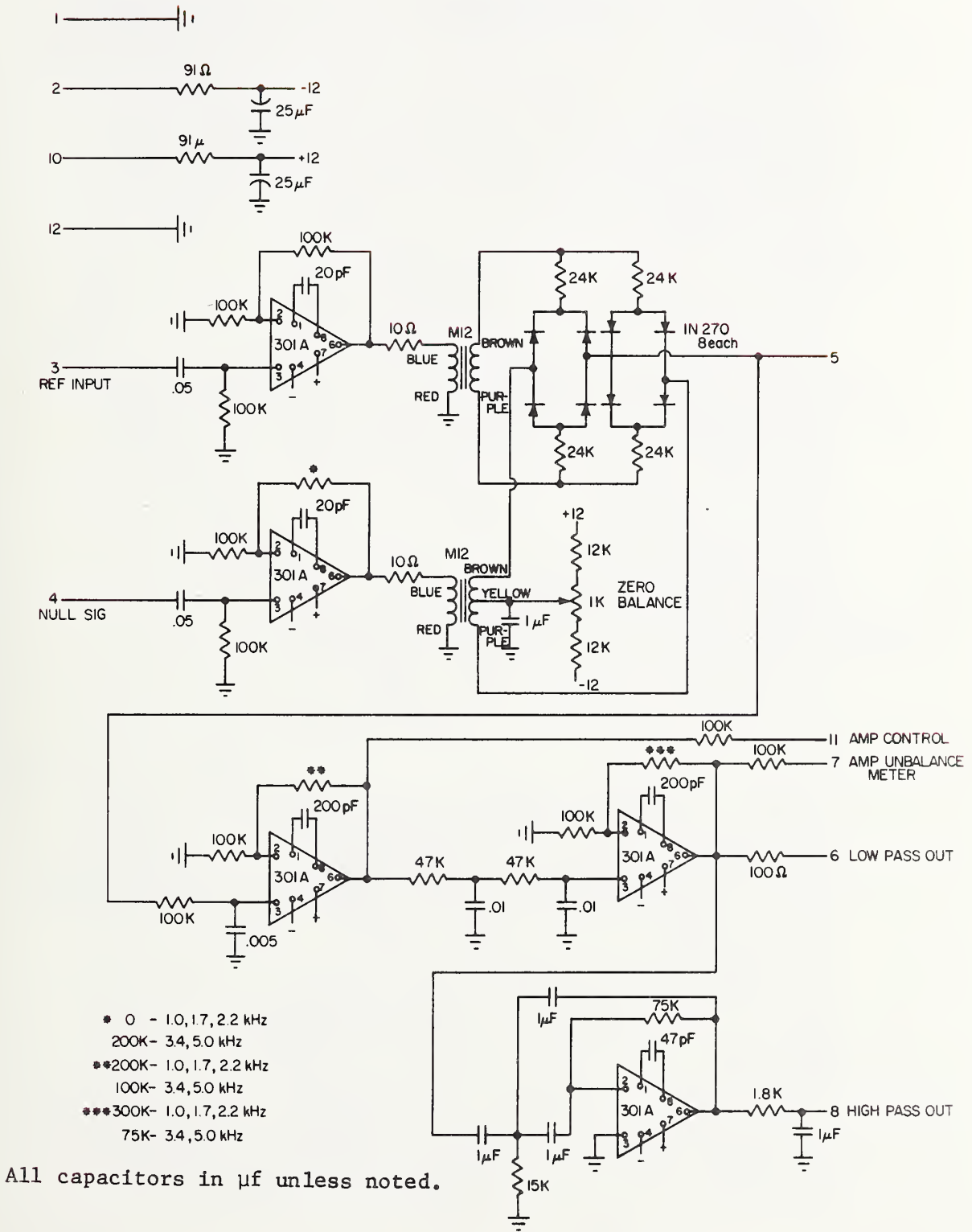


- ALL AMPLIFIERS LM301A
- Selected for center frequency
 - 10 kHz 015μF
 - 17 kHz 010
 - 2.2 kHz .0082
 - 3.4 kHz 3400 pF

All capacitors in μf unless noted.

Figure A.6

AMPLITUDE DETECTOR

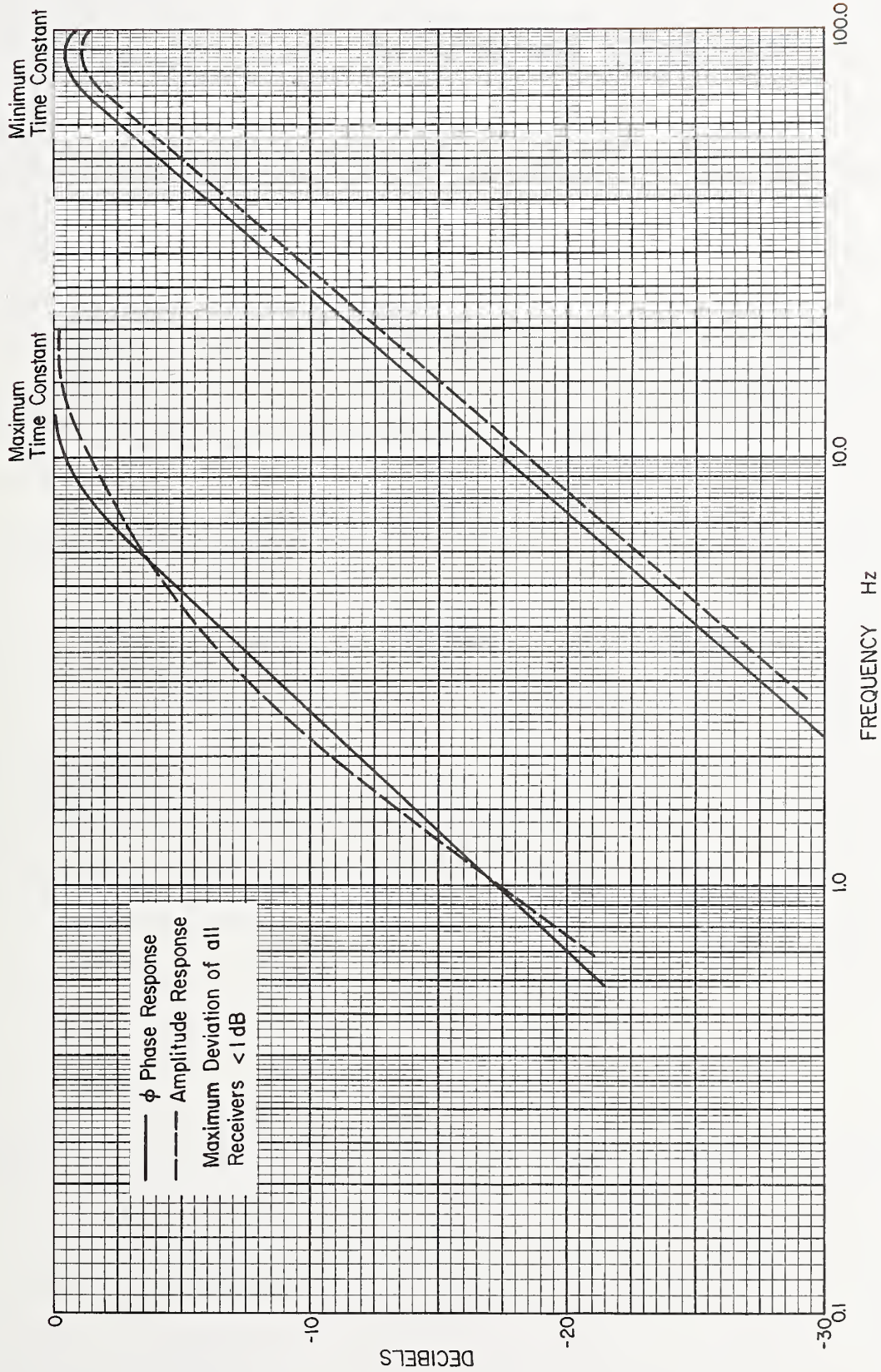


- * 0 - 1.0, 1.7, 2.2 kHz
200K - 3.4, 5.0 kHz
- **200K - 1.0, 1.7, 2.2 kHz
100K - 3.4, 5.0 kHz
- ***300K - 1.0, 1.7, 2.2 kHz
75K - 3.4, 5.0 kHz

All capacitors in μf unless noted.

Figure A.7

RECEIVER RESPONSE



0 dB is $1V/2$ degrees or $1V/3.5\%$ perturbation

Figure A.9

U.S. DEPT. OF COMM. BIBLIOGRAPHIC DATA SHEET	1. PUBLICATION OR REPORT NO. NBSIR 74-364	2. Gov't Accession No.	3. Recipient's Accession No.
4. TITLE AND SUBTITLE DETECTION OF HUMAN INTRUDERS BY LOW FREQUENCY SONIC INTERFEROMETRIC TECHNIQUES		5. Publication Date May 1974	
7. AUTHOR(S) Robert E. Stoltenberg		6. Performing Organization Code	
9. PERFORMING ORGANIZATION NAME AND ADDRESS NATIONAL BUREAU OF STANDARDS DEPARTMENT OF COMMERCE Washington, D.C. 20234		8. Performing Organ. Report No.	
12. Sponsoring Organization Name and Complete Address (Street, City, State, ZIP) Sandia Laboratories U. S. Atomic Energy Commission Albuquerque, New Mexico		10. Project/Task/Work Unit No. 2728455	
15. SUPPLEMENTARY NOTES		11. Contract/Grant No.	
16. ABSTRACT (A 200-word or less factual summary of most significant information. If document includes a significant bibliography or literature survey, mention it here.) This report examines the theory and evaluates the results of over 200 tests of the use of low frequency sonic interference techniques for the detection of a human intruder in a confined area. The conclusions are that this technique is potentially a significant improvement over conventional methods with regard to area coverage and minimum velocity detection. This work examined the intruder signature and background noise with respect to sonification frequency, source levels, intruder size, intruder velocity, source types, area coverage (to 692 sq. meters), and geometric position of the source and receiver in four radically different areas. Interference effects of the intruder signature and noise were analyzed with respect to bandwidth, spectral content, and magnitude by both computer drawn spectral displays, and specific frequency correlators.		13. Type of Report & Period Covered	
17. KEY WORDS (six to twelve entries; alphabetical order; capitalize only the first letter of the first key word unless a proper name; separated by semicolons) Human detector; interferometric technique; low frequency acoustics.		14. Sponsoring Agency Code	
18. AVAILABILITY <input checked="" type="checkbox"/> Unlimited <input type="checkbox"/> For Official Distribution. Do Not Release to NTIS <input type="checkbox"/> Order From Sup. of Doc., U.S. Government Printing Office Washington, D.C. 20402, SD Cat. No. C13 <input type="checkbox"/> Order From National Technical Information Service (NTIS) Springfield, Virginia 22151	19. SECURITY CLASS (THIS REPORT) UNCLASSIFIED	21. NO. OF PAGES	20. SECURITY CLASS (THIS PAGE) UNCLASSIFIED
		22. Price	



